LUND INSTITUTE OF TECHNOLOGY
LUND UNIVERSITY

Division of Building Materials

ASSESSMENT OF THE CHLORIDE MIGRATION COEFFICIENT, INTERNAL FROST RESISTANCE, SALT FROST SCALING AND SULPHATE RESISTANCE OF SELF-COMPACTING CONCRETE

- with some interrelated properties

Bertil Persson

TVBM-3100 Lund 2001

ISRN LUTVDG/TVBM--01/3100--SE(1-86)
ISSN 0348-7911 TVBM
ISBN 91-631-0855-0

Lund Institute of Technology
Division of Building Materials
Box 118
SE-221 00 Lund, Sweden

Telephone: 46-46-2227415
Telefax: 46-46-2224427
www.byggnadsmaterial.lth.se

LUND INSTITUTE OF TECHNOLOGY

DIVISION OF BUILDING MATERIALS, LUND UNIVERSITY, LUND

ASSESSMENT OF THE CHLORIDE MIGRATION COEFFICIENT, INTERNAL FROST RESISTANCE, SALT FROST SCALING AND SULPHATE RESISTANCE OF SELF-COMPACTING CONCRETE

- with some interrelated properties

Bertil Persson

TVBM-3100 Lund, 2001

ISRN LUTVDG/TVBM—01/3100—SE(1-86)
ISSN 0348-7911 TVBM
ISBN 91-631-0855-0

Lund Institute of Technology
Division Building Materials
P O Box 118
SE-221 00 Lund, Sweden

Telephone: +46 46 2227415
Telefax: +46 46 2224427
www.bygnadsmaterial.lth.se

PREFACE

Concrete that does not require any energy for compacting in order to cover the reinforcement or fill out the mould has attracted a great deal of interest. Swedish experience now exists from 19 full-scale bridges and other full-scale projects with Self-Compacting Concrete, SCC. The technique has also been introduced for dwelling houses and office buildings.

Regarding concrete under severe circumstances for construction of bridges, dams, tunnels and so forth, the requirements of durability are greater. Therefore a higher level of documentation is required for concrete under severe conditions than for concrete that is used for dwelling houses or office buildings. The primary durability properties are salt frost scaling, internal frost resistance, sulphate resistance and chloride ingress for concrete under severe situations.

In this project the objectives were to investigate the chloride migration coefficient, D, defined by Tang, to determine the salt frost scaling, the internal frost resistance and the sulphate resistance of SCC that contains increased amount of filler, different types of casting and air content. The objective was also to compare the result of salt frost scaling, internal frost resistance, sulphate resistance and chloride ingress of SCC with the corresponding properties of normal concrete, NC, with the same water-cement ratio, w/c = 0.39. Finally the objective was to give recommendations how to produce a SCC durable to frost and chlorides.

Financial support from the Development Fund of the Swedish Construction Industry and from Skanska Sweden Ltd is gratefully acknowledged. Acknowledgement is also due to Partek Nordkalk FoU, Pargas, Finland, for an associated project that studied the mechanism behind the effect of limestone filler on strength and structure of SCC.

Furthermore gratitude is hereby expressed to Ulf Jönsson, who coordinated the project and offered many valuable comments from the practical point of view. Finally, many thanks are due to Professor Göran Fagerlund for his critical review and to Bengt Nilsson, Ingemar Larsson and Stefan Backe who carried out most of the laboratory experiments.

Lund, 21 December 2001

Bertil Persson

CONTENTS

SUMMARY AND RECOMMENDATIONS

This report describes laboratory and analytical studies of the chloride migration coefficient, D, defined by Tang, the salt frost scaling, the internal frost resistance and the sulphate resistance of SCC that contains increased amount of filler, different types of casting and different air content. The result of studies on salt frost scaling, internal frost resistance, sulphate resistance and chloride ingress of SCC are compared with the corresponding properties of normal concrete, NC, with the same water-cement ratio, w/c = 0.39 and air content, 6%. Finally recommendations are given as to how to produce a SCC durable to frost and chlorides.

Both 28 and 90 days' age applied at the start of the testing. The strength development of the concrete, creep and shrinkage were followed in parallel. Six SCCs were studied and 2 NCs, all with water-cement ratio, w/c = 0.39. The concrete was sealed from casting until testing. The effects of normal and reversed order of mixing (filler last), increased amount of filler, type of filler, Köping 500 (branch Limus 40) or Ignaberga 200 (branch Limus 15), limestone powder, increased air content and large hydrostatic concrete pressure were investigated.

The following conclusions were found after comparative tests on mechanical properties, chloride migration coefficient, D, salt frost scaling, internal frost resistance and sulphate resistance of Self-Compacting Concrete, SCC, and of normal concrete, NC, with the same w/c-ratio, 0.39:

Mechanical properties

1. Limestone filler additives increased the strength substantially even though the cement content was somewhat lower in SCC than in NC.
2. Probably a more efficient packing of the particles was the reason for the enlarged strength of SCC.
3. Creep and shrinkage performed in the same way in SCC as in NC.

Chloride migration coefficient

1. The chloride migration coefficient was some 60% larger in SCC with limestone filler than in NC.
2. In SCC with 5% silica fume and 12% fly ash the chloride migration coefficient was 60% of that in NC.
3. At 90 days' age of testing the chloride migration coefficient was 60% of that at 28 days' age.
4. The efficiency factor of silica fume compared to Portland cement with regard to the chloride migration coefficient seems to be around 1,6.
5. The efficiency factor of blast furnace slag seems to be 1.
6. The efficiency factor of fly ash compared to Portland cement with regard to the chloride migration coefficient seems to be around 0.2.
7. Self-desiccation may had played a role in the low value of the chloride migration coefficient in concrete with low w/c.

Salt frost scaling

1. No difference was found between salt frost scaling of SCC with limestone powder and NC.
2. Larger salt frost scaling for SCC with limestone powder than for NC was found at 28 days' starting age only.

3. The salt frost scaling increased in SCC with blast furnace slag compared with NC without slag.
4. Less salt frost scaling was found for SCC with 12% fly ash and 5% silica fume than for NC without additives.
5. The mixing order had no influence on the salt frost scaling of SCC.
6. Increased air content decreased the salt frost scaling for SCC as well.
7. Salt frost scaling for SCC decreased with age at start of testing.
8. The amount of limestone filler did not affect the salt frost scaling of SCC.
9. Pouring pressure up to 5,5 m did not affect the salt frost scaling of SCC.
10. Less salt frost scaling was observed in SCC with Ignaberga limestone powder than in SCC with Köping limestone powder.

Internal frost resistance

1. The decrease of fundamental frequency and of mass of concrete was significantly larger for NC than for SCC with limestone filler.
2. SCC with 6% air content resisted internal frost better than SCC with 8% air did, which is inconsistent with previous research.

Sulphate resistance

1. No decrease of fundamental frequency (elastic modulus) or mass of any concrete was observed even after 500 days, neither when the concrete was subjected to distilled water, sea water or Sodium Sulphate, 18 g/kg in distilled water.
2. Larger increase in length due to curing 500 days in distilled water, seawater or sodium sulphate, 18 g/kg in distilled water was observed for NC than for SCC with limestone powder.
3. SCC with limestone powder exhibited larger increase of mass due to water uptake after curing in distilled water, seawater or sodium sulphate, than NC did.

Air voids structure

No correlation was found between the structure of the air voids as to explain the different behaviour of SCC and NC related to internal damage due to frost.

Recommendations

1. It is recommended that the same w/c and air content should be used in SCC with limestone filler as in NC in order to maintain the same durability in SCC as in NC.
2. The same amount of cement should be used in SCC with limestone filler as in NC in order to maintain the same chloride migration coefficient in SCC as in NC.
3. A way to lower the chloride migration coefficient is to use 5% silica fume in SCC but in this case the salt frost resistance of the concrete is to be confirmed.
4. The salt frost resistance is maintained in SCC with limestone filler if the air content is held on the same level as in NC.
5. No effect of the mix proportions of SCC with limestone filler on the internal frost resistance after 300 cycles or on the sulphate resistance after 500 days was observed.
6. All other requirements of NC are to be fulfilled for SCC in order to produce durable concrete.

SAMMANFATTNING OCH REKOMMENDATIONER

I denna rapport redovisas laboratorie- och analytiska studier av kloridmigrationskoefficienten, D, definierad av Tang, saltfrostavskalningen, den inre frostbeständigheten och sulfatbeständigheten hos självkompakterande betong, SKB, med ökat innehåll av filler, olika typer av filler och gjutmetoder. Resultaten av studierna av saltfrostavskalning, inre frostbeständigheten, sulfatresistensen och kloridinträngningen hos SKB jämförs med motsvarande egenskaper hos vibrerad betong, VB, med samma vattencementtal, vct = 0.39, och samma lufthalt, 6%. Slutligen ges rekommendationer hur beständig SKB skall produceras. Såväl 28 som 90 dygns ålder används som starttid för försöken. Hållfasthetsutvecklingen hos betongerna, krypning och krympning följdes parallellt. Sex SKB och två VB studerades, samtliga med vattencementtal, vct = 0.39. Betongen förseglades från gjutning till provning. Inverkan av normal och omvänd blandningsordning (filler sist), ökad mängd filler, typ av filler, Köping 500 (varumärke Limus 40) eller Ignaberga 200 (varumärke Limus 15) kalkstensmjöl, ökad lufthalt och ökat hydrostatisk tryck vid gjutning, undersöktes.

Följande slutsatser drogs efter jämförande studier av mekaniska egenskaper, kloridmigrationskoefficienten, D, saltfrostavskalningen, inre frostbeständighet och sulfatbeständighet hos självkompakterande betong, SKB, och vibrerad betong, VB:

Mekaniska egenskaper

1. Tillsats av kalkstensfiller ökade hållfastheten avsevärt även om cementhalten var något lägre i SKB än i VB.
2. Troligen var en mer effektiv packningsgrad hos partiklarna i SKB än hos VB orsaken till den ökade hållfastheten.
3. Krypning och krympning skedde på samma sätt i SKB som i VB.

Kloridmigrationskoefficienten

1. Kloridmigrationskoefficienten var ungefär 60% större i SKB än i VB.
2. I SKB med 5% silikastoft och 12% flygaska var kloridmigrationskoefficienten 60% av den som uppmättes i VB.
3. Vid 90 dygns ålder var kloridmigrationskoefficienten 60% av den som uppmättes vid 28 dygns ålder.
4. Effektivitetskoefficienten för silikastoft jämfört med Portlandcement med avseende på kloridmigrationskoefficienten föreföll ligga kring 1,6.
5. Effektivitetskoefficienten för masugnsslagg jämfört med Portlandcement med avseende på kloridmigrationskoefficienten föreföll ligga kring 1.
6. Effektivitetskoefficienten för flygaska jämfört med Portlandcement med avseende på kloridmigrationskoefficienten föreföll ligga kring 0,2.
7. Självuttorkning kanske spelade en viktig roll för att förklara den låga kloridmigrationskoefficienten vid låga vct.

Saltfrostavskalning

1. Ingen skillnad erhölls mellan saltfrostavskalning hos SKB med kalkstensfiller och VB.
2. Vid 28 dygns startålder erhölls dock något större frostavskalning hos SKB än hos VB.

3. Saltfrostavskalningen var större i SKB med masugnsslagg än i SKB utan masugnsslagg
4. Saltfrostavskalningen var mindre i SKB med 5% silikastoft och 12% flygaska än i SKB utan dessa tillsatsmaterial.
5. Blandningsordningen hade ingen inverkan på saltfrostavskalningen.
6. En ökad lufthalt minskade saltfrostavskalningen även hos SKB.
7. Saltfrostavskalningen för SKB minskade med ökad startålder.
8. Mängden kalkstensfiller i SKB påverkade ej saltfrostavskalningen
9. Gjuttryck upp till 5,5 m påverkade ej saltfrostavskalningen hos SKB
10. Mindre saltfrostavskalning observerades hos SKB med Ingaberga kalkmjöl än hos SKB med Köping kalkmjöl.

Inre frostbeständighet

1. Minskningen av inre egenfrekvensen (elasticitetsmodulen) och vikten var signifikant större hos VB än hos SKB med kalkstensfiller.
2. SKB med 6% lufthalt erhöll bättre inre frostbeständighet än SKB med 8% lufthalt.

Sulfatresistens

1. Ingen minskning av inre egenfrekvensen (elasticitetsmodulen) eller vikten hos någon betong observerades efter 500 dygns lagring i endera avjoniserat vatten, havsvatten eller avjoniserat vatten med 18g/l natriumsulfat.
2. Längdökningen, efter 500 dygns lagring i endera avjoniserat vatten, havsvatten eller avjoniserat vatten med 18 g/l natriumsulfat, var större hos VB än hos SKB med kalkstensfiller.
3. SKB med kalkstensfiller uppvisade en större viktökning än VB efter lagring 500 dygn i endera avjoniserat vatten, havsvatten eller avjoniserat vatten med 18 g/l natriumsulfat.

Luftporstruktur

Inget samband återfanns mellan luftporstruktur och inre förstöring av normal betong till följd frost.

Rekommendationer

1. Det rekommenderas att använda samma vct och lufthalt i SKB som i VB i syfte att bibehålla samma beständighet i SKB som i VB.
2. Samma cementmängd rekommenderas i SKB som i VB för att erhålla samma kloridmigrationskoefficient i SKB som i VB.
3. Ett sätt att minska kloridmigrationskoefficienten i SKB är att använda 5% silikastoft i SKB men i detta fall skall saltfrostavskalningen bekräftas.
4. Saltfrostavskalningen hos SKB med kalkstensfiller bibehålls vid samma lufthalt i SKB som i VB.
5. Efter 500 dygn hade sammansättningen hos SKB ingen inverkan på inre frostbeständigheten eller på sulfatresistensen.
6. Alla övriga krav på VB skall uppfyllas för SKB i syfte att erhålla en beständig betong.

1. INTRODUCTION, LIMITATIONS AND OBJECTIVE

1.1 Introduction

Concrete that does not require any energy for compacting in order to cover the reinforcement or fill out the mould has attracted a great deal of interest in recent years. Swedish experience now exists from 19 full-scale bridges and other full-scale projects with SCC [1]. The technique has also been introduced for dwelling houses and office buildings [2]. Recently SCC has been introduced for the production of poles, piles and pillars [3], Appendix 1.

Regarding concrete under severe circumstances for the construction of bridges, dams, tunnels and so forth, the requirements of durability are greater. Therefore a higher level of documentation is required for concrete under severe conditions than for concrete that is used for dwelling houses or office buildings. The primary durability properties are salt frost scaling, internal frost resistance, sulphate resistance and chloride ingress for concrete under severe situations. In this project the objectives were to investigate the chloride migration coefficient, D, defined by Tang, to determine the salt frost scaling, the internal frost resistance and the sulphate resistance of SCC that contains increased amount of filler, different types of casting and air content and to compare the result of salt frost scaling, internal frost resistance, sulphate resistance and chloride ingress of SCC with the corresponding properties of normal concrete, NC, with the same water-cement ratio.

1.2 Limitations

The testing of the chloride migration coefficient, D, internal frost resistance, sulphate resistance and salt frost scaling started at both 28 and 90 days' age. Eight concretes were studied, 2 normal concrete, NC, and 6 self-compacting concrete, SCC, all with water-cement ratio, w/c = 0.39 (c was defined as Portland cement). The concrete was sealed from casting until testing. All the specimens were core-drilled from a larger specimen of concrete. In this way the effects of bleeding, carbonation, concrete skin, crazing, segregation and so forth were avoided. The following parameters were studied:

1. Normal and reversed order of mixing (filler first or last).
2. Different filler amount (low or high).
3. Limestone powder of old or young type from the geological point of view (≈ 200 or 20 million years old).
4. Different air content (normal or increased air-entrainment).
5. Hydrostatic pressure on the fresh concrete mass.
6. Different ambient environment such as fresh water, sea water, salt water, sulphate water, frost cycles or 5°C.

1.3 Objectives

The objectives of the project was to investigate the chloride migration coefficient, D, defined by Tang [4], to determine the salt frost scaling, the internal frost resistance and the sulphate resistance of SCC that contains increased amount of filler. The results were to be compared with the corresponding durability resistance components of NC.

2. PREVIOUS RESEARCH

2.1 Effect of w/c on the chloride migration coefficient, D

Figure 2.1 shows the chloride migration coefficient, D, of SCC with quartzite filler and of NC. All concrete mixes contained Slite Standard Portland cement except for concrete with w/c = 0.27, in which the low-alkali Portland cement Degerhamn was used, Appendix 2.1. The mix compositions of the concrete of series 1 are given in Appendices 2.2-3. The measurement was performed with a Rapid Test Method developed by Tang at Chalmers Technical University [4]. The results of the measurement are shown in Figure 2.1 and Appendix 2.4. For SCC with w/c = 39%, the chloride migration coefficient, $D = 14 \cdot 10^{-12}$ m^2/s was obtained.

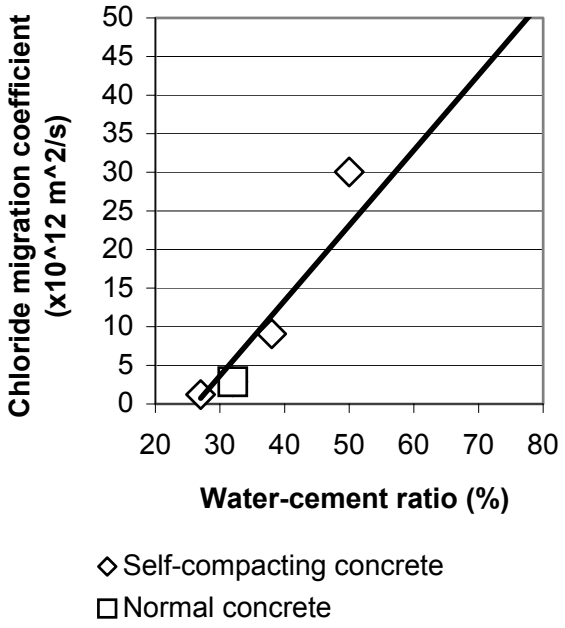

Figure 2.1 - The chloride migration coefficient, D versus w/c.

The following expression for the chloride migration coefficient, D at 3 years' age was obtained (10^{-12} m^2/s, w/c in%), c:

$$D = (0.97 \cdot w/c - 25) \cdot 10^{-12} \text{ m}^2/\text{s}$$

$$\{0.27 < w/c < 0.80;\ R^2 = 0.96\} \quad (2.1)$$

2.2 Effect of additives on the chloride migration coefficient

The chloride migration coefficient, D, was studied for 3 Portland cement concretes and one silica fume concrete Figure 2.2 [5]. The mix proportions are found in Appendix 2.5. The chloride migration coefficient, D, was greatly decreased in concrete with silica fume.

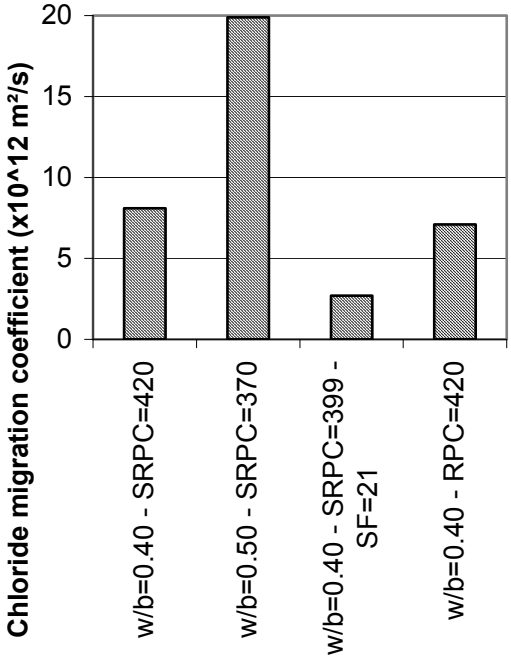

Figure 2.2. - The chloride migration coefficient, D, for NCs with different cement types and 5% silica fume, w/b=0.4-0.5 [5].

For Portland cement based concrete the active porosity was found to be significantly lower when 5% of the cement was replaced by silica fume compared with a pure Portland cement based concrete with the same water-

binder ratio [6]. Two different concrete mixes based on the different cements and pozzolans having the same active porosity can have very different shape of the pore system, therefore resulting in different tortuosity factors [6]. The relation between the binding capacity of chlorides and the cement content follows the same pattern as the relation between the tortuosity factor and porosity, i.e. for the same type of cement and Pozzolan based concrete with different water-binder ratios the binding capacity decreases with the cement content [6].

The electrical conductivity was studied on concrete discs of NCs for the Great Belt Link [7-9]. The mix proportions of the experiment are given in Appendix 2.6. Especially in silica fume concrete the conductivity of NCs was reduced substantially [8]. The effect of fly ash on the electrical conductivity in Portland cement concrete was unclear [8], Figure 2.3.

In another project 4 types of SCCs and one NC for marine environment were studied, Figure 2.4 [10]. The mix proportions of the concrete of series 2 in the experiment are given in Appendix 2.7. A large decrease of the chloride migration coefficient, D, was observed when using slag cement or silica fume concrete. Also in this case the effect on the chloride migration coefficient, D, of fly ash in Portland cement concrete was found to be unclear [10]. When using as much as 68% slag of the slag cement, the chloride binding ability of the concrete increased and therefore a low chloride migration coefficient, D, was found, Figure 2.4 [10].

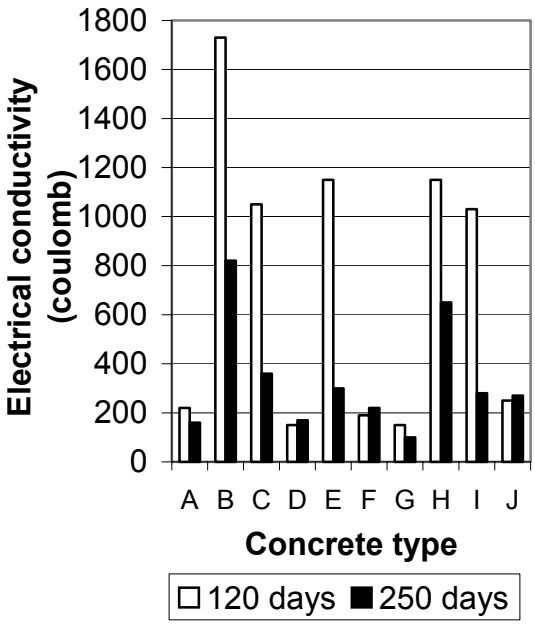

Figure 2.3 - Electrical conductivity for concrete discs of NCs for the Great Belt Link [7-9]. Notations: A-E = SRPC (sulphate resistant cement); F-J = RPC (rapid cement); A = PFA (fly ash) + SF (silica fume); C, E = PFA; D = SF; G = PFA (fly ash) + SF (silica fume); I = PFA; J = SF [7-9].

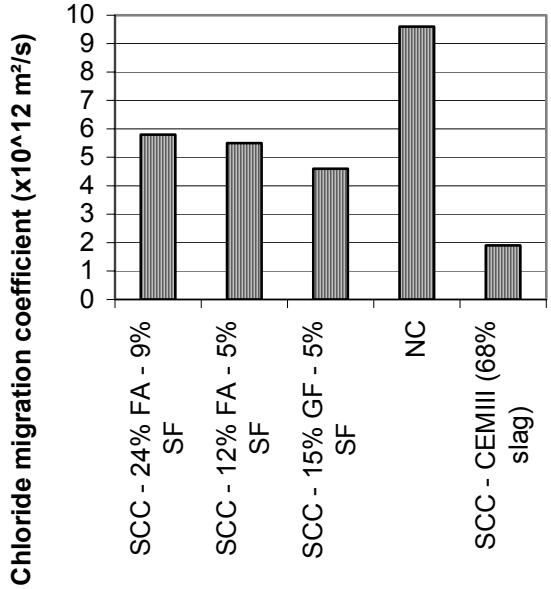

Figure 2.4 - The chloride migration coefficient, D, for SCC with additives [10]. FA = fly ash; SF = silica fume.

An extensive summary of the effect of additives on the chloride migration coefficient is given in [11-12] also taking into account w/c, Figures 2.5-6. It is quite clear that silica in concrete decreased the chloride migration coefficient substantially as compared to the chloride migration coefficient in concrete without silica fume, Figure 2.5. The concrete in the study was non-exposed and studied after 6 months. The effect of the cement type on the chloride migration coefficient seemed to be minor in comparison to the effect of 5% silica fume. Still the effect of the water-binder ratio dominated the chloride migration coefficient [11].

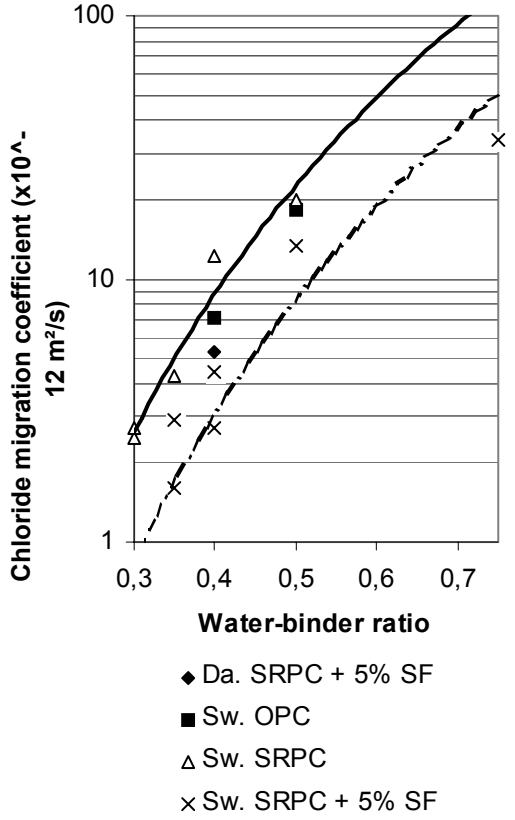

Figure 2.5 - Chloride migration coefficient in concrete without silica fume (full line, above) and in concrete with 5% silica fume (dotted line, below) [11-12].

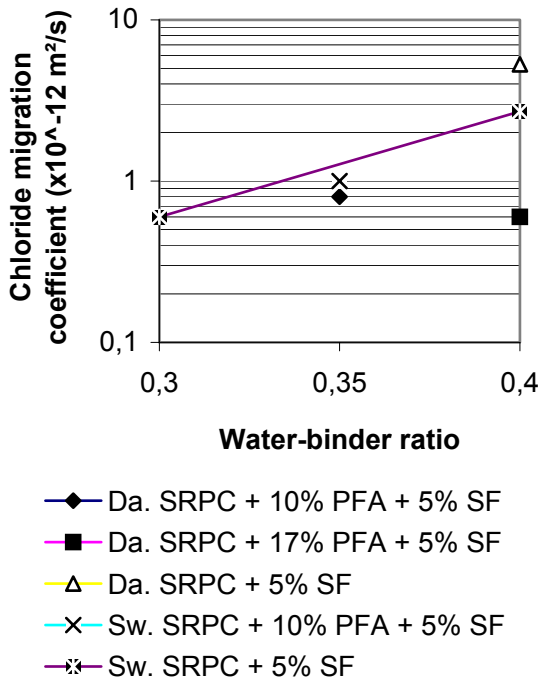

Figure 2.6 - Chloride migration coefficient of concrete with 5% silica fume and varying amount of fly ash [11-12].

At water-binder ratios varying between 0.3 and 0.4 it seemed as if it was an advantage to add about 17% fly ash in concrete with 5% silica fume in order to further decrease the chloride migration coefficient [11-12], Figure 2.6. At 10% addition of fly ash in the concrete the effect was more dubious [11-12], Figure 2.6.

In resource-saving concretes a lot of the cement was replaced by silica fume and fly ash, Figure 2.7 [13]. Even though the water-binder ratio (1:1) was larger in concrete with additives the chloride migration coefficient was substantially lower, less than one third of that of concrete based on pure Portland cement, one fourth with 40% fly ash and 5% silica fume [13], Figure 2.7.

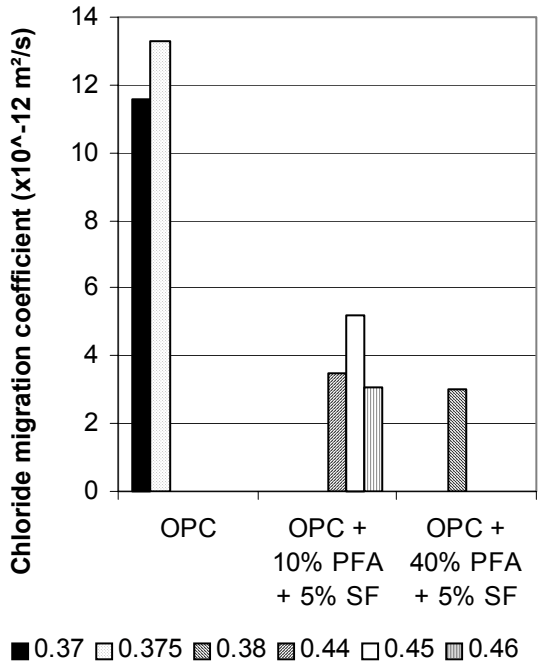

Figure 2.7 - Chloride migration coefficient of resource-saving concretes with cement replaced by silica fume and fly ash at different water-binder ratios (1:1) [13].

2.3 Effect of self-desiccation and time on the chloride migration coefficient, D

Buenfeld [14] called attention to the detail that chlorides could not be transported in air. During self-desiccation in concrete with low w/c, chlorides may be transported from the surface of the concrete to the depth of liquid water front but no further since the pores at self-desiccation are partly disconnected by air-filled voids. For concrete presently being used in severe environments, i.e. with low w/c $\leq$ 0.40, this depth of water ingress varies from 2 cm up to 5 cm even after 7 years of exposure, Figure 2.5 [15-17].

Over 7 years the value of the chloride migration coefficient, D, decreases substantially as compared to the initial value at young age. Hydration products will occupy all space in the concrete since the volume is limited for those to increase at low w/c [18]. The shortage of space in concrete with low w/c will actually stop both hydration and chloride ingress hand in hand with the effect of self-desiccation in the cover layer of the reinforcement. The cover layer of reinforcement exceeds 5 cm in severe conditions, Figure 2.8 [19]. As close as 10 mm from the exposed surface there seemed to be a substantial self-desiccation even after 2 years.

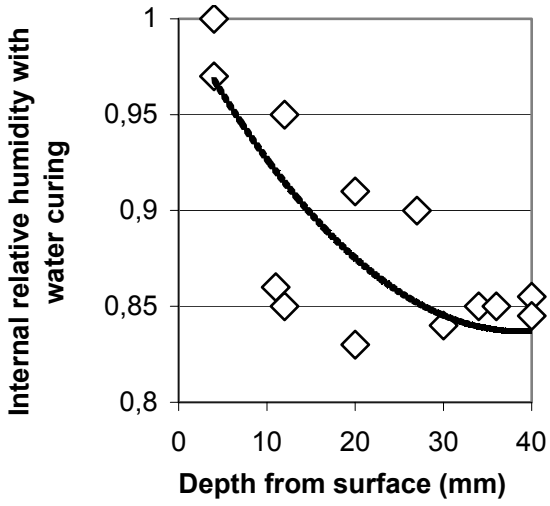

Figure 2.8 - RH measured after 2 years vs depth from water-cured surface (w/b=0.4, 5% SF) [16].

The question was whether the self-desiccation would be only temporary and the pores finally saturated also by chlorides. A 7-year study of the effect of ageing on self-desiccation is shown in Figure 2.9 [20]. The following equations apply to self-desiccation [20]:

$$RH(t,w/c)_s = 1.13\cdot[1-0.065\cdot\ln(t)]\cdot \cdot(w/c)^{0.24\cdot[1-0.1\cdot\ln(t)]}$$

$$\{0.22<w/c<0.58;\ R^2=0.76\} \qquad (2.2)$$

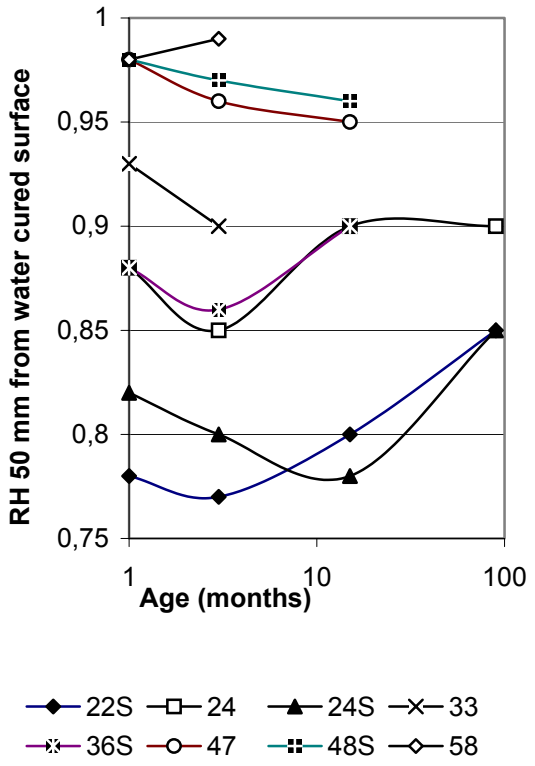

Figure 2.8 - RH at a depth of 50 mm from the free water vs age. R = normal; S = 10% silica fume; 20 = w/c (%) [20].

$$RH(t,w/c) = 1.09\cdot(w/c)^{0.17\cdot(1+0.0451\cdot t)}$$

$$\{0.22<w/c<0.58;\ R^2=0.54\} \qquad (2.3)$$

t denotes the age ($1<t<15$ months)
s denotes 10% silica fume

c denotes cement content (kg/m^3)
w denotes water content (kg/m^3)

$$RH(wbr_{eff}, t) = 0.38\cdot[w/(c+2\cdot s)+2.4 -0.1\cdot lnt]+\Delta RH_{sl}$$

$$\{R^2= 0.83\} \qquad (2.4)$$

t denotes the age ($1<t<1000$ days)
wbr_{eff} denotes water to equivalent cement ratio ($0.22<w/(c+2\cdot s)<0.38$)

ΔRH_{sl} = - 0.035 for 5-10% silica fume slurry at age, $t \leq 28$ days

In another long-term study the 17-year effect of ageing on the chloride diffusion coefficient was shown on the Farø Bridge, Denmark [21], Figure 2.9. The concrete with 12% fly ash but no silica fume had a water-binder ratio, w/b = 0,42 (1:1).

According to measurements on drilled cores by grinding the chloride diffusion coefficient remained at about 0.7 x 10^{-12} m²/s even after 17 years. The chloride ingress was then 40 mm at 0.1% chloride content (the cover layer of the concrete being 50 mm). The surface chloride content was not affected by ageing, about 1% chlorides in the concrete surface [21].

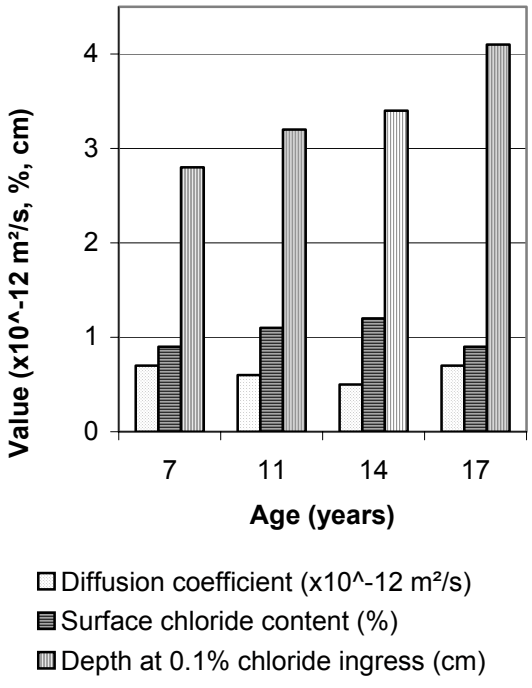

Figure 2.9 - The 17-year effect on the chloride diffusion coefficient at the Farø Bridge, Denmark [21]. Surface chloride content and depth at 0.1% chloride content are shown [21].

Reinforcement corrosion owing to chloride ingress will normally be slowed down by use of High Performance Concrete, HPC, with sufficiently low w/b < 0.40, an adequate concrete cover provided that the surface is free from cracks [22]. Formulas in general used for estimating the chloride ingress were introduced some 30 years ago for water-saturated structural concrete in use at that time, i.e. with w/c > 0.40. These formulas do not account for self-desiccation since concrete with sufficiently low w/c was not in use at the time [23].

A great step in the understanding of the chloride migration coefficient, D, in NC with w/c > 0.40 was taken when the binding capacity related to the cement content was clarified [24]. Rapid tools for examining concrete were a great advantage when optimising concrete in use under severe conditions in sea [25]. Different models for estimating chloride ingress were put forward but still the relation to self-desiccation was not considered nor understood [26,27].

2.4 Salt frost scaling

The general effects of concrete constituents on the chloride ingress are given in an overview [28]. The effects of the following parameters on the salt frost scaling of concrete after 56 cycles were studied, Figure 2.10:

1. Air content (%)
2. Fly ash (%)
3. Specific surface of air voids (1/mm)
4. Silica fume (%)
5. Water-binder ratio (x10)

The following general equation was found from Figure 2.10:

$$P = a \cdot \ln(Sc) + b \qquad (2.5)$$

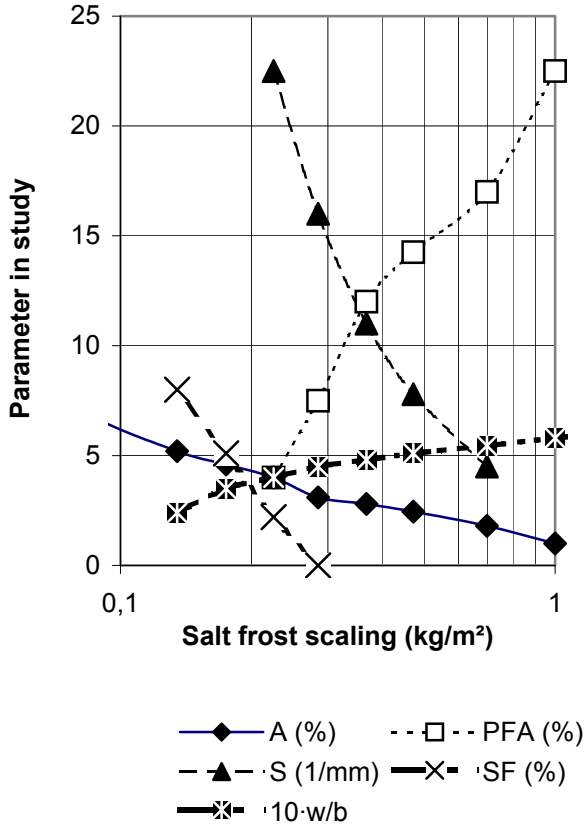

Figure 2.10 - Effect of air content (%), fly ash (%), specific surface of air voids (1/mm), silica fume (%) and water-binder ratio (x10) on the salt frost scaling of concrete [28].

a denotes constants given in Table 2.1
b denotes constants given in Table 2.1
P denotes the value of the parameter
Sc denotes salt frost scaling (kg/m²)

Table 2.1 - Constants of equation (2.5)

P	A	PFA	S	SF	10w/b
Sort	(%)	(%)	/1/mm)	(%)	-
a	-2.78	11.8	-15.6	-10.8	1.23
b	0.28	22.3	-2.8	-13.7	5.70

The salt frost scaling increased with increasing amounts of fly ash and at higher w/b but decreased with all other parameters such as higher air content, higher silica fume content and with a larger specific surface of the air voids.

The salt frost scaling of concrete with pure Portland cement, OPC, and of concrete with additives was compared [13], Figure 2.11. Concrete with OPC contained 4% air, concrete with 10% fly ash, PFA, and 5% silica fume, SF, 6.2% air and concrete with 40% fly ash and 5% SF 5.2% air.

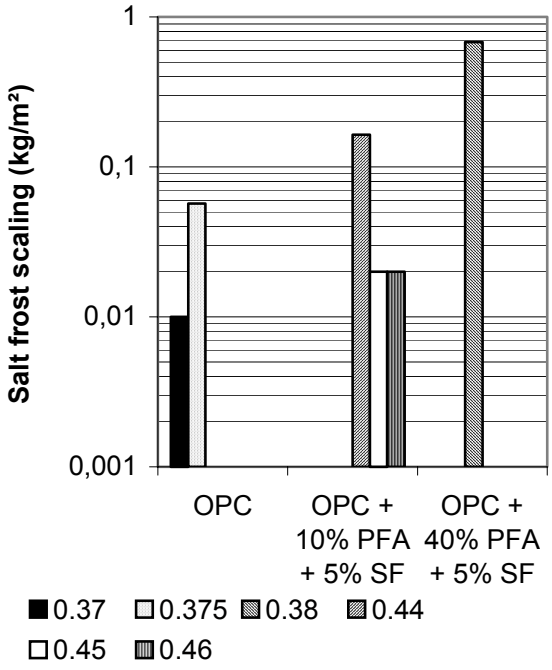

Figure 2.11 - Salt frost scaling of concrete with pure Portland cement and of concrete with additives was compared [13]. The water-binder ratio, w/b, is given.

However, the increase of salt frost scaling shown in Figure 2.11 for concrete with additives may also be as a result of an increasing w/b. At about w/b = 0.38 the salt frost scaling of concrete with 40% fly ash and 5% silica fume (5.2% air content) was 20 times that of concrete with pure Portland cement (4% air content) [13], which more or less confirms the results of [28], Figure 2.10. In another study the effect of fly ash, ground blast furnace slag and silica fume on the salt frost scaling was investigated [10]. Appendix 2.7 shows the mix proportions of the concrete of series 2 in this study and the saltfrost scaling. The air content of all the studied concrete was close or equal to 6%. Salt frost scaling increased in concrete with large amounts of slag compared with the corresponding scaling of Portland cement concrete, Figure 2.11 [10].

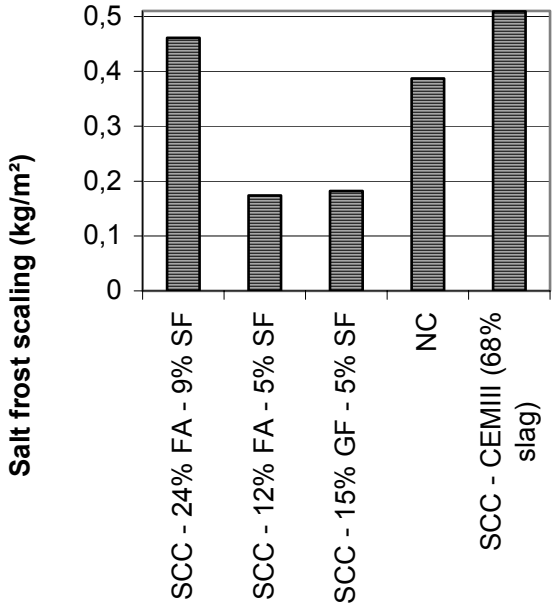

Figure 2.11. - Salt frost scaling of SCCs with additives [10]. FA = fly ash; GF = glass filler; SF = silica fume [10].

However, for concrete with 12% fly ash and 5% silica fume as calculated on the cement content, less salt frost scaling was observed than for a normal concrete without these additives. For 24% fly ash and 10% silica fume larger salt frost scaling was obtained than for the normal concrete, Figure 2.11. It must be underlined that the salt frost scaling of concrete to a great degree depends on the air void system created in the concrete. The salt frost scaling is not only dependent on the type of binder.

Salt frost scaling and internal frost resistance of SCC and NC were also studied by Rougeau, Maillard and Mary-Dippe [29]. Mix composition, properties, salt frost scaling and fundamental transversal frequency from this investigation are shown in Appendix 2.8. The fundamental transversal frequency gives a measurement of dynamic elastic modulus, which in turn is a measurement of the internal damage caused by frost, Appendix 2.8. The following conclusion were drawn by Rougeau, Maillard and Mary-Dippe [29]:

1. The salt frost scaling and the loss of fundamental transversal frequency were much larger for NC than for SCC [29].
2. The salt frost scaling increased with time for NC but remained constant for SCC at 0.9 kg/m², which was obtained after just 28 cycles [29].
3. NC exhibited a total loss of the internal solidity after 150 frost cycles while SCC lost only 7% of the cohesion (elastic modulus) during the corresponding period of time [29].
4. After 300 frost cycles the decline of the elastic modulus was only 12% of SCC [29].

Most probably the vibration technique used for the compaction of the specimen more or less damaged the air void system in NC [29]. In SCC, however, the entrained air was unaffected since no vibration was used in this kind of concrete. The salt frost scaling of concrete with pure Portland cement (CEM I) and that of concrete with cement CEM II (14% limestone filler) was compared [30], Figure 2.12.

The water-binder ratio, w/b, varied between w/b = 0.42 for concrete with pure Portland cement and w/b = 0.43 for concretes with limestone filler. The air content varied as follows:

1. Concrete with pure CEM I: 5.8% air
2. Concrete with CEM I + 13% PFA + 5% SF: 5.4 % air
3. Concrete with CEM II: 5.8% air
4. Concrete with CEM II +13% PFA + 5% SF: 7.2 % air

No significant effect of limestone filler in concrete on salt frost scaling was observed (CEM I and CEM II) [30]. Concrete with CEM I, 13% PFA and 5% silica fume exhibited a substantial increase of salt frost scaling as compared to concrete with no additives. The effect of additives in concrete on the salt frost scaling of concrete with CEM II could not be settled since the air content was not kept constant [30].

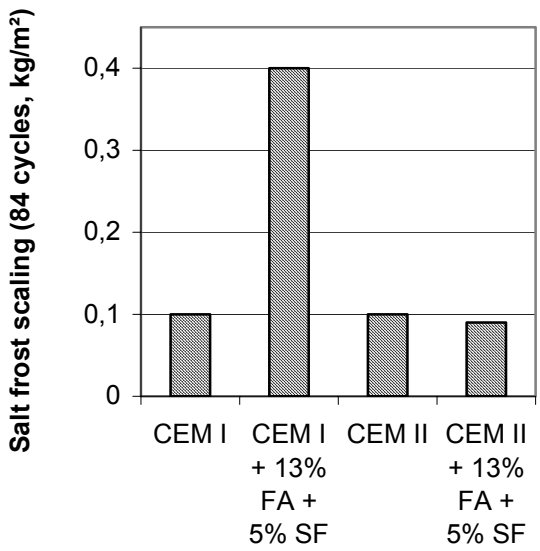

Figure 2.12 - Salt frost scaling of concrete with pure Portland cement (CEM I) and of concrete with cement CEM II (14% limestone filler) [30].

Salt frost scaling after 56 frost cycles at 28 days' starting age of concrete with 5% silica fume, SF, or with 30% blast furnace slag was compared with that of concrete without additives (pure OPC). All concrete had 4.6% air content [31]. Figure 2.13 shows salt frost scaling after 56 cycles [31] as a function of the water-binder ratio, w/b (1:1).

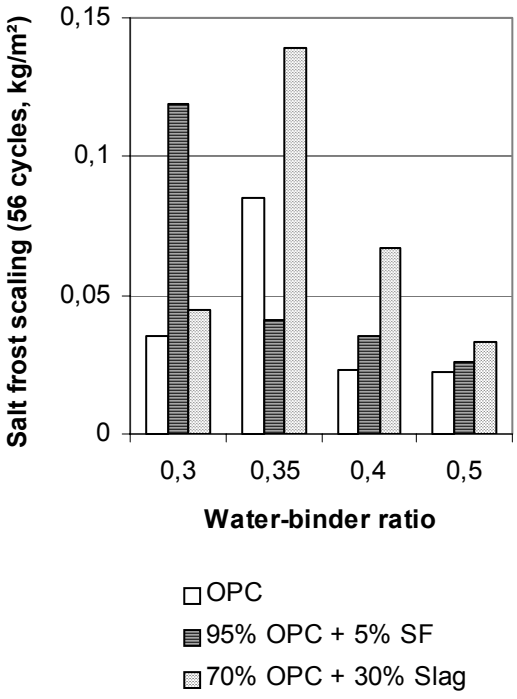

Figure 2.13 - Salt frost scaling after 56 cycles [31] as a function of the water-binder ratio, w/b, of concrete with pure OPC, additives of either 5% silica fume, SF, or 30% blast furnace slag (air content 4.6%) [31].

Generally, the salt frost scaling decreased with w/b, which is astonishing since the general trend demonstrated by [28] was an increasing salt frost scaling with w/b. At w/b = 0.35 the salt frost scaling of concrete with OPC was about 4 times that of concrete with w/b = 0.5. At w/b = 0.35 the salt frost scaling of concrete with 5% SF was about half that of concrete without silica fume, SF. Concrete without SF exhibited larger salt frost scaling than concrete with 5% SF at w/b = 0.3, 0.4 and 0.5. On average concrete with 5% SF obtained about 35% larger salt frost scaling than concrete with pure OPC (concrete with 30% slag obtained about 70% larger scaling on average than concrete with pure OPC). As related to strength the salt frost scaling seemed to be increasing at higher strength (the air content was kept constant at about 4.6%, Figure 2.14. Concrete with 30% slag and 85 MPa strength (w/b = 0,35) obtained three times the frost scaling of concrete with 30% slag and 90 MPa strength (w/b = 0.3), which may be an effect of self-desiccation. Self-desiccation is much more pronounced at low w/b. However, for concrete with 5% silica fume the opposite results were found: at w/b = 0.30 (100 MPa strength) the salt frost scaling was about three times that of concrete with w/b = 0.35 and about 90 MPa strength.

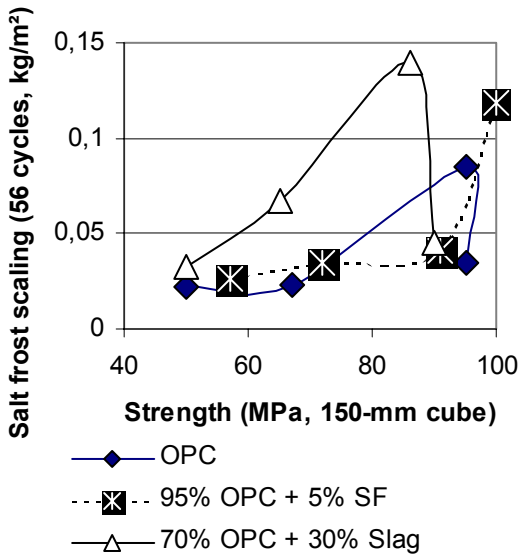

Figure 2.14 - Salt frost scaling after 56 cycles of concrete with pure OPC, 5% silica fume, SF, or 30% blast furnace slag (air content 4.6%) [31].

Recently the water absorption after capillary suction or 56 salt frost tests, the loss of internal elastic modulus and the sulphate resistance of self-compacting concrete with different amount of filler were studied [32]. The fillers in use were fly ash, PFA, or silica fume, SF or combinations of these two additives. No air-entrainment was used in the concrete (about 1.5% natural air content at higher water-binder ratio, w/b, and about 3% air content at low w/b. As expected, the water-absorption increased with larger w/b, Figures 2.15-16 [32]. However, in concrete with more additive of fly ash less absorption was observed. Probably the structure became denser due to the pozzolanic interaction between OPC and fly ash.

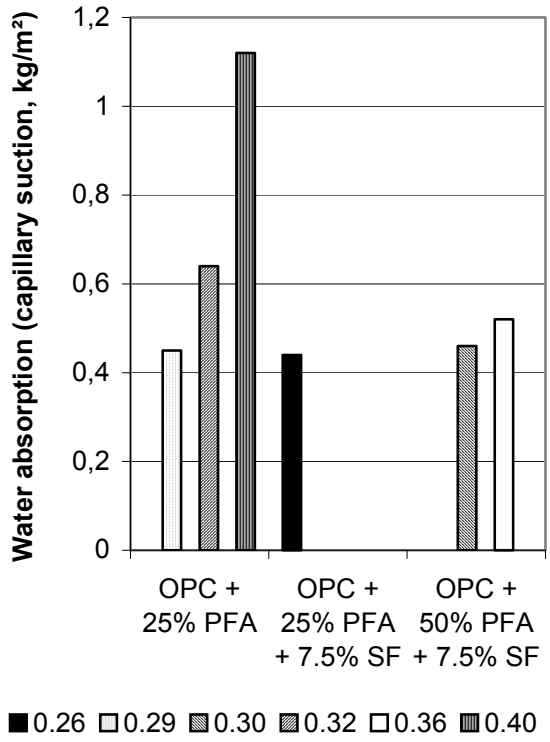

Figure 2.15 - The water-absorption (capillary suction) decreased with larger amount of fly ash [32]. The water-binder ratio is given.

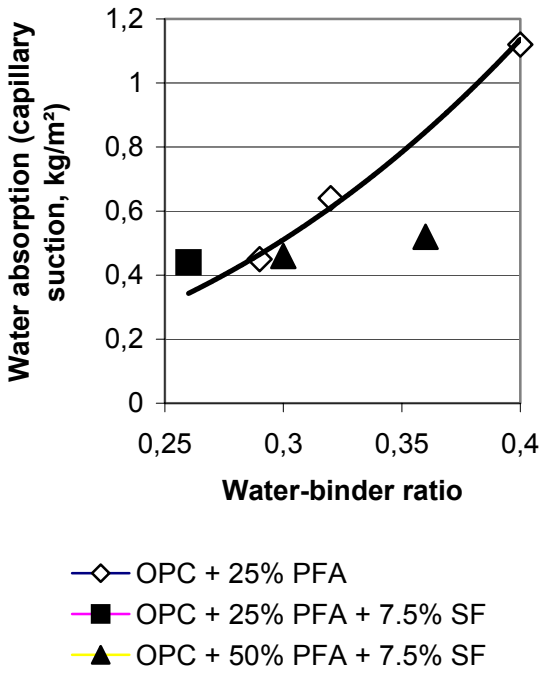

Figure 2.15 - The water-absorption increased with larger water binder ratio [32].

The salt frost tests were performed according to [33], Figures 2.16-17.

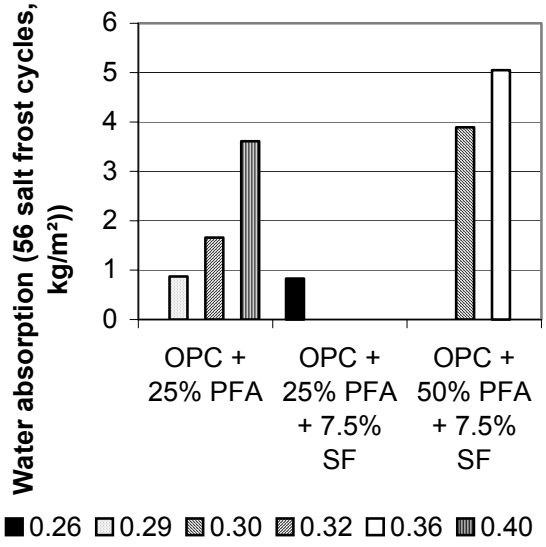

Figure 2.17 - The water-absorption (after 56 salt frost cycles) increased with larger amount of fly ash [32]. The water-binder ratio is given.

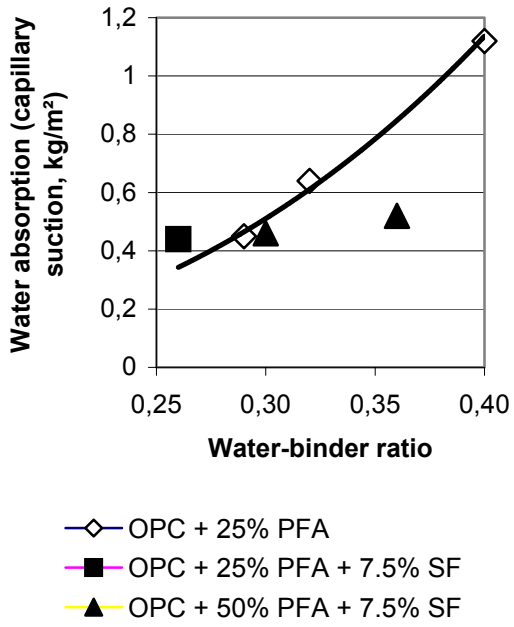

Figure 2.18 - The water-absorption (after 56 salt frost cycles [33]) increased with the water binder ratio and with larger amount of fly ash [32].

Since no air-entrainment was used in the concrete the denser structure with more fly ash (50% instead of 25%) caused larger expansion during the frost cycles followed by larger water absorption [32]. The relative elastic modulus of concrete after 56 frost cycles was also examined [32], Figure 2.19-20. Evidently the large water absorption of concrete with 50% fly ash or with w/b = 0.4 caused large internal destruction in order to withstand salt frost attacks (the concrete did not contain air-entrainment). As shown in Figure 2.20, it seems as if concrete at low w/b < 0.30 did not require any air-entrainment at all in order to withstand 56 salt frost cycles, which also was indicated by [34]. In this case the self-desiccation of the concrete probably prohibited internal expansion large enough to damage the concrete. On the other hand, the loss of elastic modulus was very large in concrete with 50% fly ash despite a low w/b = 0.3.

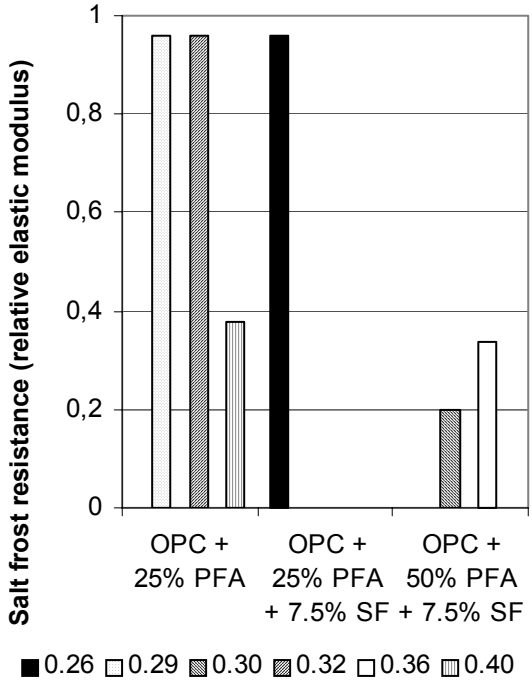

Figure 2.19 - Relative elastic modulus of concrete after 56 frost cycles [32]. The water-binder ratio is given.

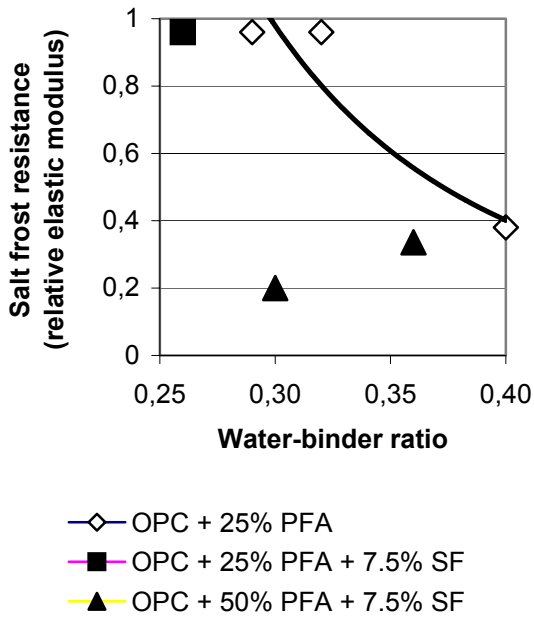

Figure 2.20 - The relative elastic modulus of concrete after 56 frost cycles versus the water-binder ratio [32]. The amount of additives is given.

2.5 Sulphate resistance

The sulphate resistance after 30 d in pH = 2 was estimated according to [32,35]. Figures 2.21-22 show the dependence of additives and water-binder ratio on the sulphate resistance [32]. The mass loss increased at low w/b since the cement content was larger in this case [32]. The High Performance Concrete was not better during sulphate attack than the reference concrete. No difference was found between resistance to sulphate attack of concrete with 5% silica fume and concrete without silica fume [32]. Concrete with sulphate-resisting cement showed considerably worse durability than concrete with normal Portland cement [32]. The self-compacting concrete with high amount of fly ash showed the best resistance to sulphate attack at pH = 2.

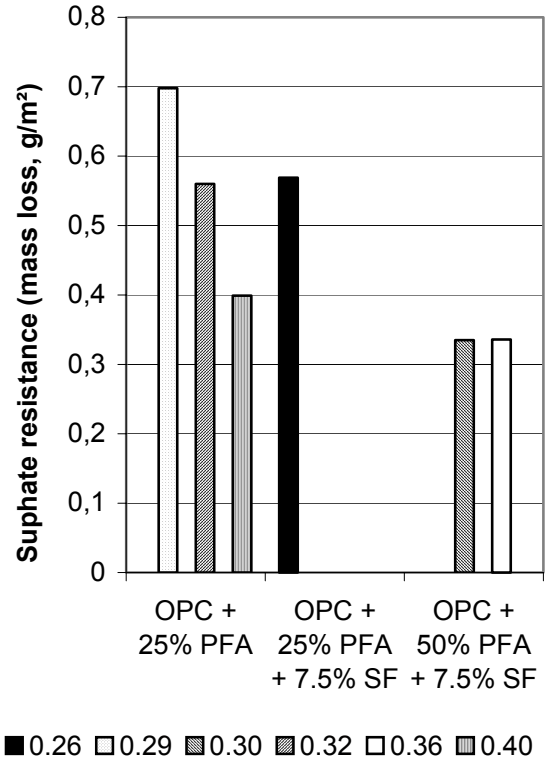

Figures 2.21 - Dependence of additives on the sulphate resistance [32]. The water-binder ration is given.

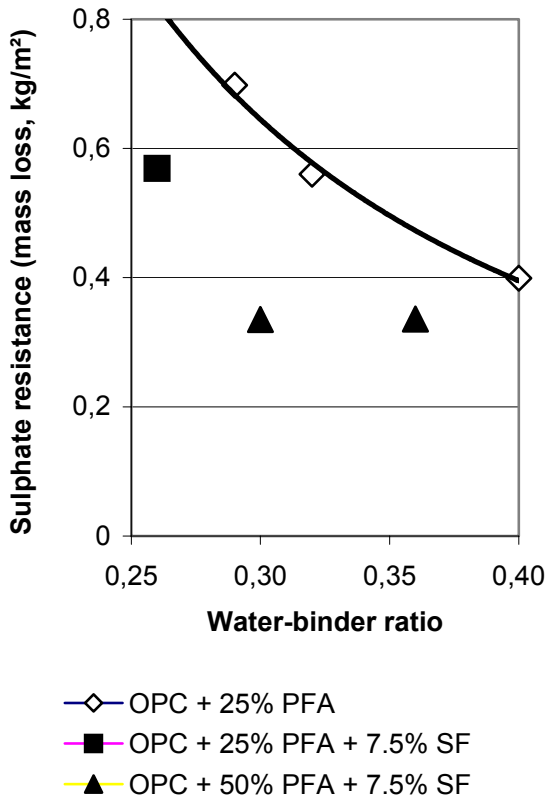

Figures 2.22 - Dependence of the water-binder ratio on the sulphate resistance [32].

3. MATERIALS, MANUFACTURE AND METHODS

3.1 Material

Crushed gneiss (E-modulus 61 GPa and strength 230 MPa), natural sand, limestone filler Köping 500 (branch Limus 40) or Ignaberga 200 (branch Limus 15) and Degerhamn cement were used in the mix compositions, Appendices 2.1 and 3.1. Melamine-based superplasticiser was used for NC (branch Flyt 97M), polycarboxyl ether for SCC (branch Glenium 51) and air-entertainment agent based on fir oil and fatty acids (branch Microair).

3.2 Manufacture of specimen

3.2.1 Durability properties

Manufacturing and curing of the large specimen of concrete (until the test specimen were core drilled) were performed in the following way:

1. New mixing order (N) with material except for filler mixed for ½ min. with water and air-entertainment.
2. Then half the amount of superplasticiser mixed for ½ min.
3. Finally the remaining superplasticiser with filler mixed for 2 min. [36].
4. Ordinary mixing order (O) with all dry material at the start mixed for ½ min. with water and air-entertainment.
5. Then all the material with the superplasticiser mixed for 2½ min.
6. Casting of large specimen in steel mould with 0.23 m in diameter and 0.3 m or 6 m in height filled with concrete.
7. NC vibrated 10 + 10 + 10 s.
8. SCC was not vibrated.
9. Sealed curing at 20 °C until the specimens were core-drilled from the large specimen.

From the pour the following specimens were cored at 28 and 90 days' age:

1. For determination of the chloride migration coefficient, D: 3 discs 100 mm in diameter and 50 mm in height [4].
2. For salt frost scaling: 3 discs 94 mm in diameter and 40 mm in height
3. For determination of the internal frost resistance, sulphate resistance and performance in sea water or fresh water, 3 cylinders 50 mm in diameter and 150 mm in height
4. When testing the effect of hydrostatic pressure the specimen was cored 0.5 m from the bottom of the 6 m long specimen
5. Between drilling and testing the cylinders were stored in water saturated by adding limestone powder.

3.2.2 Mechanical properties

Specimens for mechanical tests were obtained in the following way:

1. Ordinary mixing order (O) with dry material at the start mixed for ½ min. with water and air-entertainment
2. Then all the material with the superplasticiser mixed for 2½ min.
3. Casting of cubes 100 mm and cylinder specimen 100 mm in diameter and 500 mm in length in steel mould with concrete.
4. NC vibrated 10 + 10 + 10 s.
5. SC was not vibrated.
6. Sealed curing or air curing at an ambient relative humidity, RH = 60% until testing of strength, creep and shrinkage.

3.3 Methods

3.3.1 Determination of the chloride migration coefficient, D

Between drilling and rapid testing the specimens were stored in water saturated with limestone powder. The determination of the chloride migration coefficient, D, was performed in an apparatus developed by Tang, Appendix 3.2 [4]. After sawing, brushing and washing away any burrs from the surface of the specimen, excess of water was wiped off the surface of the specimen. When the specimens were surface-dry, they were placed in a vacuum container to a pressure in the range of 1-5 kPa within a few minutes, Figure 3.1 [4]. The vacuum was maintained for 3 h, and then, with the vacuum pump still running, the container was filled with water saturated with $Ca(OH)_2$ in order to immerse the specimen. The vacuum was maintained another h before air was allowed to enter the container. The specimen was then kept in the solution for 18 h. The catholyte solution was 10% NaCl (100 g NaCl in 900 g water, about 2 N) and the anolyte solution 0.3M NaOH in distilled water (about 12 g NaOH in 1 l water). The testing procedure was performed in the following way:

1. The catholyte solution, 10% NaCl was poured to fill the 12-l container, Figure 3.2.
2. A rubber sleeve was assembled to the specimen, Appendix 3.2.
3. The specimen were placed on the plastic support in the catholyte reservoir (10% NaCl), Appendix 3.2
4. The sleeve was filled with 300 ml anolyte (0.3 M NaOH), Figure 3.3.
5. An anode was immersed into the anolyte solution, Appendix 3.2.
6. The cathode was connected to the negative pole and the anode to the positive pole of the power supply.

Figure 3.1 - When the specimens were surface-dry, they were placed in a vacuum container to a pressure in the range of 1-5 kPa within a few minutes [4].

Figure 3.2 - The catholyte solution, 10% NaCl filled in the 12-l container.

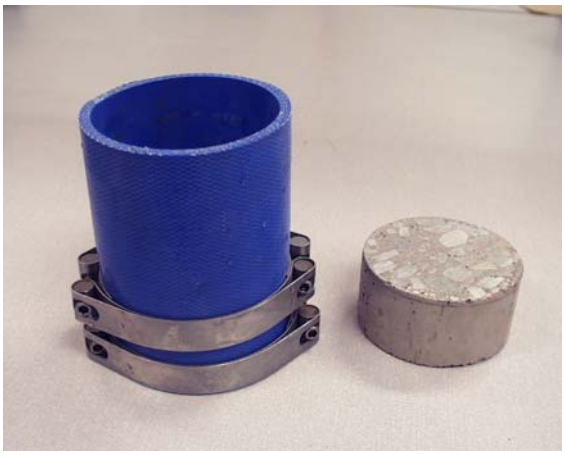

Figure 3.3 - A rubber sleeve was assembled to the specimen [4].

7. The initial current through the specimen was measured with a power supply at 30 V.
8. Voltage was adjusted, Appendix 3.3
9. The temperature in anolyte solution was recorded by thermocouple.
10. The test duration was chosen according to Appendix 3.3.
11. The final current and temperature were recorded before the test was terminated.

The chloride penetration depth was determined in the following way:

1. The specimen was disassemblde in the reverse way of assembly, Figure 3.3
2. The specimen was split into two pieces, Figure 3.4
3. Point-one M silver nitrate solution was sprayed several times on the freshly split specimen, Figure 3.5-7
4. When the white silver chloride precipitation was clearly visible on the surface of the specimen it was measured with an accuracy of 0.1 mm from the centre to both edges at intervals of 10 mm to obtain seven depths, Figure 3.7

Figure 3.4 - The split specimen [4].

Figure 3.5 - Point-one M silver nitrate solution sprayed several times to the freshly split specimen [4].

Figure 3.6 - Test specimen after preparation for chloride penetration depth measurement [4].

Figure 3.7 - Specimen for test of the chloride migration coefficient, D [4].

3.3.2 Resolve of the salt frost scaling

Salt frost scaling was studied by a method previously used by Lindmark [37]. The specimen was placed in a plastic container, fully immersed into 3% NaCl, Figure 3.8. Two frost cycles daily varying between -20 and 20 °C were used, Appendix 3.4. The temperature was held at - 20 °C and + 20 °C internally for 3 h. The tests were started at either 28 or 90 days' age. The salt frost scaling was determined after 28, 56 and 112 frost cycles by weighing.

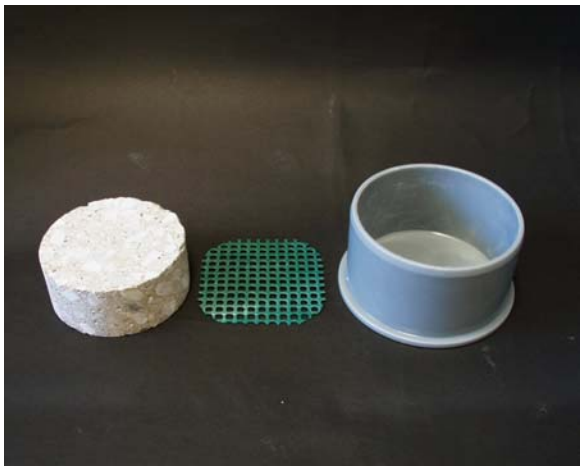

Figure 3.8 - Specimen for tests of salt frost scaling [37].

3.3.3 Determination of the internal frost resistance

The specimen was placed in a rubber container, fully immersed in distilled water, Figure 3.9. Two frost cycles daily varying between -20 and 20 °C were used, Appendix 3.4. The tests were started at either 28 or 90 days' age. The frost scaling was determined after 90 and 300 frost cycles by weighing. The decrease of the elastic modulus due to internal damage was obtained by measurement of the fundamental resonance frequency in a Grindosonic apparatus. The length change of the specimen was measured.

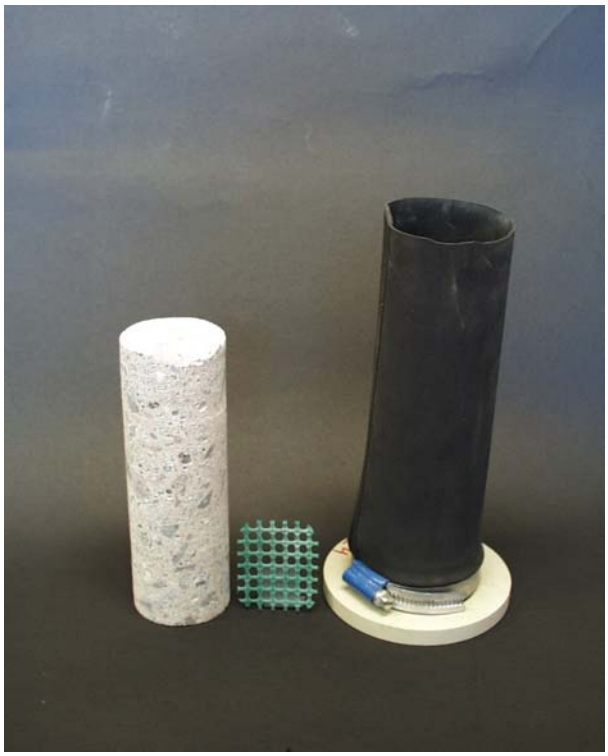

Figure 3.9 - Specimen in a rubber container, immersed in distilled water (internal frost resistance tests) or in a Sodium sulphate solution, 18 g/l distilled water [37], seawater from Barsebäck with 1% NaCl or distilled water (sulphate attack; performance in sea or fresh water).

3.3.4 Resistance to sulphate attack; performance in sea or fresh water

The specimen was placed in a rubber container, fully immersed in a sodium sulphate solution, 18 g/l distilled water [38], sea water from Barsebäck with about 1% NaCl or distilled water, Figure 3.9. The temperature was held constant at 5 °C. The tests were started at either 28 or 90 days' age. Resistance to sulphate attack, performance in sea or fresh water, was determined after 90 and 500 days. The decrease of the elastic modulus due to internal damage was obtained by measurement of the fundamental resonance frequency in a Grindosonic apparatus. The length change of the specimen was measured.

3.3.5 Strength

The cube was measured and tested for compressive strength. The ultimate stress was applied at a rate of 1 MPa/s in a Seidner testing machine. The testing machine was calibrated. The accurate strength would be 1 MPa higher, which is a small error. An eccentricity in placing the cube or the cylinder may have affected the test result. A special gauge was therefore used to centre the cube or the cylinder. The fault of eccentricity was less than 1 mm. The hourglass shape of fragments after testing the cube indicated a highly centric placing. At high strength a circular conical part of the cube remained after testing. The corners of the cube seemed to fail before the ultimate strength was reached.

3.3.6 Shrinkage

Early drying shrinkage up to 1 day's age was obtained on a horizontal specimen with a square size of 100 mm and 400 mm in length, Figure 3.10.

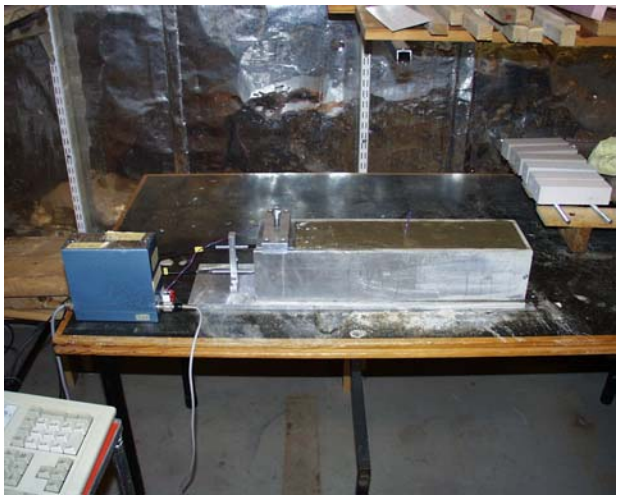

Figure 3.10 - Equipment for shrinkage measurement of up to 1 day's age.

The end of the mould for the specimen was movable and connected to two separate LVDT displacement and gauging transducers collecting data measured the deformations by a separate computer, Figure 3.10. Studies of long-term shrinkage were performed on horizontal (lying) cylinders, Figure 3.11. Adhesive aluminium cloth insulated the autogenous shrinkage specimens. Aluminium cloth was also placed at the ends of the cylinder. The specimens were stored in a 20 °C climate chamber. Some temperature movements took place in the concrete due to hydration, which was compensated for by $1{,}0 \cdot 10^{-5}$/°C. The maximum temperature was 24 °C about 15 hours after casting. After 30 hours the temperature varied between 21 and 20 °C. The cylinders were turned a third of a full turn at each measurement to avoid bending effects. The cylinder was continuously weighed. All the short-term and long-term studies were performed on cylinders (diameter: 100 mm, length: 500 mm). Autogenous shrinkage and drying shrinkage were studied for the same type of cylinders.

Figure 3.11 - Specimen for studies of long-term shrinkage.

3.3.7 Creep

The specimen was sealed or dried at RH = 60% in the same way as the shrinkage specimen. Right before testing of creep the adhesive aluminium cloth at the ends of the specimen was removed. Two-year creep tests on cylinders (100 mm in diameter and 500 mm in length) were performed in traditional mechanical spring-loading devices, Figure 3.12. After demoulding and insulation (in the case of studies of autogenous shrinkage), 6 stainless steel screws were fixed into cast-in items in the cylinder 100 mm from each end. Measurements were taken on three sides of the cylinder on a length of 300 mm within 1 h of demoulding. The specimen was placed in a 20 °C climate chamber with a relative humidity, RH= 60%. Mechanical devices performed the measuring. These studies also provided results on the long-term creep rate and on the elastic modulus. The exact specified loading of the springs was applied at all times of measurement. The loading of the spring device was applied at a rate of 1 MPa/s. The cylinders were weighed before and after the studies.

Figure 3.12 - Long-term creep studies.

The following routine was carried out in the spring-loading device:

1. The first measurements were recorded within 2 minutes of loading by the mechanical device.
2. Loading was manually kept constant for 1 h in the spring-loading devices.
3. A second measurement was recorded.
4. After 1 h the nuts on the screws of the spring-loading were tightened until a 10% decrease of the loading was recorded on the display of the load cell in the device.
5. The decrease of loading on the display corresponded to a constant length between the measurement point when the external loading was removed and only the spring acted.
6. The position of the precision-turned screws in both sealed and drying cylinders was measured.

7. The internal temperature of the cylinders was measured.
8. The loading was applied in the spring-loading devices; one device for a sealed HPC, another for the air-cured HPC.
9. The loading rate was about 1 MPa/s.
10. The age at loading was either 2 d (40% of the 28-day strength) or 28 d.
11. The stress to strength level was 30% of the present strength.
12. After 3 hours 90% of the specified loading of the specimen was applied in the load-cell.
13. The nuts of the screws in the device were loosened.
14. The external loading was adjusted to within $\pm$ 0.05 kN.
15. The measurement was recorded between the 6 screws on both the cylinders.

3.3.8 Air void structure

Some of the concrete (mix proportions KN, KO, KOT and RO I) was studied as related to the air void structure [37]. Three specimens, 100 mm in diameter, from the same pour of concrete that was used for the other studies, were prepared to study the air voids system. Reduction was performed as related to air at the rim of the specimen.

4. RESULTS ON MECHANICAL PROPERTIES, CHLORIDE MIGRATION COEFFICIENT AND SALT FROST SCALING

4.1 Mechanical properties

4.1.1 Grading curves of all solid particles in the fresh mix and strength

The choice of mix composition may be linked to the derived strength and is influenced by the grading curve of all solid particles in the fresh mix composition (silica fume, cement filler, sand, gravel and stone fraction). Figure 4.1 shows the grading curve of the mix composition in the present tests, Appendix 3.1. The strength development of the tests is shown in Figure 4.2 and Appendix 4.1. The following most important points were found from the influence of particle grading on strength of SCC:

1. Gap grading was not feasible.
2. Filler had a large effect on strength
3. The particle distribution could be improved by a suitable choice of the type and amount of filler.

For this investigation the following expression was found for the grading of the particles in the fresh mix:

$$p_m = 0.102 \cdot \ln(d) + 0.583 \qquad \{R^2 = 0{,}96\} \quad (4.1)$$

ln(d) denotes natural logarithm of sieve dimension (0.002<d<10 mm)

p_m denotes the material passing through (by weight)

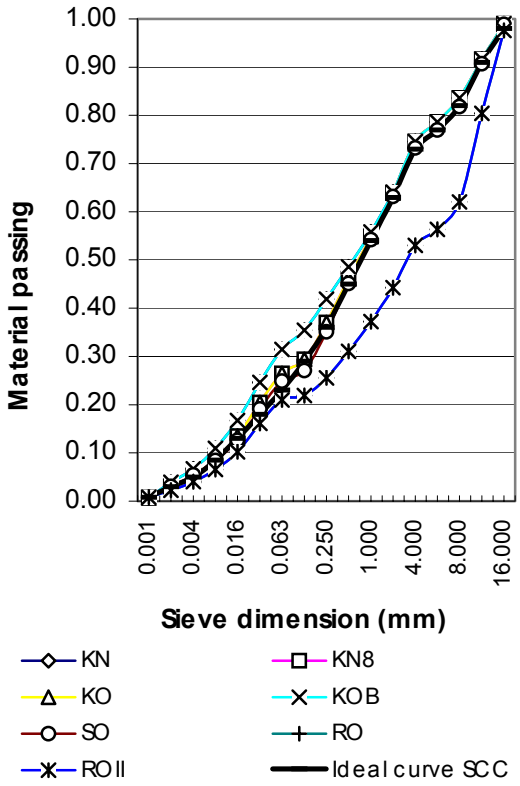

Figure 4.1 – Grading of solid particles in the fresh mix. B = increased amount of filler; K = Köping 500 limestone filler; N = new way of mixing (filler last); O = ordinary way of mixing (filler first); R = reference; S = Ignaberga 200 limestone filler; II = second.

In addition it was found that the following empirical relationships existed between strength and filler content also taking into account the type of filler and the effect of air-entrainment:

$$f_{cc} = k_N \cdot k_S \cdot k_8 \cdot\cdot [(14.6 \cdot p + 12.3) \cdot \ln(t) + 51 \cdot p + 23] \qquad \{R^2 = 0.70\} \quad (4.2)$$

f_{cc} denotes compressive strength (100-mm cube, MPa)

k_N = 0.89 applies for new order of mixing (filler last); k_N = 1 otherwise

k_S = 0.82 applies for Ignaberga 200 limestone filler in these tests; k_S = 1 otherwise

k_8 = 0.74 applies for 8% air content; k_8 = 1 for 6% air content.

ln(t) denotes the natural logarithm of concrete age (1 < t < 100 days)

p denotes content of limestone powder (0.03 < p < 0.15 by vol.)

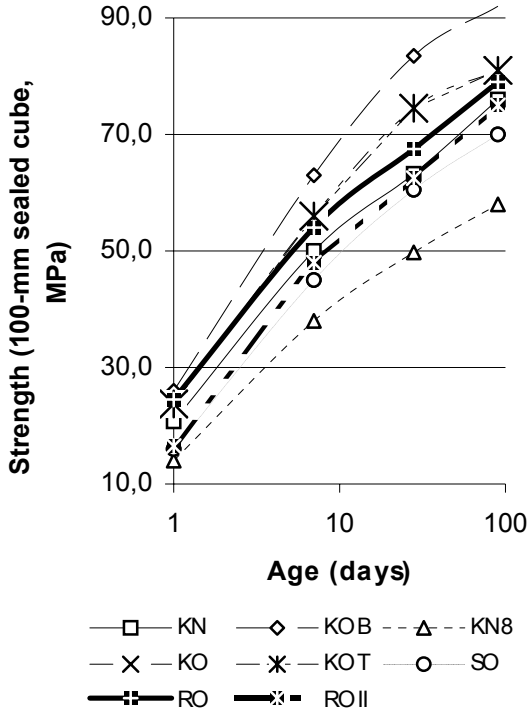

Figure 4.2 – Strength development of concrete in the tests. Notations: B = increased amount of filler; K = Köping 500 limestone filler; N = new way of mixing (filler last); O = ordinary way of mixing (filler first); R = reference; S = Ignaberga 200 limestone filler; T = 5.5 m hydrostatic pouring pressure instead of 0.5 m; II = second reference.

Figure 4.3 shows the strength estimated with equation (4.2) versus the measured one. The agreement was good between the strength estimated with equation (4.2) and the measured strength.

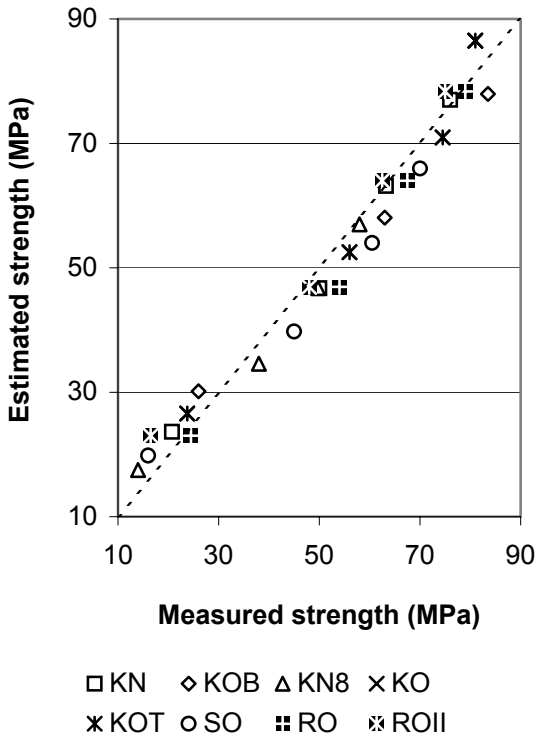

Figure 4.3 – Strength estimated by equation (4.2) vs measured strength. B = increased amount of filler; K = Köping 500 limestone filler; N = new way of mixing (filler last); O = ordinary way of mixing (filler first); R = reference; S = Ignaberga 200 limestone filler; T = 5.5 m hydrostatic pouring pressure instead of 0.23 m; II = second.

4.1.2 Early free shrinkage

Figure 4.4 and Appendix 4.2 show the drying shrinkage up to 1 day's age. A part of this shrinkage is called plastic shrinkage, which takes place before the concrete sets at about 6 hours' age. Also the property of the amount of fines seemed to have a substantial effect, Figure 4.5. The surface dries out at early age and plastic shrinkage occurs.

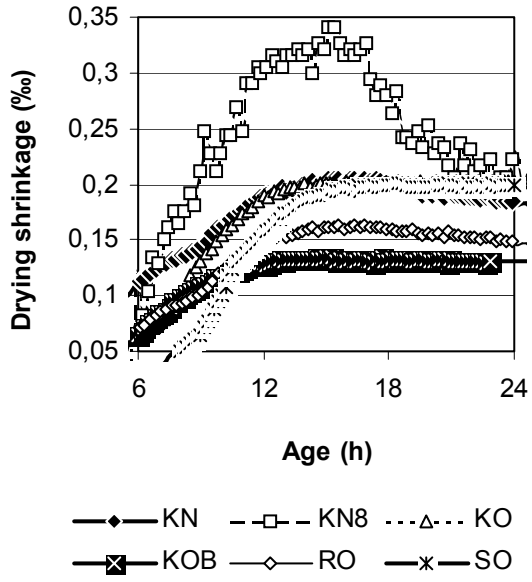

Figure 4.4 – Free drying shrinkage up to 1 day's age. B = increased amount of filler; K = Köping 500 limestone filler; N = new way of mixing (filler last); O = ordinary way of mixing (filler first); R = reference; S = Ignaberga 200 limestone filler.

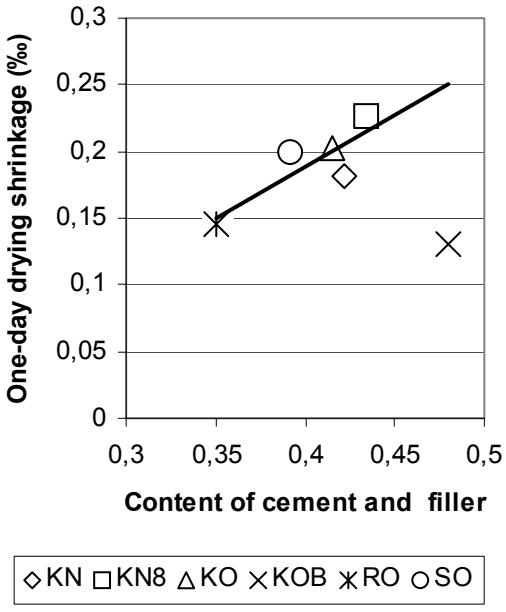

Figure 4.5 - One-day drying shrinkage of concretes in series 3 versus content of fines. Notations see above.

However, the concrete with the largest amount of cement and filler, KOB, obtain the lowest early shrinkage, which was inconsistent, Figure 4.5. Instead the first-day shrinkage was better correlated to the strength development, which was reasonable, Figure 4.6. The following equation was calculated for the early shrinkage in this investigation:

$$\varepsilon_{1d} = 0{,}30 - 0{,}0060 \cdot f_{c1d}$$

$$\{R^2 = 0{,}67\} \quad (4.3)$$

ε_{1d} denotes one-day drying shrinkage (‰)

f_{c1d} denotes one-day strength (MPa)

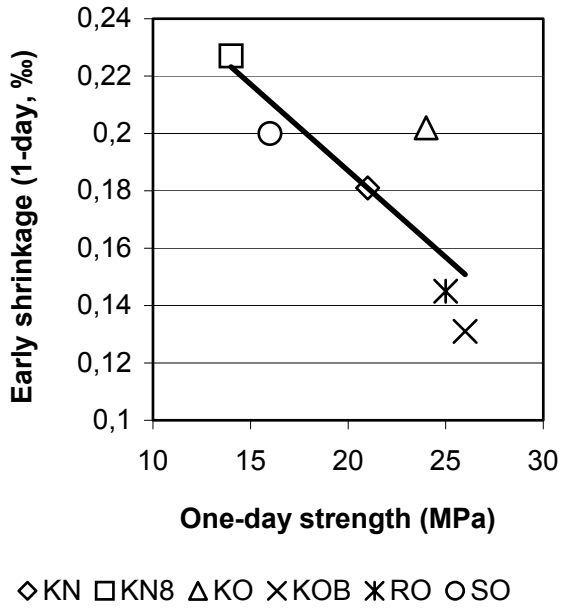

Figure 4.6 – One-day drying shrinkage of concretes in series 3 versus one-day strength. Notations: B = increased amount of filler; K = Köping 500 limestone filler; N = new way of mixing (filler last); O = ordinary way of mixing (filler first); R = reference; S = Ignaberga 200 limestone filler.

4.1.3 Long-term shrinkage

Figure 4.7 shows long-term shrinkage of NC (mix proportion RO) and SCC (mix proportion KO). Only small differences were observed between long-term shrinkage of NC and long-term shrinkage of SCC even though SCC contained less coarse aggregate (more fines). However, the content of cement paste was equal in NC and SCC (0.65), which was most important as regards long-term shrinkage.

4.1.4 Creep

Creep was also studied for NC (mix proportion RO) and SCC (mix proportion KO). Figures 4.8-9 show the creep compliance (including the elastic deformation) for starting age 2 and 28 days respectively (stress/strength 30%).

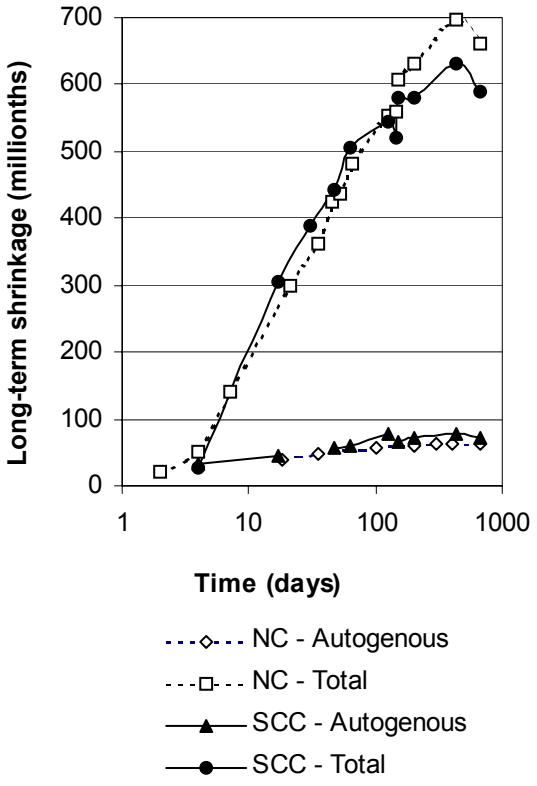

Figure 4.7 – Long-term shrinkage of NC and SCC both with w/c = 0.39. NC = mix proportions RO; SCC = mix KO.

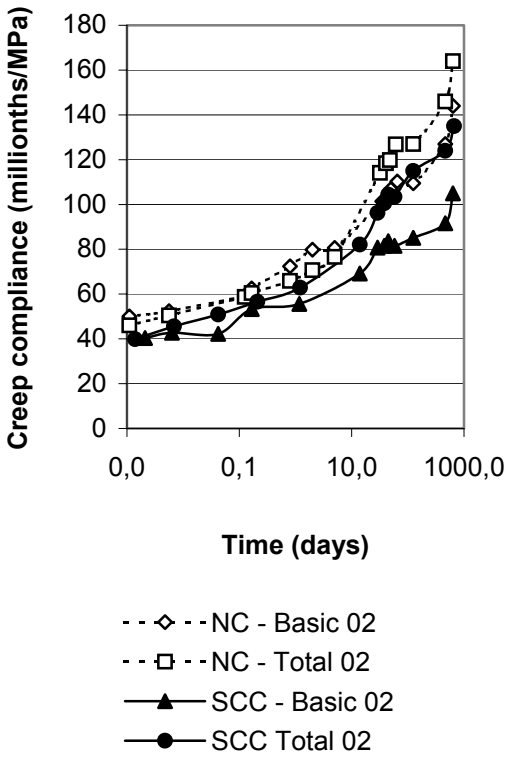

Figure 4.8 – Creep compliance for starting age 2 days. Concrete with w/c = 0.39. NC = mix RO; SCC = mix KO.

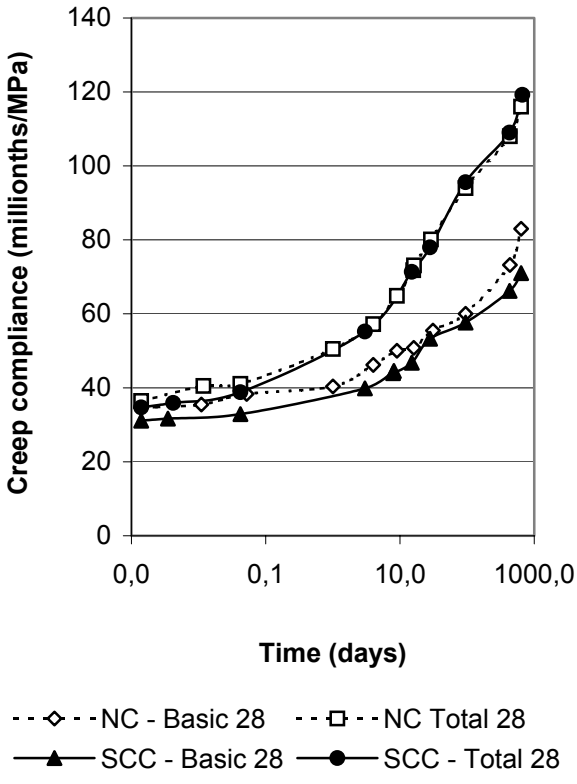

Figure 4.9 – Creep compliance for starting age 28 days. Concrete with w/c = 0.39. NC = mix RO; SCC = mix KO.

At 2-day starting age creep seemed to be less for SCC than for NC, which may be due to higher early strength of SCC than of NC, see above, Figure 4.8. However, at 28-day starting age creep of NC and SCC performed more or less equal while the other parameters were kept constant, which was also confirmed by other research [39-42], Figure 4.9.

4.2 Chloride migration coefficient, D

The following equation was used to calculate the chloride migration coefficient, D [4]:

$$D= 0.0239\cdot(273+T)\cdot L\cdot/[(U-2)\cdot t]\cdot \cdot\{x_d-0.0238\cdot[(273+T)\cdot L\cdot x_d)/(U-2)]^{½}\} \quad (4.4)$$

t denotes the test duration (h)
x_d denotes the average chloride penetration depth (mm)
D denotes the non-steady-state migration coefficient, x10 $^{-12}$ m²/s
L denotes the thickness of the specimen (mm)
T denotes the average initial and final temperatures in the anolyte solution (°C)

Significant differences were obtained between the chloride migration coefficient, D, of SCC and that of NC, Figure 4.10 and Appendix 4.3. An average 60% increase of the chloride migration coefficient, D, was observed in SCC compared with that of NC. The reasons for the enlargement of the chloride migration coefficient, D, in SCC compared with D in NC are not clarified. The effect of filler on strength makes it possible to use less cement in SCC than in NC. On the other hand less cement in concrete lowers the porosity, which works in the other direction.

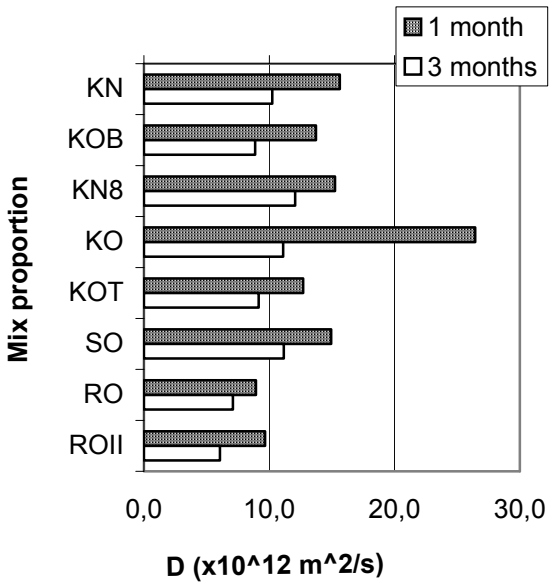

Figure 4.10 – Chloride migration coefficient, D, for concrete in series 3, Appendix 4.3. Notations: B = increased amount of filler; K = Köping 500 limestone filler; N = new way of mixing (filler last); O = ordinary way of mixing (filler first); R = reference; S = Ignaberga 200 limestone filler; T = 5.5 m hydrostatic pouring pressure instead of 0.23 m; II = second.

More cement in the concrete increased the ability of the concrete to bind chlorides [6]. Figure 4.11 shows that less cement content in SCC than in NC increased D. The studies described here and also those described in Chapters 2.1-2 for concrete without mineral additives were used to obtain the following empirically based equations for D, Figures 4.12-14 [5,10]:

$$D=\{[(0.0055\cdot\ln(t)-0.2122)\cdot c-3.5\cdot\ln(t)+104]\cdot(4\cdot w/b-1.2)/0.4\}\cdot(10^{-12}) \quad \{R^2=0.88\} \quad (4.5)$$

c denotes the cement content ($375 < c < 450$ kg/m³)

D denotes the chloride migration coefficient ($x10^{-12}$ m^2/s)

ln(t) denotes the natural logarithm of concrete age ($1 < t < 36$ months)

w/b denotes the water-binder ratio, 1:1 ($0.35 < w/b < 0.50$)

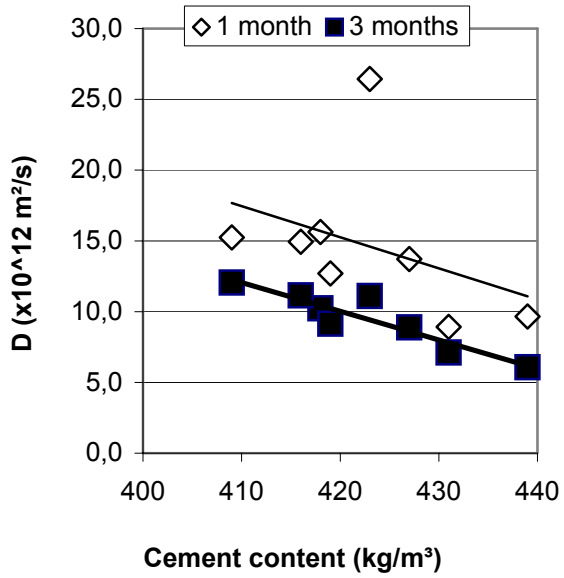

Figure 4.11 – The chloride migration coefficient, D, versus cement content, Appendix 4.3. Starting age is given.

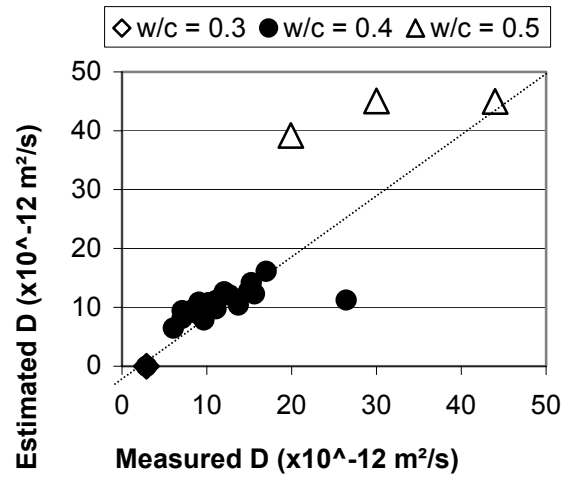

Figure 4.12 – Comparison between values of the chloride migration coefficient, D, estimated with equation (4.5) and measured values of the chloride migration coefficient, D [5,10].

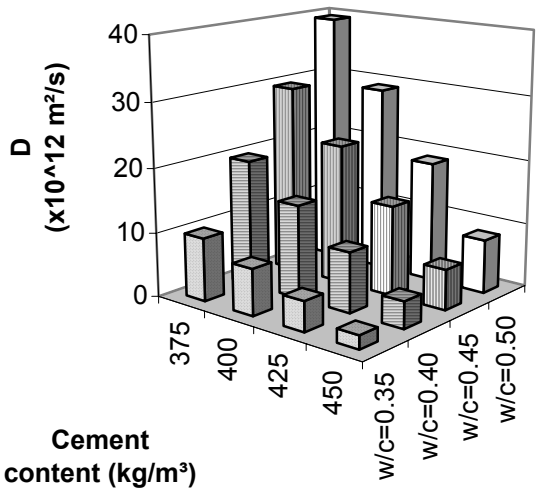

Figure 4.13 – Values of the chloride migration coefficient, D, at 3 months' age estimated with equation (4.5) at different cement content and w/c.

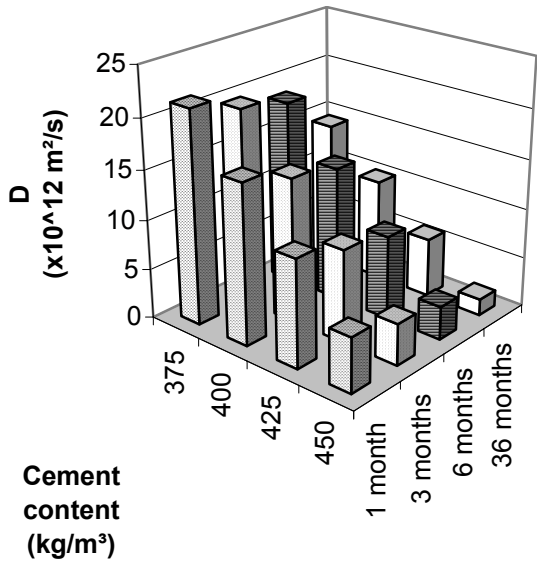

Figure 4.14 - Values of the chloride migration coefficient, D, at w/c = 0.4 estimated with equation (4.5)

4.3 Salt frost scaling

Figure 4.15 and Appendix 4.4 show results of salt frost scaling at 28, 56 and 112 frost cycles. SCC obtained the same salt frost scaling as NC did. Based on the studies the following conclusions were drawn after 112 cycles:

1. More filler did not increase the amount of salt frost scaling.
2. At 28 days' but not at 90 days' age at start of testing salt frost scaling was larger in SCC than in NC.
3. SCC with 5.5 m hydrostatic pouring pressure instead of 0.23 m did not obtain a different salt frost scaling.
4. In this studies SCC with Köping 500 filler obtained larger salt frost scaling than SCC with Ignaberga 200 did.

According to the Swedish rules based on the Borås method the concrete performs excellent with less than 0.2 kg/m³ salt frost scaling after 56 cycles, and has good salt frost resistance with less than 0,5 kg/m³ after 56 cycles. Since the method in the present investigation differs from the Borås method, only comparison between the different concretes may be done.

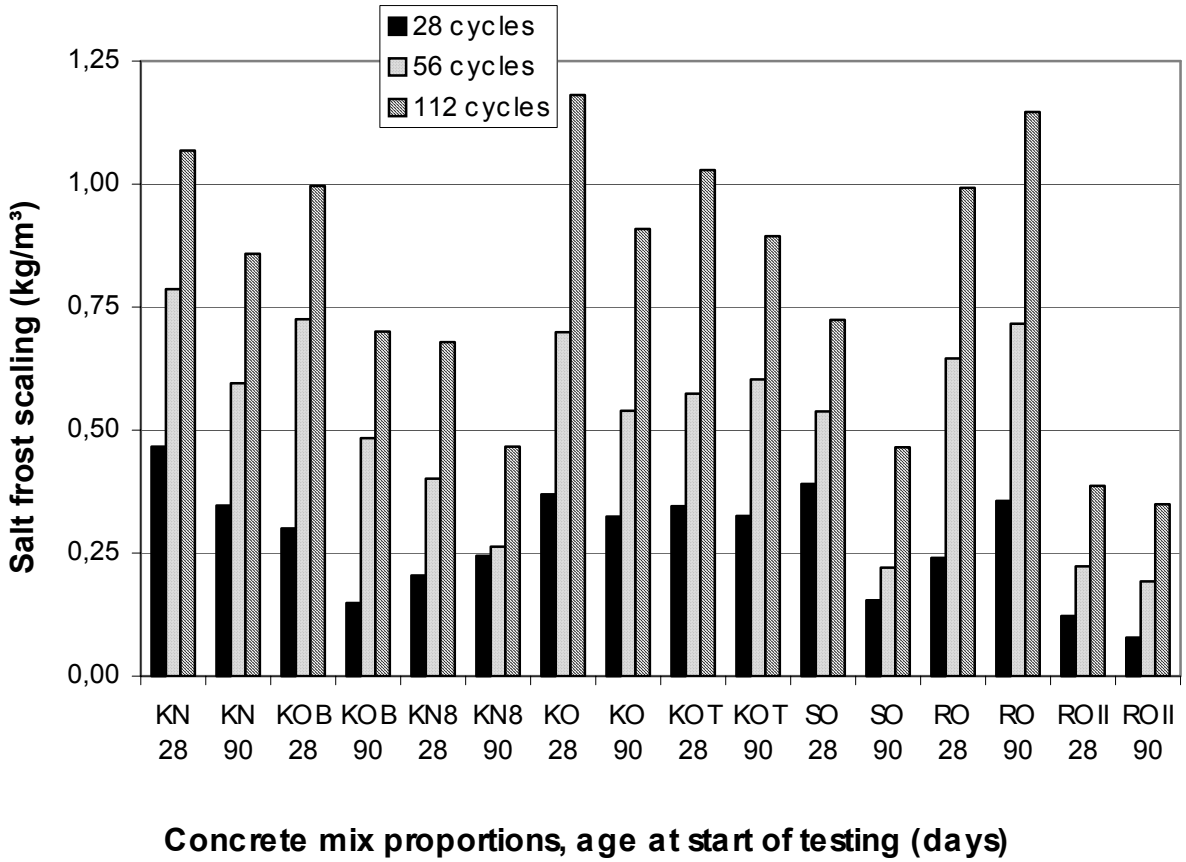

Figure 4.15 – Salt frost scaling of concrete at 28, 56 and 112 frost cycles (see also Appendix 4.4). Notations: B = increased amount of filler; K = Köping 500 limestone filler; N = new way of mixing (filler last); O = ordinary way of mixing (filler first); R = reference; S = Ignaberga 200 limestone filler; T = 5.5 m hydrostatic pouring pressure instead of 0.23 m; II = second.

5. RESULTS ON INTERNAL FROST AND SULPHATES RESISTANCE AND AIR VOIDS

5.1 Internal frost resistance

Figures 5.1-3 show results of concrete in series 2 as regards change of fundamental frequency (closely related to the elastic modulus), length change and change of mass after 100 and 300 frost cycles in distilled water (± 20 °C). For the mix proportions D (Danish fly ash mix composition) and RO (reference mix composition) the decrease of fundamental frequency after 300 frost cycles coincided well with the loss of weight. For other mix proportions, F (optimum fly ash mix composition), G (glass filler mix composition) and T (German slag mix composition), small changes of the measured properties were observed, which indicates that the later concrete performed better as related to internal frost resistance than concrete D and RO II. After length changes the fundamental frequency increased due to water absorption, Figure 5.4.

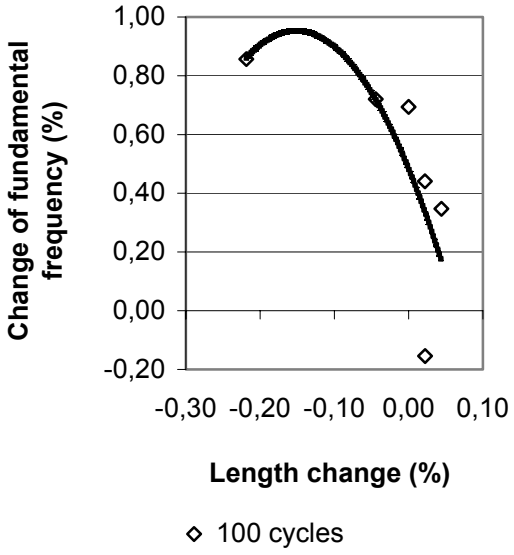

Figure 5.4 – A small length change increased the fundamental frequency.

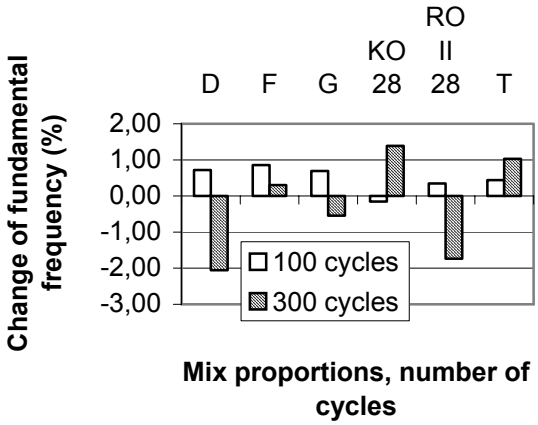

Figures 5.1 – Change of fundamental frequency of concrete in series 2 (closely related to the elastic modulus) after 100 and 300 frost cycles in distilled water (± 20 °C).

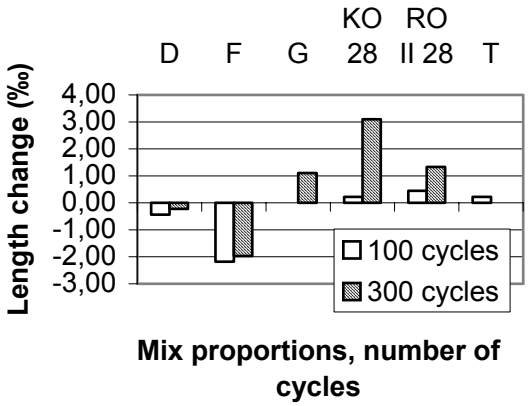

Figures 5.2 – Length change of concrete in series 2 after 100 and 300 frost cycles in distilled water (± 20 °C).

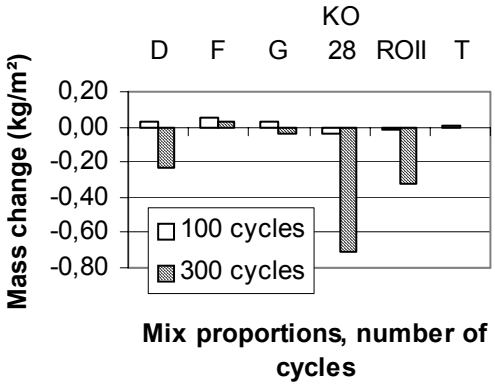

Figures 5.3 – Change of mass of concrete in series 2 after 100 and 300 frost cycles in distilled water (± 20 °C).

As shown in Figure 5.1-3 and Appendices 5.1-3 the largest length increase (3.1 ‰) and the largest loss of mass for SCC (0.71 kg/m²) was obtained for concrete with limestone filler.

Figures 5.5-7 and Appendices 5.2-3 show results of concrete in series 3 as regards the change of fundamental frequency (closely related to the elastic modulus), length change and change of mass after 100 and 300 frost cycles in distilled water (± 20 °C). SCC in series 3 exhibited much larger changes in fundamental frequency, length and mass than concrete in series 2, which indicated the resistance to internal frost to be of lower in SCC with limestone filler than in concretes with silica fume, fly ash, slag or glass filler, filler.

The first reference concrete in series 3, RO, was almost destroyed after 300 frost cycles (about 80% loss of fundamental frequency, about 1% increase in length and about 2,5 kg/m³ loss of weight). The comparative figures for concrete RO II were 2% loss of fundamental frequency, about 0.1% increase in length and about 0.3 kg/m³ loss of weight after 300 cycles. The reason for the large differences of the results on internal frost resistance with the same mix proportion is not known. The mix proportions, the handling and the measurements of the two reference concretes were identically performed by the same laboratory personal. Figure 5.8 shows the change of fundamental frequency versus the length change.

On average SCC exhibited much better internal frost resistance than NC. Remarkable, besides the low repeatability of the internal frost resistance test of NC, was the large frost scaling of SCC mix proportion KN8 (Köping 500 limestone filler; new way of mixing (filler last); 8% air content). The following equation was estimated:

$$\Delta f = -43{,}755 \cdot \Delta l^{2} - 57{,}642 \cdot \Delta l + 0{,}16 \qquad \{R2 = 0{,}85\} \qquad (5.1)$$

Δf denotes change of fundamental frequency of concrete after frost
Δl denotes length change of concrete

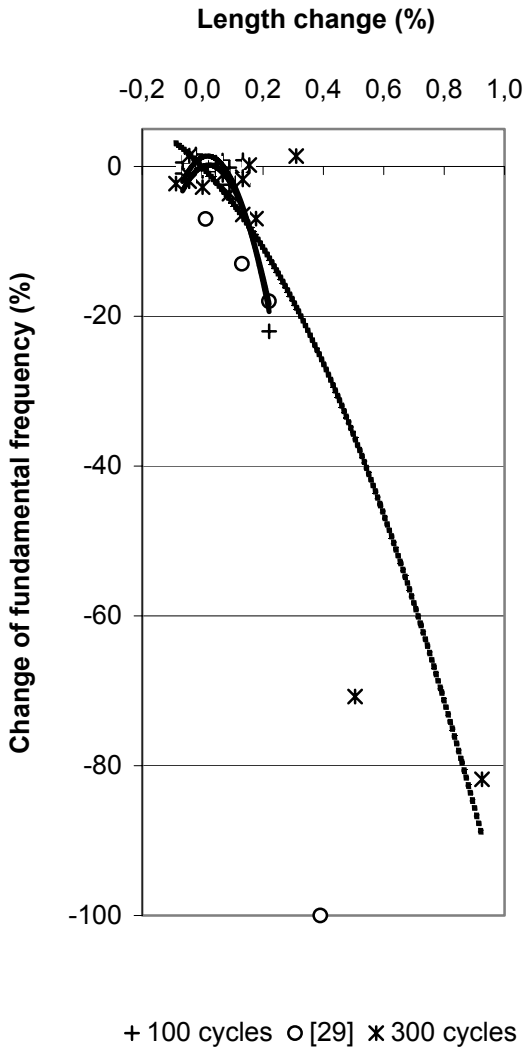

Figure 5.8 – Change of fundamental frequency versus the length change.

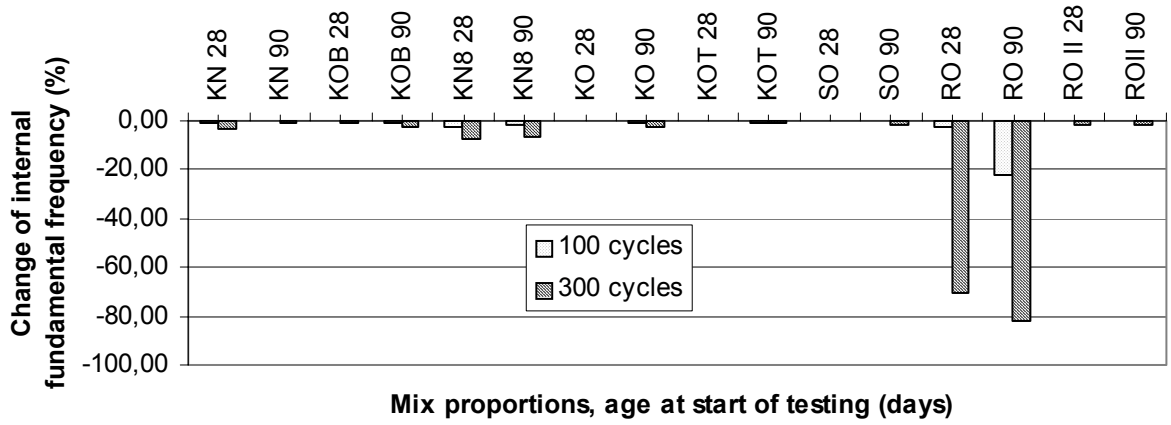

Figure 5.5 – Change of fundamental frequency of concrete in series 3 (closely related to the elastic modulus) after 100 and 300 frost cycles in distilled water (± 20 °C). B = increased amount of filler; K = Köping 500 limestone filler; N = new way of mixing (filler last); O = ordinary way of mixing (filler first); R = reference; S = Ignaberga 200 limestone filler; T = 5.5 m hydrostatic pouring pressure instead of 0.23 m; II = second.

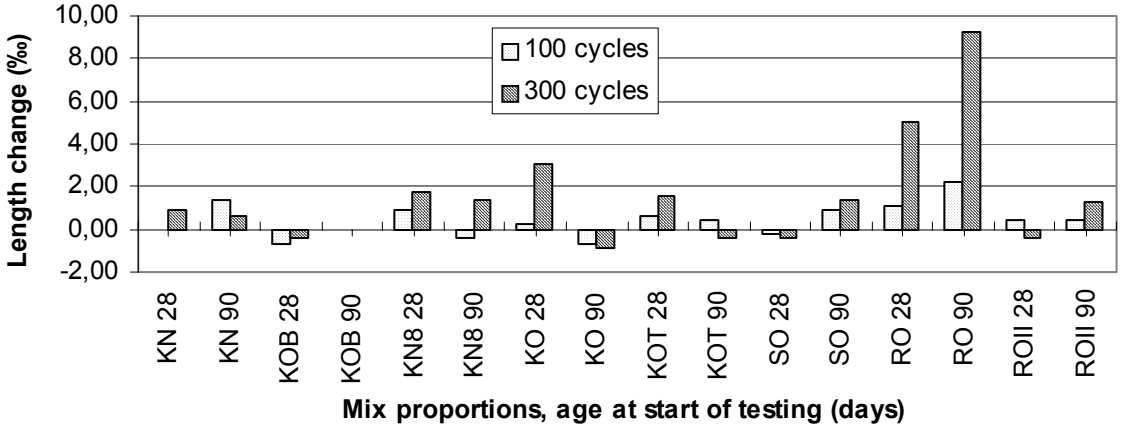

Figure 5.6 – Length change of concrete in series 2 after 100 and 300 frost cycles in distilled water (± 20 °C).

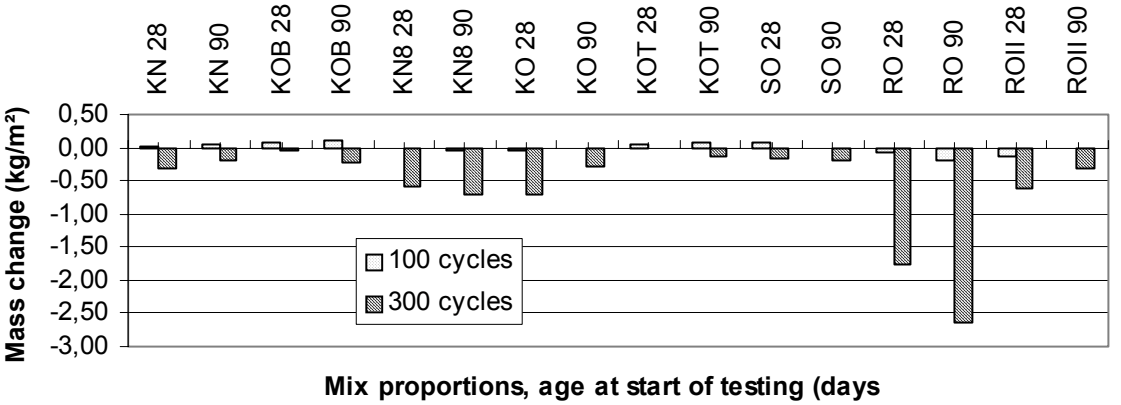

Figure 5.7 – Change of mass of concrete in series 2 after 100 and 300 frost cycles in distilled water (± 20 °C).

5.2 Sulphate resistance

Appendix 5.4 shows results of fundamental frequency, length and mass for specimens stored in distilled water, seawater or sodium sulphate, 18 g/kg distilled water, all specimens at 5 °C. In Figures 5.8-10 the change of fundamental frequency, length and mass after 90 days are shown. In Figures 5.11-13 the change of fundamental frequency, length and mass after 500 days are shown. Generally no large differences between the change of fundamental frequency, length and mass of NC and SCC were observed, whether subjected to distilled water, sea water or sodium sulphate, 18 g/kg distilled water. No decrease of fundamental frequency of any of the concrete was observed even after 500 days, which is most important for the internal structure. The largest increase in length was observed for NC. SCC exhibited larger increase of mass due to water uptake than NC did.

5.3 Air void structure

Figure 5.14 shows the accumulated air void structure of the concrete KN, KO, RO I and KOT. The fresh and hardened concrete contained the amount of air voids given in Table 5.1 (% air voids).

Table 5.1 – The fresh and hardened concrete air voids given in (% volume).

State	Fresh	Hardened voids < 2 mm
KN	5.6	4.7
KO	5.5	4.8
KOT	6.3	2.8
RO I	5.8	4.2

K = Köping limestone powder: N = new order of mixing (filler last); O = ordinary order of mixing; R = reference (normal) concrete; T = 5.5 m fresh concrete pressure; I = first casting.

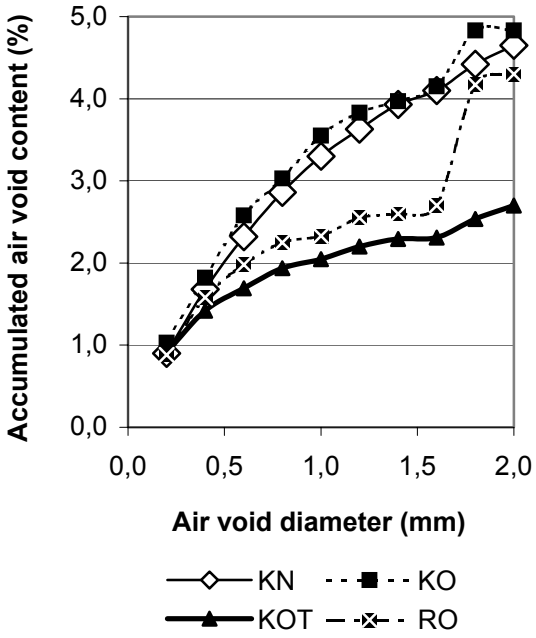

Figure 5.14 – Accumulated air void structure of the concrete KN, KO, RO I and KOT. K = Köping limestone powder: N = new order of mixing (filler last); O = ordinary order of mixing; R = reference (normal) concrete; T = 5.5 m fresh concrete pressure; I = first.

The precise air void structure in each test is shown in Appendices 5.6-9. A substantial decrease of the air void content less than 2 mm in diameter was observed in concrete that was subjected to 5.5 m concrete pressure during the casting. Evidently the air voids were enlarged in diameter since no increase of small air voids was observed, Figure 5.14. It was also of great interest to correlate the air void structure to the chloride migration coefficient and the frost resistance of the concrete. Figure 5.15 shows the chloride migration coefficient versus the air void structure less than 1 mm in diameter, Figure 5.16 the salt frost resistance versus the air void structure less than 1 mm in diameter and Figure 5.17 the internal frost resistance versus the air void structure less than 1 mm in diameter.

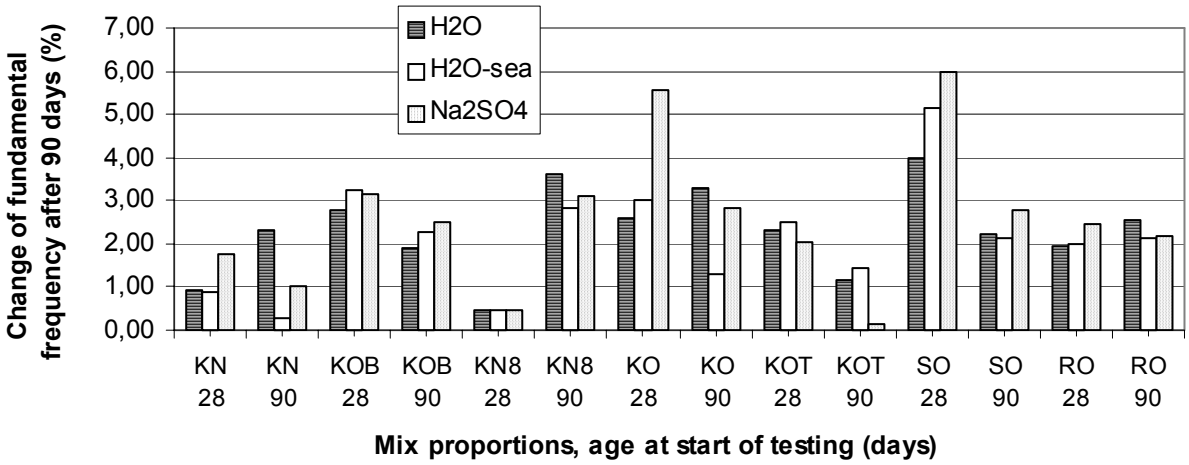

Figure 5.8 – Change of fundamental frequency after 90 days (%).

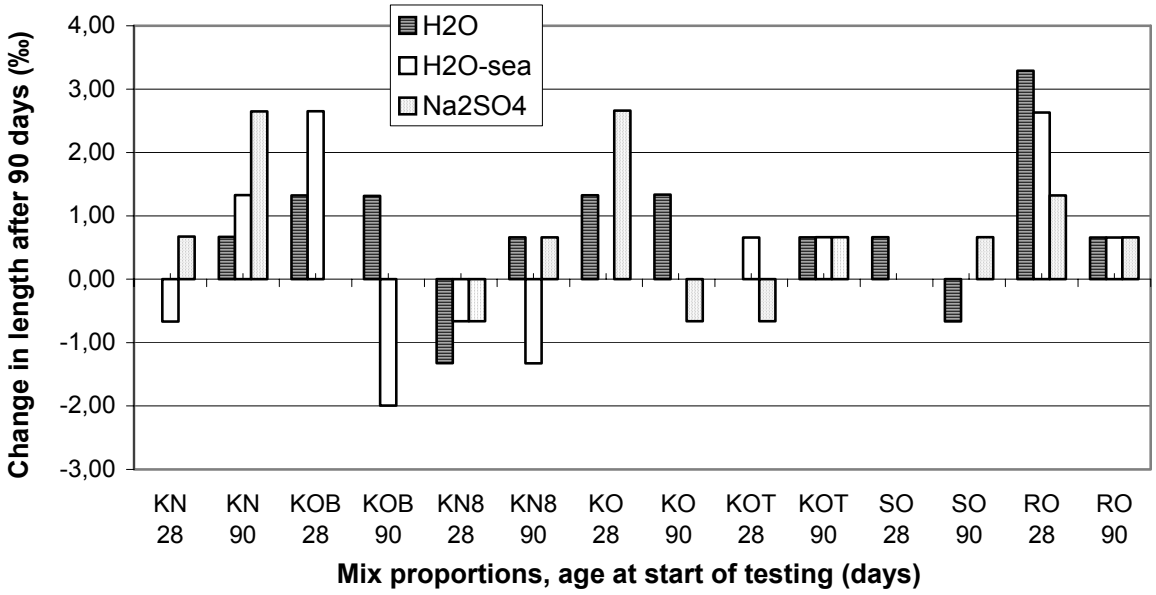

Figure 5.9 – Change of length frequency after 90 days (‰).

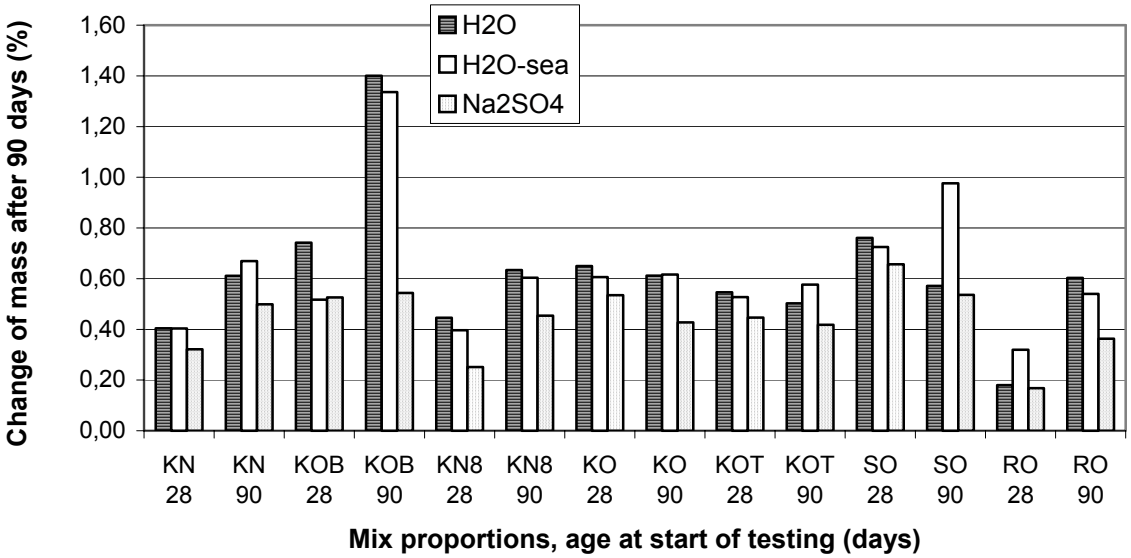

Figure 5.10 – Change of mass after 90 days (%).

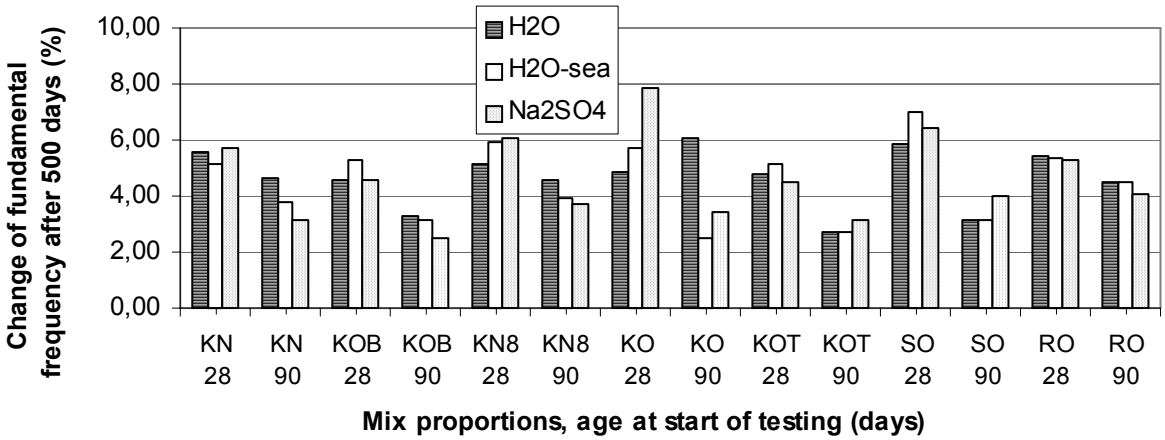

Figure 5.11 – Change of fundamental frequency after 500 days (%).

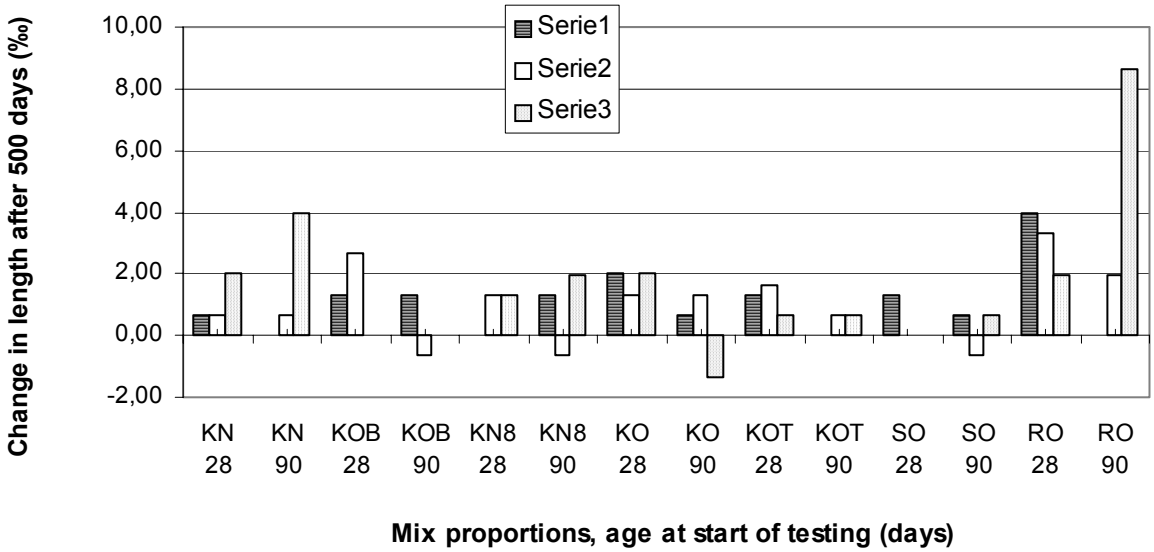

Figure 5.12 – Change of length frequency after 500 days (‰).

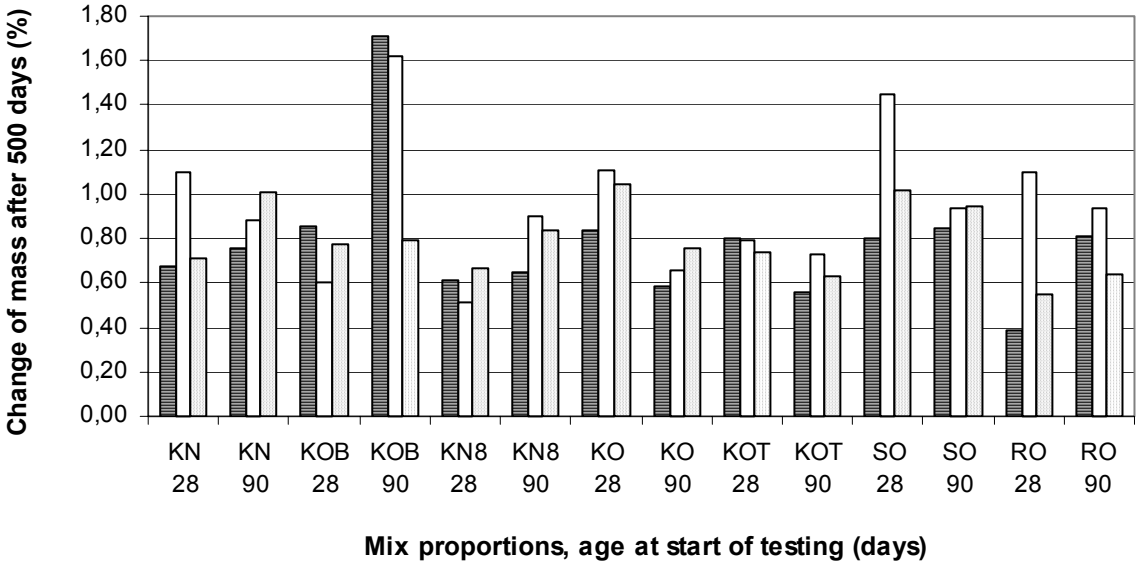

Figure 5.13 – Change of mass after 500 days (%).

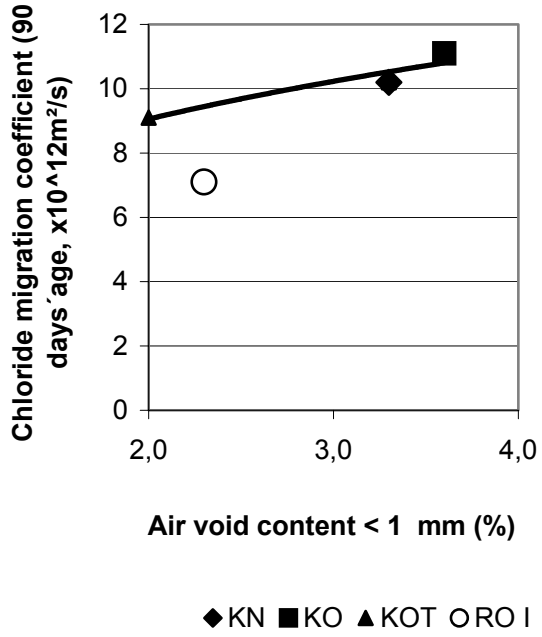

Figure 5.15 – Chloride migration coefficient versus the air void structure less than 1 mm in diameter. K = Köping limestone powder: N = new order of mixing (filler last); O = ordinary order of mixing; R = reference (normal) concrete; T = 5.5 m fresh concrete pressure; I = first casting.

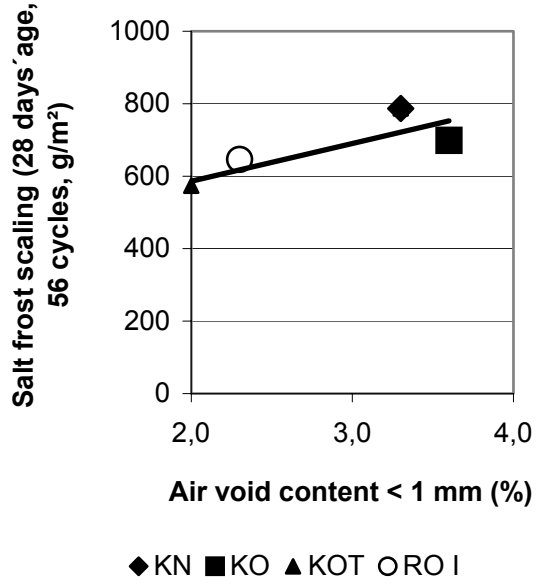

Figure 5.16 – Salt frost resistance versus the air void structure less than 1 mm in diameter.

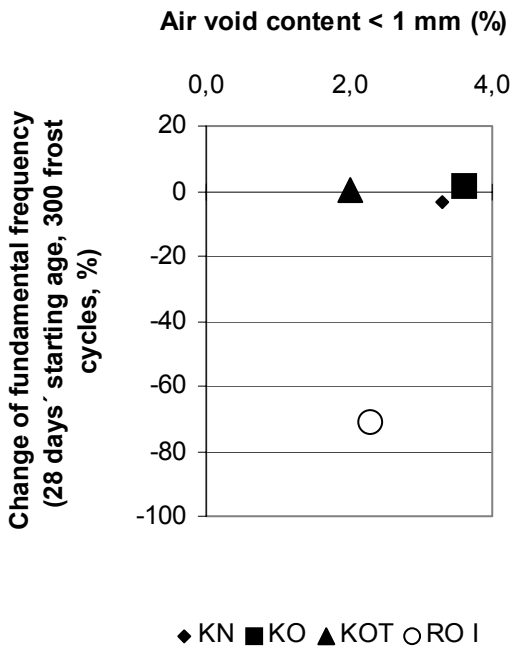

Figure 5.17 – Internal frost resistance versus the air void structure less than 1 mm in diameter.

Figure 5.15 shows that the chloride migration coefficient increased slightly with the air void structure less than 1 mm in diameter. This observation seems to be logical since the porosity also increases with the air content (the concrete was vacuum treated before testing the chloride migration coefficient. Figure 5.16 shows that the salt frost resistance did not vary much with the air void structure less than 1 mm in diameter. Usually more small air voids decreases the salt frost scaling but not in this experiment. On the contrary more air voids less than 1 mm in diameter seemed to increase the salt frost scaling in this case, which cannot be explained. Normally the salt frost scaling decreases with increasing air void content. Figures 5.18-20 show the chloride migration coefficient, the salt frost scaling and the internal frost resistance related to the air void content less than 0.5 mm in diameter.

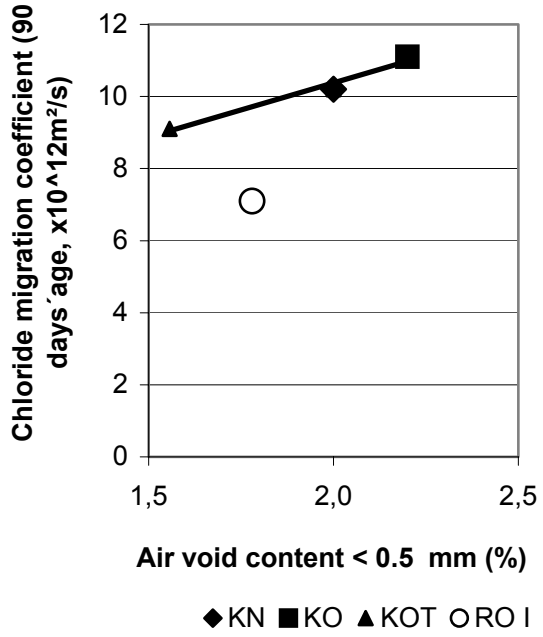

Figure 5.18 – Chloride migration coefficient versus the air void structure less than 0.5 mm in diameter. K = Köping limestone powder: N = new order of mixing (filler last); O = ordinary order of mixing; R = reference (normal) concrete; T = 5.5 m fresh concrete pressure; I = first casting.

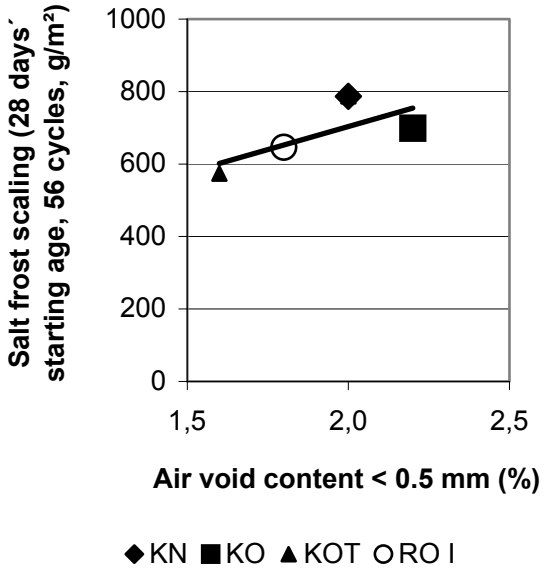

Figure 5.16 – Salt frost resistance versus the air void structure less than 0.5 mm in diameter.

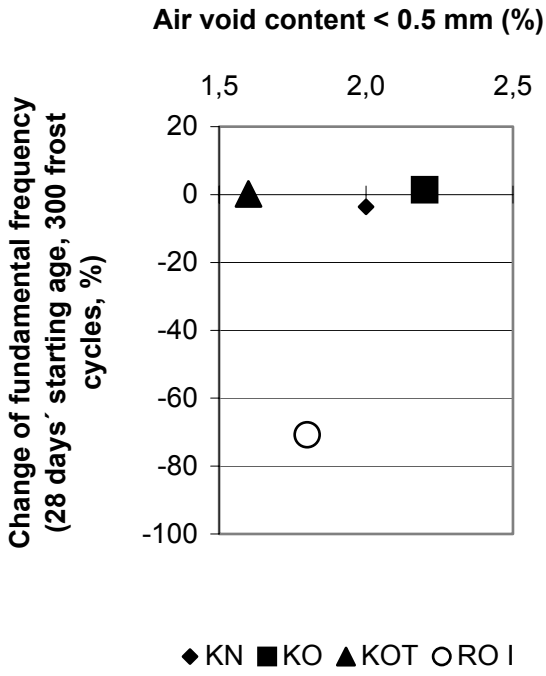

Figure 5.17 – Internal frost resistance versus the air void structure less than 0.5 mm in diameter.

6. DISCUSSION

6.1 Chloride migration coefficient, D

6.1.1 Effect of method of compaction on coefficient of variation of testing

In Appendix 6.1 the coefficient of variation between the repeated tests of chloride migration coefficient, D (standard deviation to average the chloride migration coefficient, D ratio) is given in order of the estimated accuracy.

On average the tests of SCC showed smaller coefficient of variation than the tests of NCs did, probably due to the fact that vibration was avoided in SCCs. The transition zone remained unaffected in SCC but was affected in NC due to different movements of cement paste and aggregate in NC in turn due to vibrations. Appendix 6.2 shows that the chloride migration coefficient, D, of SCC with large significance was larger than that of NC ($z = 3.15 > 2$).

6.1.2 Effect of method of mixing on the chloride migration coefficient, D

Appendix 6.3 shows the effect of mixing order and type of concrete on the chloride migration coefficient, D, for concretes in series 3 ($x10^{12}$ m^2/s). It was shown in Appendix 6.3 that the mixing order did not affect the chloride migration coefficient, D, and that the chloride migration coefficient, D, was about 60% lower for NC than for SCC.

6.1.3 Effect of age on the chloride migration coefficient, D

Appendix 6.4 shows the effect of age at testing and way of compaction on the chloride migration coefficient, D, for concretes in series 3 ($x10^{-12}$ m^2/s). Again it was shown that the chloride migration coefficient, D, was 60% lower for NC than for SCC, independent of age at testing. However, on average the chloride migration coefficient, D, was 60% lower at 90 days' age at testing than at 28 days' age at testing.

6.1.4 Effect of filler additives on the chloride migration coefficient, D

Figure 6.1 shows that the chloride migration coefficient, D, increased in concrete at higher cement-powder ratio, c/p, i.e. concrete pure cement binder (c/p = 1) had a lower chloride migration coefficient, D, than concrete with cement and limestone powder did. Obviously concrete with pure cement without filler binds more chloride than concrete based on cement with limestone powder does.

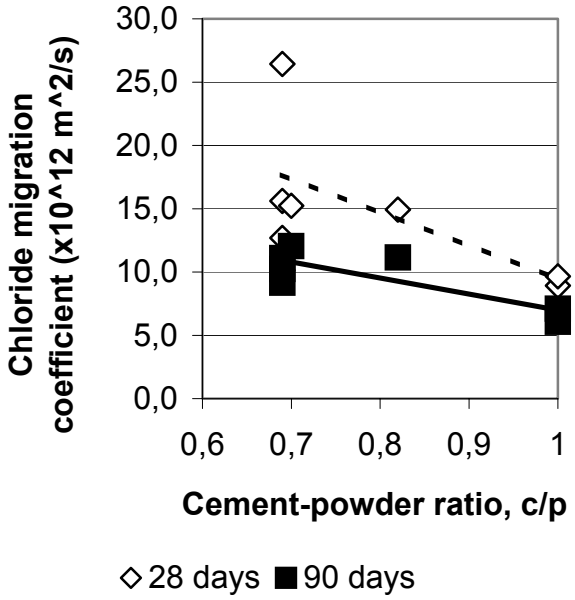

Figure 6.1 – The chloride migration coefficient, D, increased in concrete at higher cement-powder ratio, c/p.

6.1.5 Effect of aggregate content on the chloride migration coefficient, D

Figure 6.2 shows that the chloride migration coefficient, D, was lower at higher aggregate content, which seems logical. It is not possible for chloride to pass aggregate. The migration of chlorides takes place in the cement paste.

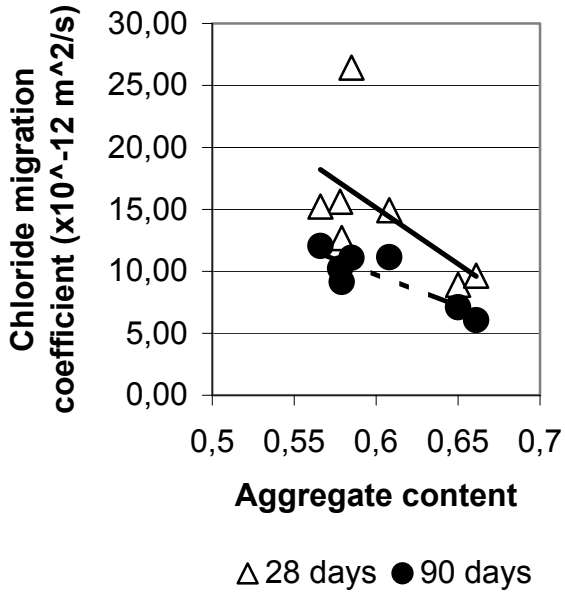

Figure 6.2 – Chloride migration coefficient, D, versus aggregate content. Testing age indicated.

6.1.6 Effect of silica fume, fly ash and slag on chloride migration coefficient, D

From the results and from the references [5,10] it was obvious that pozzolans like silica fume and slag had an effect on the value of the chloride migration coefficient, D. From the results obtained by Tang and Nilsson [5] and further by Boubitsas and Paulou [10] it was possible to estimate the effect of pozzolans on the chloride migration coefficient, D, assuming that the concrete performed in accordance with equation (4.5) above.

The effect of one kg of the different additives was adjusted to the effect of 1 kg cement content on the chloride migration coefficient, D, in equation (4.5) for the measured results to coincide with the estimations. The ratio of the effect of 1 kg of the additive to 1 kg of cement on the chloride migration coefficient, D, is here called the efficiency factor. The recalculation of the amount of cement into an equivalent amount achieved this.

From previous research it was known that silica fume had a substantial effect on strength, self-desiccation and hydration [20]. For strength large efficiency factors were obtained at early ages but declining to less than 0 after about 90 months [43-46]. For hydration the opposite results were found.

The present results were obtained only at 1 and 6 months' age, i.e. the efficiency factor (effect of 1 kg additive to the effect of 1 kg cement on the chloride migration coefficient, D) may very well be time-dependent.

The following equation was obtained for the pozzolanic interaction between Portland cement, silica fume, fly ash and slag as regards the chloride migration coefficient, D [4,5,10,47]:

$$c_{eq.} = c + 0{,}21 \cdot fl + 1{,}6 \cdot sf + 1{,}03 \cdot sl$$

$$\{R^2 = 0{,}81\} \quad (6.1)$$

$c_{eq.}$ denotes the equivalent amount of cement to be used in equation (4.5)
c denotes amount of Portland cement
fl denotes the amount of fly ash
sf denotes the amount of silica fume
sl denotes the amount of slag

6.1.7 Effect of porosity on the chloride migration coefficient, D

Porosity was calculated in order to detect its effect on the chloride migration coefficient, D [48]. Figure 6.3 shows little influence of the calculated porosity on the chloride migration coefficient, D. Even though the calculated porosity was somewhat larger for NC than for SCC, the chloride migration coefficient, D, of NC was smaller, probably due to the chloride binding ability of the cement gel [6].

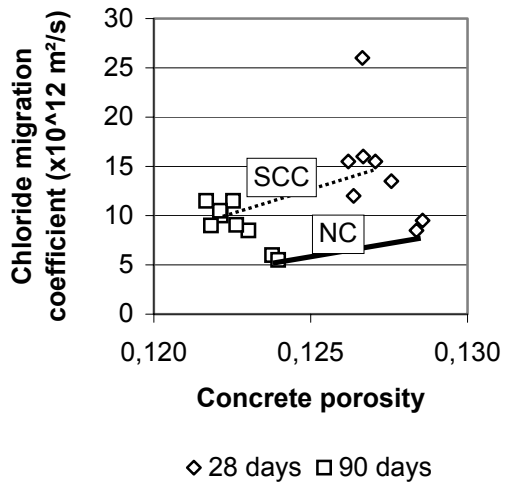

Figure 6.3 – Chloride migration coefficient versus calculated porosity.

6.1.8 Effect of self-desiccation on the chloride migration coefficient, D

As shown above, chlorides cannot be transported in the air or in voids of vacuum that were obtained due to self-desiccation. However, it is not feasible to measured RH in concrete during chloride transport since water is required for this transport to take place. Therefore the chloride migration coefficient, D, from these tests and from other tests [5,10] was related to RH with self-desiccation, equation (2.4). Factors of the efficiency factor (effect of 1 kg additive to the effect of 1 kg cement on the chloride migration coefficient, D) shown in equation (6.1) were used in order to estimate RH. The dependence of the cement content on the chloride migration coefficient, D, was dominating besides the effect of RH, Figure 6.4. The following formula was calculated in order to describe the effect of self-desiccation on the chloride migration coefficient, D, taking into account the cement content ($x10^{12}$ m²/s):

$$D = 3000 \cdot e^{-0,0118 \cdot c} \cdot (RH)^{0,04 \cdot c - 9,1} \quad (6.2)$$

c denotes cement content (kg/m³)

RH denotes the internal relative humidity with self-desiccation, equation (2.4)

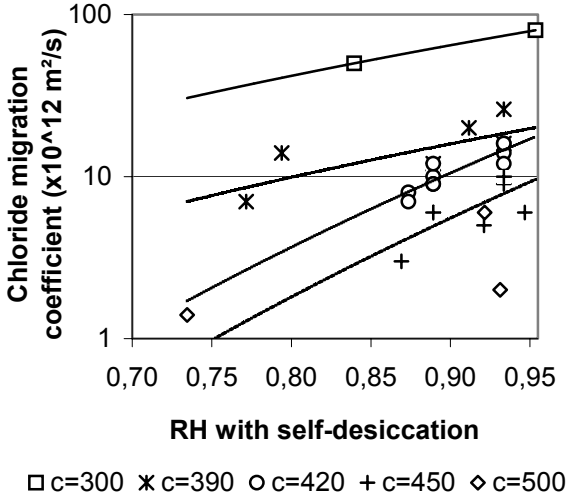

Figure 6.4 – Comparison between chloride migration coefficient, D, measured acc. to [5,10] and self-desiccation calculated acc. to equation (2.4).

6.2 Salt frost scaling

6.2.1 Effect of mixing order on the salt frost scaling of concrete

Pettersson stated that a new order of mixing (filler at last) had a substantial effect on the salt frost scaling of SCC. The salt frost scaling decreased in SCC with filler added at the end of the mixing procedure as compared to the salt frost scaling of SCC with filler added at the beginning of the mixing [25], Appendix 6.5.

Appendix 6.5 shows that SCC with ordinary mixing order on average did not significantly have larger salt frost scaling after 112 cycles than NC did ($z \approx 1.5 < 1.96$). However, at a testing age of 28 days with $z = 2.2$ a tendency was observed that SCC with ordinary mixing had larger salt frost scaling than the reference concrete, RO, with ordinary mixing had. At 90 days' age of testing the opposite was observed, i.e. no significant difference between salt frost scaling due to mixing order ($z = 0.8$).

6.2.2 Effect of way of compaction on the salt frost scaling of concrete

Appendix 6.6 shows salt frost scaling of concrete with different age at start of testing, amount of filler and air content. All these parameters affected the salt frost scaling. No significant difference was obtained between salt frost scaling of SCC and salt frost scaling of NC at constant air content except for 28 days' age at start of testing. At 28 days' age at start of testing the salt frost scaling was significantly larger in SCC than in NC ($z = 2{,}75 > 2$). It was also observed from Appendix 6.6 that the salt frost scaling generally decreased at larger age of testing.

6.2.3 Effect of air content on the salt frost scaling of SCC

Figure 6.5 shows the salt frost scaling of all concretes in series 3 versus air content. Increased amount of air resulted in lower salt frost scaling as expected. Appendix 6.7 shows that air content had high significance for the salt frost scaling ($z \approx 7.4$).

6.2.4 Effect of filler content on the salt frost scaling of SCC

Appendix 6.8 shows the effect of filler content on the salt frost scaling of SCC. No significant difference of salt frost scaling existed due to the filler content ($z = 1.9 < 2$).

6.2.5 Effect of the pouring pressure on the salt frost scaling of SCC

Appendix 6.9 shows the effect of pouring pressure on the salt frost scaling of SCC. No significant difference of salt frost scaling existed due to the pouring pressure up to 5.5 m ($z = 0.8 < 2$).

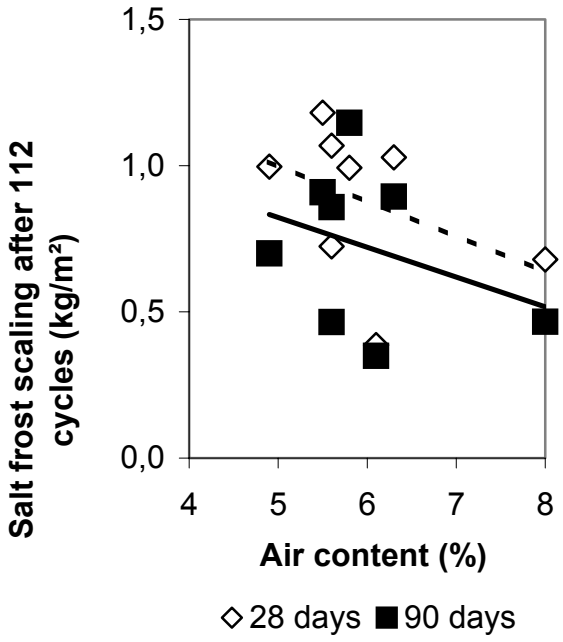

Figure 6.5 – Salt frost scaling of all concretes in series 3 versus air content.

6.2.6 Effect of the type of filler on the salt frost scaling of SCC

It was shown above that the amount of filler did not have any significant influence on the salt frost scaling of SCC. It was then possible to compare the salt frost scaling of SCC with different types of filler, Köping or Ignaberga, even though the content of filler was not the same of the two SCCs.

SCC with Köping filler contained 184 kg/m³ limestone powder and SCC with Ignaberga filler only about half the amount, 84 kg/m³ limestone powder. Appendix 6.10 shows that SCC with Ignaberga filler had significantly lower salt frost scaling than SCC with Köping filler had ($z = 3.5 > 2$).

6.3 Internal frost resistance

Appendices 6.11-12 show a summary of change on average of fundamental frequency, length and loss of weight of SCC mix proportions with Köping limestone filler and 6% or 8% air content. Appendix 6.13 shows a summary of change on average of fundamental frequency, length and loss of weight of NC mix proportions with 6% air content. Figure 6.6 shows a summary of change on average of fundamental frequency, Figure 6.7 shows a summary of length change and Figure 6.8 a summary of the loss of weight of SCC mix proportions with Köping limestone filler and 6% or 8% air content and of NC with 6% air content independent of the age at start of testing.

It may be observed from Appendices 6.11-13 and Figures 6.6-8 that the SCC with 6% air content resisted internal frost better than SCC with 8% air, i.e. inconsistent with previous research.

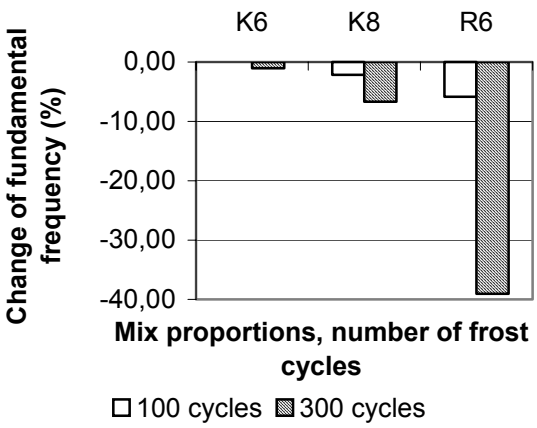

Figure 6.6 – Summary of change on average of fundamental frequency. K = SCC with Köping limestone filler. R = NC; 6 = 6% air content.

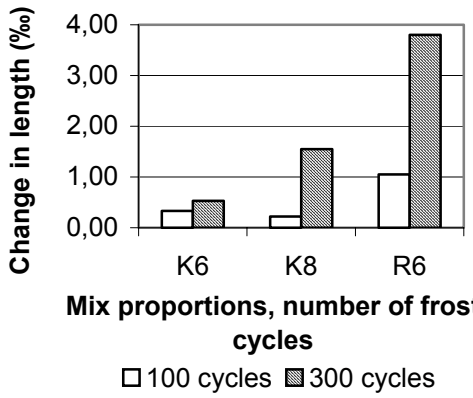

Figure 6.7 – Summary on average of length change.

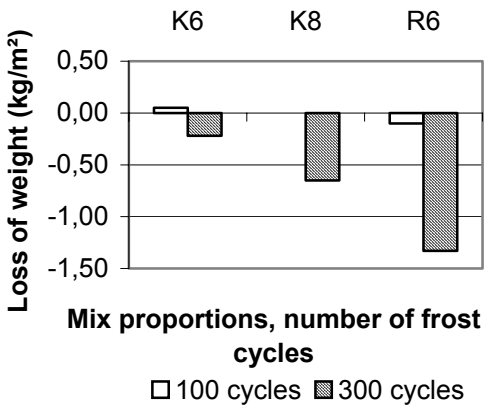

Figure 6.8 – Summary of the loss of weight.

Increased amount of air content normally increases the internal frost resistance as well. Therefore tests of the significance of the results on the effect of air-entrainment were performed on mix proportions KN and KN8 in Appendices 6.14-16. Appendices 6.14-16 show that the change of fundamental frequency and mass of concrete was significantly larger for SCC with 8% than for than for SCC with 6% air ($z > 2$; the difference in length change was not significant different since $z < 2$).

Tests of significance of the results on the effect of compaction method were performed on mix proportions KO, RO and RO II in Appendices 6.17-19. Appendices 6.17-19 show that the change of fundamental frequency and mass of concrete was significantly larger for NC than for both SCC mixes with 6% air ($z > 3$; difference in length change showed a significant different at 90 days' age at start of testing; $z = -5.7$).

6.4 Sulphate resistance

Even though no decrease of fundamental frequency of any of the concrete was observed after 500 days, some deterioration may occur later on due to effect of sulphates on the internal structure. Still the largest increase in length was observed for NC. On the other hand SCC exhibited the largest increase of mass due to water uptake than NC did, which may lead to weakening of the structure later on.

6.5 Air void structure

Significant effect of the air void structure was observed on the chloride migration coefficient and on salt frost scaling. The following relationships were used to describe the effect of the air void structure:

$$D = 3 \cdot A_{0.5} + 4.4 \quad (6.3)$$

$$D = 1.1 \cdot A_1 + 6.8 \quad (6.4)$$

$$SC = 0{,}25 \cdot A_{0.5} + 0{,}19 \quad (6.5)$$

$$SC = 0{,}1 \cdot A_{0.5} + 0{,}38 \quad (6.6)$$

$A_{0.5}$ denotes air voids less than 0.5 mm
A_1 denotes air voids less than 1 mm
D chloride migration coefficient
SC denotes the salt frost scaling after 56 frost cycles (28 days' starting age, kg/m³)

Also from these equations it was observed that the chloride migration and also the salt frost scaling increase with the air void content. Figure 6.9 shows the salt frost scaling versus Powers spacing factor:

$$SC = 55{,}806 \cdot a - 6{,}58 \quad (6.7)$$

a denotes Powers spacing factor for a unfilled system (mm)
SC notations see above

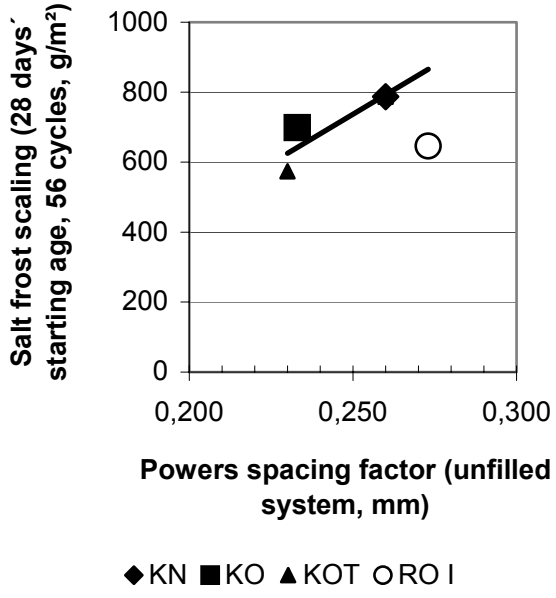

Figure 6.9 Salt frost scaling versus Powers spacing factor.

7. CONCLUSIONS AND RECOMMENDATIONS

The following conclusions were drawn and recommendations given:

Mechanical properties

1. Limestone filler additives increased the strength substantially even though the cement content was somewhat lower in SCC than in NC.
2. Probably a more efficient packing of the particles was the reason for the enlarged strength of SCC.
3. Creep and shrinkage performed in the same way in NC as in SCC.

Chloride migration coefficient

1. The chloride migration coefficient was some 60% larger in SCC with limestone filler than in NC.
2. In SCC with 5% silica fume and 12% fly ash the chloride migration coefficient was 60% of that in NC.
3. At 90 days' age of testing the chloride migration coefficient was 60% of that at 28 days' age
4. The efficiency factor of silica fume compared to Portland cement with regard to the chloride migration coefficient seems to be around 1.6.
5. The efficiency factor of blast furnace slag seems to be 1.
6. The efficiency factor of fly ash compared to Portland cement with regard to the chloride migration coefficient seems to be around 0.2.
7. Self-desiccation probably played a vital roll to explain the low value of the chloride migration coefficient in concrete with low w/c.

Salt frost scaling

1. No difference was found between salt frost scaling of SCC and NC.
2. Larger salt frost scaling for SCC than for NC was found at 28 days' starting age only.
3. The salt frost scaling increased in SCC with blast furnace slag compared with NC without slag.
4. Less salt frost scaling was found for SCC with 12% fly ash and 5% silica fume than for NC without additives.
5. The mixing order had no influence on the salt frost scaling of SCC.
6. Increased air content decreased the salt frost scaling for SCC as well.
7. Salt frost scaling for SCC decreased with age at start of testing.
8. The amount of filler did not affect the salt frost scaling of SCC.
9. Pouring pressure up to 5.5 m did not affect the salt frost scaling of SCC.
10. Less salt frost scaling was observed of SCC with Ignaberga limestone powder than of SCC with Köping limestone powder.

Internal frost resistance

1. The decrease of fundamental frequency and of mass of concrete was significantly larger for NC than for SCC.
2. SCC with 6% air content resisted internal frost better than SCC with 8% air did, which is inconsistent with previous research.

Sulphate resistance

1. No decrease of fundamental frequency (elastic modulus) or mass of any concrete was observed even after 500 days, whether the concrete was subjected to distilled water, sea water or sodium sulphate, 18 g/kg in distilled water.
2. The largest increase in length due to curing to distilled water, seawater or sodium sulphate, 18 g/kg in distilled water was observed for NC.

3. SCC exhibited larger increase of mass due to water uptake after curing in distilled water, seawater or sodium sulphate, than NC did.

Recommendations

1. It is recommended to use the same amount of cement in SCC with limestone filler as in NC in order to maintain the same chloride migration coefficient in SCC as in NC.
2. A way to lower the chloride migration coefficient is to use 5% silica fume in SCC but in that case the salt frost resistance must be confirmed by measurements.
3. The salt frost resistance is maintained in SCC if the air content is held on the same level as in NC.
4. No effect of the mix proportions of SCC with limestone filler on the internal frost resistance after 300 cycles or on the sulphate resistance after 450 days was observed.

REFERENCES

1. M. Nilsson, Ö. Petersson. The First Bridge Made of Self-compacting Concrete. Väg- och Vattenbyggaren 2/98 (1998) 28-31.
2. L. Söderlind. Full-scale Tests of Self-compacting Concrete for Dwelling Houses. RILEM Symposium on Self Compacting Concrete. Ed.: Skarendahl and Petersson (1999) 723-728.
3. B. Persson. Mix Proportions and Strength of Self-compacting Concrete for Production of High Strength Poles, Piles and Pillars. Contribution to "1. Münchener Baustoffseminar Selbstverdichtender Beton" 9 Oktober 2001. Ed.: Peter Schiessl (2001) 31-39.
4. CTH Rapid Test for Determination of the Chloride Migration Coefficient, D, in Concrete. NT BUILD 492 (2000).
5. L. Tang, L.-O. Nilsson, Modelling of chloride penetration into concrete – Tracing five years' field exposure. Concrete Science Engineering. 2 (2000) 170-175.
6. B. Johannesson. Transport and Sorption Phenomena in Concrete and Other Porous Media. TVBM-1019. LTH Byggnadsmaterial. Lund (2000) 491 pp.
7. AASHTO T 271-831. Rapid Determination of Chloride Permeability of Concrete.
8. M. Geiker, N. Thaulow, P. J. Andersen, Assessment of Rapid Test of Concrete Permeability Test of Concrete with and without Mineral Admixtures. Durability of Concrete and Components. Brighton. Chapman & Hall (1990) 52-61.
9. B. Persson. A Background for the Choice of Mix Design of the Concrete for the Great Belt Link. Report U91.02 Div. Building Materials (1991) 102 pp.
10. D. Boubitsas, K. Paulou. Self Compacting Concrete for Marine Environment. TVBM-5048. Lund Institute of Technology. Lund University. Lund (2000) 55 pp.
11. Lindvall, L.-O. Nilsson. Studies on the Effect of Secondary Cementitious Materials on Chloride Ingress. Nordic Seminar on Durability of Exposed Concrete Containing Secondary Cementitious Materials. Hirtshals. Ed.: D. Bager (2001) 18 pp.
12. L. Tang. Chloride Penetration Profiles and Diffusivity in Concrete under Different Exposure Conditions. Report E-97:3. Building Materials. Chalmers University of Technology. Gothenburg (1997).
13. M. T. Jepsen, D. Mathiesen, C. Munch-Petersen, D. Bager. Durability of Resource Saving "Green" Types of Concrete. Durability of Exposed Concrete Containing Secondary Cementitious Materials. Hirtshals. Ed.: D. Bager (2001) 10 pp.
14. N. Buenfeld. Personal information. Imperial College. London (2001).
15. Persson. Moisture in Concrete Subjected to Different Kinds of Curing. Materials and Structures 30 (1997) 533-544.
16. Persson. Self-desiccation and Its Importance in Concrete Technology. Nordic Concrete Research 20 (1998) 120-129.
17. B. Persson. Shrinkage of High Performance Concrete. Proceedings of an International RILEM Conference on Early Age Cracking

in Concrete. Haifa. 2001. Ed. by A Bentur (2001) 301-311.
18. T.G. Powers, T.L. Brownyard. Studies of the Physical Properties of Hardened Portland Cement Paste. PCA 22 (1948) 473-488, 845-864.
19. L.-O. Nilsson, G. Hedenblad, K. Norling-Mjörnell. Suction after Long Time, HPC Handbook, Svensk Byggtjänst. 2000, 209-226.
20. B. Persson. Seven-year Study of the Effect of Silica Fume. ABCM 7 (1998) 139-155.
21. E. Stoltzer, B. Buhr, S. Engelund. The Faroe Bridges – Chloride Penetration Rate Estimated on a Basis of Measurements from 1988 to 1997. Durability of Exposed Concrete Containing Secondary Cementitious Materials. Hirtshals. Ed.: D. Bager (2001) 19 pp.
22. R. Castel, G. Francois, A. Arliguie. Clarification of Corrosion of Reinforcement in Concrete Structures Exposed to Chloride Environment. Contribution at the fib Meeting and Nordic Mini Seminar. Gothenbourg (2001) 10 pp.
23. M. Collepardi et al. The Kinetics of Chloride Ions Penetration in Concrete. Il Cemento. 67 (1970) 157-164.
24. K. Tuutti. Corrosion of Steel in Concrete. Report 4:82. CBI. Stockholm (1982).
25. L. Tang, L.-O. Nilsson. Rapid Determination of Chloride Diffusitivity of Concrete by Applying an Electric Field. ACI Material Journal 49/1 (1992) 49-53.
26. M. Maage, S Helland, J. E. Carlsen. Chloride Penetration in HPC Exposed to Marine Environment. RILEM Workshop on Durability. Ed.: H. Sommer (1994) 194-207.
27. Poulsen. Prediction Models. STAR 53. Danish Road Direct. Ed. L.-O. Nilsson (1996).
28. M. T. Jepsen. Predicting Concrete Durability by Using Artificial Neural Network. Nordic Seminar on Durability of Exposed Concrete Containing Secondary Cementitious Materials. Hirtshals. Ed.: D. Bager (2001) 11 pp.
29. P. Rougeau, J. L Maillard, C. Mary-Dippe. Comparative Study on Properties of Self Compacting Concrete and HPC Concrete Used in Precast Construction. RILEM Symposium on Self Compacting Concrete. Stockholm. Ed.: Skarendahl and Petersson (1999) 251-261.
30. D. Bager. Aalborg Portland's Durability Project – 18-year judgement. Durability of Exposed Concrete Containing Secondary Cementitious Materials. Hirtshals. Ed.: D. Bager (2001) 30 pp.
31. Peter Utgennant, Per-Erik Petersson. Frost Resistance of Concrete Containing Secondary Cementitious Materials – Experience from Three Field Exposure Sites. Durability of Exposed Concrete Containing Secondary Cementitious Materials. Ed.: D. Bager (2001) 17 pp.
32. M. Friebert. Durability of High Performance Concrete Containing Fly Ash and Silica Fume. Durability of Exposed Concrete Containing Secondary Cementitious Materials. Ed.: D. Bager (2001) 11 pp.
33. R. Auberg. Zuverlässige Prüfung des Frost und Frost-Tausalz. Widerstands von Beton mit dem CDF und CIF Test. University of Essen (1998)
34. Effect of Self-desiccation on Internal Frost Resistance of

Concrete. Self-Desiccation and Its Importance in Concrete Technology. Ed.: B. Persson, G. Fagerlund. TVBM-3075. Lund University. Lund (1997) 227-238.
35. W. Kaempfer, M. Berndt. Estimation of Service Life of Concrete Pipes in Sewer Networks. Durability of Building Materials and Components 1 (1999) 36-45.
36. Ö. Pettersson. Dispersion and Frost Resistance. Investigation of Four Types of Limestone Filler for Self Compacting Concrete. Report 2000-27. Cement and Concrete Research Institute. Stockholm (2000) 14 pp.
37. S. Lindmark. Mechanisms of Salt Frost Scaling of Portland Cement-bound Materials: Studies and Hypotheses. TVBM-1017. Lund University (1998) 266 pp.
38. K. Moir. Sulphate Resistance Test Method. TG 1. CEN/TC51/WG 12. Düsseldorf. (2000) 13 pp.
39. B. Persson. Deformations of House Construction Concrete – Effect of Production Methods on Elastic Modulus, Creep and Shrinkage. TVBM-3088 Lund University. Lund (1999) 71 pp.
40. B. Persson. A Comparison between Deformations of Self Compacting Concrete and Corresponding Properties of Normal Concrete. Cement and Concrete Research 31 (2001) 193-198.
41. E. Prost, G. Pons. Macroscopic and Microscopic Behavior of Self-compacting Concrete Creep and Shrinkage. Creep, Shrinkage and Durability Mechanics of Concrete and Other Quasi-Brittle Materials. Ed.: F.-J. Ulm; Z. P. Bažant, Elsevier Science Ltd (2001) 569-574.
42. A.-M. Poppe; G. de Schütter, Creep and Shrinkage of Self-compacting Concrete. Creep, Shrinkage and Durability Mechanics of Concrete and Other Quasi-Brittle Materials. Ed.: F.-J. Ulm; Z. P. Bažant, Elsevier Science Ltd (2001) 563-568.
43. B. Persson. Long-term Shrinkage of High Performance Concrete. 10th Congress on the Chemistry of Cement. 2ii073. Gothenburg (1997) Ed.: Justnes, H., 9 pp.
44. B. Persson. Shrinkage of High Performance Concrete. Proc. RILEM Conference on Early Age Cracking in Concrete. Haifa. 2001. Ed. by A Bentur (2001) 301-311.
45. B. Persson. Long-term Effect of Silica Fume on the Principal Properties of Low-Temperature-Cured Ceramic. Cement and Concrete Research 27 (1997) 1667-1680.
46. B. Persson. B., Pozzolanic Interaction between Portland Cement and Silica Fume in Concrete. Sixth CANMET/ACI Int. Conference. Bangkok (1998) 631-660.
47. B. Persson. Chloride Diffusion Coefficient and Salt Frost Scaling of Self-Compacting Concrete and of Normal Concrete. Nordic Seminar and fib Meeting. Chalmers University of Technology. Gothenburg. Ed. by L.-O Nilsson (2001) 13 pp.
48. A.M. Neville, J. J. Brooks. Concrete Technology. Longman Singapore Publ (1987) 101.

APPENDICES

APPENDIX 1

Appendix 1.1 – Highway bridge made of Self-compacting Concrete

Appendix 1.1 – Stäket Tunnel made of Self-compacting Concrete

Appendix 1.3 – A pile cap made of Self-compacting Concrete, 60 mm in thickness [3].

Appendix 1.1 – High-way bridge made of Self-compacting Concrete

Photo: Thomas Österberg.

Appendix 1.2 – Stäket Tunnel made of Self-compacting Concrete

Appendix 1.3 – A pile cap in Self-compacting Concrete, 60 mm in thickness [3].

Photo: Giovanni Terrasi.

APPENDIX 2

Appendix 2.1 – Chemical composition and physical properties of cements (%).

Appendix 2.2 – Summary of mix composition (kg/m³) and strength of concrete (series 1) (MPa).

Appendix 2.3 – Mix composition (kg/m³ dry); strength of concrete series 1 (MPa)

Appendix 2.4 – Chloride migration coefficient, D, for normal (NC) and self-compacting (SCC) concrete series 1 ($x10^{12}$ m^2/s)

Appendix 2.5 – Mix composition and chloride migration coefficient, D of NCs [5].

Appendix 2.6 – Mix composition NC mixes tested for use on Great Belt Link [8].

Appendix 2.7 – Mix composition and chloride migration coefficient of SCCs series 2 [10].

Appendix 2.8 – Mix composition and frost resistance of NC and SCC [24].

Appendix 2.1 – Chemical composition and physical properties of cements (%).

Components	Slite Std, N	Degerhamn, SL
CaO	62	65
SiO_2	20	21.6
Al_2O_3	4.4	3.5
Fe_2O_3	2.3	4.4
K_2O	1.4	0.58
Na_2O	0.2	0.05
MgO	3.5	0.78
SO_3	3.7	2.07
Ignition losses	2.4	0.47
CO_2	1.9	0.14
Clinker minerals: C_2S	14	21
C_3S	57	57
C_3A	8	1.7
C_4AF	7	13
Water demand	28%	25%
Initial setting time	154 min.	145 min.
Density	3122 kg/m^3	3214 kg/m^3
Specific surface	364 m^2/kg	305 m^2/kg

N = normal hardening cement; SL = slowly hardening cement

Appendix 2.2 – Summary of mix composition (kg/m³) and strength of concrete (series 1) (MPa).

Mix	Cement, c	Type	Silica fume, s	w/(c+s)	Sand filler	Air (%)	Strength
SCC27	500	SL	50	0.24	50	1.3	141
NC 32	389	N		0.32	106	12	55
SCC38	400	N		0.38	145	1.4	86
SCC50	340	N		0.50	165	3.5	61
SCC80	260	N		0.80	185	1.9	27

Notations: N = normal hardening cement; NC = normal compacting concrete; SCC = self-compacting concrete; SL = slowly hardening cement

Appendix 2.3 – Mix composition (kg/m³ dry); strength of concrete series 1 (MPa)

Material/w/c (%)	**SCC27**	**NC32**	**SCC38**	**SCC50**	**SCC80**
Quartzite 11-16 mm	800	660	620	525	270
Quartzite 8-11 mm	60	135	305	285	395
Sand 0-8 mm, Åstorp	880	694	790	840	1000
Sand, Baskarp, B7 + B6	50	106	145	165	135+50
Cement, Degerhamn Standard	500				
Cement, Slite Standard		389	400	340	260
Silica fume	50				
Air-entrainment agent, L14 (g/m^3)		50		24	
Superplasticiser, branch Cementa 92M		3.6			
Superplasticiser, branch Glenium 51	5.0		2.0	1.2	1.0
Water reducer, branch LP40		1.7			
Water	133	126	153	170	207
Aggregate content	0.72	0.75	0.77	0.78	0.80
Density	2478	2115	2415	2325	2318
Air content (%)	1.3	12	1.4	3.5	1.9
Slump (flow) (cm x cm)	70x72	11	53x54	56x60	54x57
Compr. strength (sealed, MPa): 1 d	19	36	26	23	9
2 d	63	59	65	43	18
7 d	110		76	52	27
28 d	141		86	61	32
90 d	158	55	98	67	34
1 year	171	61	108	76	36
2 years		68			
Compressive strength (air, MPa): 2 d	63	50	65	43	18
7 d	103	54	79	55	27
28 d	124		86	63	32
90 d	134	55	94	67	
1 year	120	64	93	70	35
2 years		62			35
RH, 1 d (sealed):	0.95		0.89	0.95	0.97
2 d	0.91	0.91	0.87	0.95	0.96
7 d	0.88		0.86	0.92	0.92
28 d	0.86		0.88	0.93	0.96
90 d	0.78		0.85	0.88	0.98
1 year	0.82	0.78	0.84	0.90	0.97
2 years		0.82			
RH, 2 d (air):	0.91	0.88	0.87	0.95	0.96
7 d	0.84		0.81	0.91	0.92
28 d	0.82	0.82	0.85	0.83	0.88
90 d	0.71		0.73	0.82	0.67
1 year	0.62	0.70	0.66		0.56
2 years		0.60		0.77	

Appendix 2.4 – Chloride migration coefficient, D, for normal (NC) and self-compacting (SCC) concrete series 1 (x10^{12} m^2/s)

Concrete	Specimen 1 1						Specimen 2						Specimen 3						Average
Measured value	**U**	**T**	**L**	**x_d**	**t**	**D**	**U**	**T**	**L**	**x_d**	**t**	**D**	**U**	**T**	**L**	**x_d**	**t**	**D**	**$D_{average}$**
SCC27	60	21.8	50	21.6	96	1.26	60	21.8	50	12	96	0.68	60	21.8	50	29.6	96	1.74	1.22
NC32	50	23.3	50	10.6	24	2.84	50	23.3	50	11.3	24	3.04	50	23.3	50	10.3	24	2.75	2.88
SCC38	30	21.6	50	20.2	24	9.30	30	21.6	50	20.6	24	9.49	30	21.6	50	18.44	24	8.43	9.07
SCC50	20	21.7	50	40.9	24	29.79	20	21.7	50	40.5	24	29.48	20	21.7	50	42.25	24	30.83	30.04
SCC80	15	22.1	50	50	24	50.11	15	22.1	50	50	24	50.11	15	22.1	50	50	24	50.11	50.11

Notations [4]: $D = \{0.0239\cdot(273+T)\cdot L\cdot/[(U-2)\cdot t]\cdot\cdot[x_d-0.0239\cdot[(273+T)\cdot l\cdot x_d)/(U-2)]^{½}$

t denotes the test duration (h)

x_d denotes the average chloride penetration depth (mm)

D denotes the non-steady-state migration coefficient, x10^{-12} m^2/s

L denotes the thickness of the specimen (mm)

T denotes the average initial and final temperatures in the anolyte solution (°C)

.

Appendix 2.5 – Mix composition and chloride migration coefficient, D of NCs [5].

Material/mix – water-binder ratio (%)	1-40	1-50	H40	2-40
Cement Degerhamn	420	370	399	420 (Slite Std)
Silica fume			21	
Water	168	185	168	168
Air content (% vol.)	6	6.4	5.9	6.2
Aggregate	1692	1684	1685	1675
D (10^{-12} m^2/s)	8.1	19.9	2.7	7.1

Appendix 2.6 – Mix composition NC mixes tested for use on Great Belt Link [8].

Material/mix	A	B	C	D	E	F	G	H	I	J
SRPC (sulphate resistant cement)	310	405	370	345	370	345				
RPC (rapid cement)							310	405	370	345
PFA (fly ash)	70		70		70		70		70	
SF (silica fume)	30			30		30	30			30
w/c	0.34	0.33	0.32	0.33	0.31	0.32	0.36	0.34	0.33	0.35
Current pass. (coulomb)	220	1730	1050	150	1150	190	150	1150	1030	250

Appendix 2.7 – Mix composition and chloride migration coefficient of SCCs series 2 [10].

Material/mix composition	D	F	G	RO II	T
Crushed aggregate Bålsta 8-16	496	494	580	876	495
Natural sand Bålsta 0-8	699	728	800	727	714
Natural sand SÄRÖ 0-2	505	465	220	149	521
Fly ash	89	55			
Glass filler			60		
Cement Aalborg (CEMI)	375				
Cement Degerhamn (CEMI)		440	420	438	
Slag cement (CEMIII, 68% slag)					470
Silica fume Elkem (granulate)	35	18	21		
Air-entrainment (wet, g, 10% dry)	0,498	0,501	0,500	482	0,498
Superplasticiser (wet, 35% dry)	5,25		4,24	5,92	3,52
Water	191	172	162	171	183
w/b	0,38	0,38	0,37	0,39	0,39
Slump (flow) (mm)	690	725	720	150	737
Flow time until diameter 500 mm (s)	7	8	8		6,5
Density	2247	2300	2306	2368	2281
Aggregate content (>0.125, % vol.)	0,64	0,64	0,60	0,66	0,65
Air content (%)	6,4	6,2	6,3	6,1	5,7
28-day cube strength (100 mm, MPa)	61	70	64	63	79
D (x10^{12} m^2/s)	5,8	5,5	4,6	9,6	1,9
Salt frost scaling 112 cycles (kg/m^2)	0,461	0,174	0,182	0,387	0,509

Notations: D = Danish fly ash mix composition; F = optimum fly ash mix composition; G = glass filler mix composition; RO II = reference mix composition; T = German slag mix composition

Appendix 2.8 – Mix composition and frost resistance of NC and SCC [29].

Material, cement type, w/c	BAP3	BAP5	HPC
Coarse aggregate 6-14 mm	267	267	
Sand 3-6 mm	543	544	
Sand 0-4 mm	886	887	
Limestone powder	101	100	
Cement CEMI 52.5 R	352	350	323
Plasticiser	3.2	5.0	
Superplasticiser	2.3	0.9	
Water	197	190	
w/c	0.56	0.54	
Water-powder ratio, w/p	0.44	0.42	
Aggregate content (>0.125 mm, % vol.)	0.64	0.64	
Slump flow (mm)	600	580	
28-day strength (MPa)	56	58	72
Decrease of internal transversal resonance (%):			
150 frost cycles	0	13	100
300 frost cycles	7	18	-
Increase of length (%):			
150 frost cycles	0.01	0.13	0.39
300 frost cycles	0.01	0.22	-
Salt frost scaling (kg/m²):			
28 frost cycles	0.9	1.3	1.8
56 frost cycles	0.9	1.4	3.7

APPENDIX 3

Appendix 3.1 – Mix composition and properties of NC and SCC in series 3.

Appendix 3.2 – The determination of the chloride migration coefficient, D, in an apparatus developed by Tang [4].

Appendix 3.3 – Test voltage and duration for concrete with normal binder content during determination of the chloride migration coefficient, D, in an apparatus developed by Tang [4].

Appendix 3.4 – Two frost cycles daily varying between – 20 and 20 °C during the frost tests.

Appendix 3.1 – Mix composition and properties of NC and SCC in series 3.

Material/mix composition	KN	KOB	KN8	KO	KOT	SO	RO	ROII
Crushed aggregate Bålsta 8-16	363	371	355	367	363	402	862	876
Natural sand Bålsta 0-8	853	872	836	864	855	786	715	727
Natural sand SÄRÖ 0-2	316	135	309	320	316	422	146	149
Limestone filler Köping 500	183	375	180	186	184	94	0	
Cement Degerhamn	418	427	409	423	419	416	431	438
Microair (wet, g, 10% dry)	585	213	1203	106	117	125	474	482
Superplasticiser(wet, 35% dry)	2,97	4,13	3,2	3,39	3,69	2,99	7,32	5,92
Water	163	167	160	165	163	162	168	171
w/c	0,39	0,39	0,39	0,39	0,39	0,39	0,39	0,39
Air content (%)	5,6	4,9	8	5,5	6,3	5,6	5,8	6,1
28-day cube strength (MPa)	63	84	50	75	75	61	68	63
Slump flow (mm)	720	780	735	620	640	710	110	150
Flow time until 500 mm (s)	5	7	8	10	8	5	-	-
Density	2297	2348	2250	2323	2300	2285	2325	2368
Aggregate with filler (% vol.)	0,643	0,654	0,630	0,652	0,645	0,641	0,650	0,661

Notations: B = increased amount of filler; K = Köping 500 limestone filler; N = new way of mixing (filler last); O = ordinary way of mixing (filler first); R = reference; S = Ignaberga 200 limestone filler; T = 5.5 m hydrostatic pouring pressure instead of 0.23 m; II = second; 8 = 8 % air content.

Appendix 3.2 – The determination of the chloride migration coefficient, D, in an apparatus developed by Tang [4].

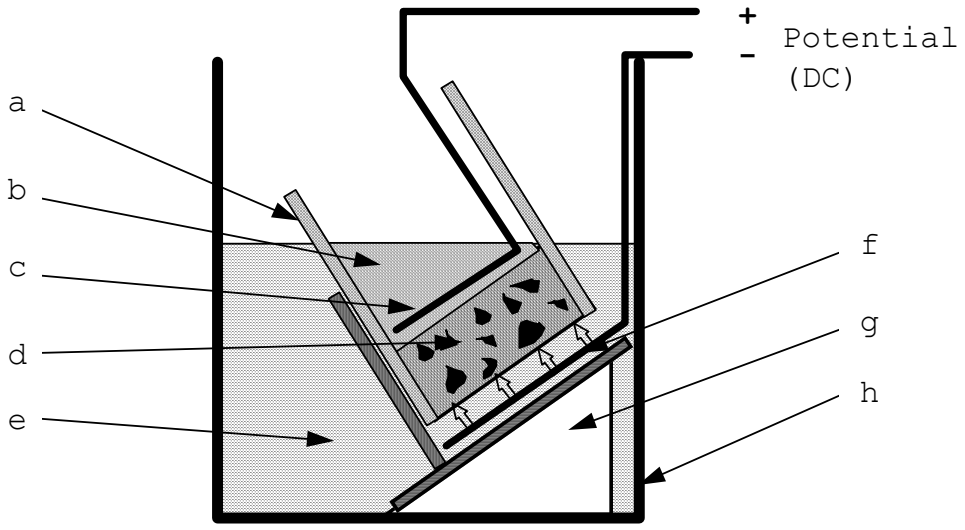

a. Rubber sleeve
b. Anolyte
c. Anode
d. Specimen
e. Catholyte
f. Cathode
g. Plastic support
h. Plastic box

Appendix 3.3 – Test voltage and duration for concrete with normal binder content during determination of the chloride migration coefficient, D, in an apparatus developed by Tang [4].

Initial current I_{30V} (mA)	Adjusted voltage (V)	Approximate new initial current I_0 (mA)	Test duration (h)
$I_{30V} < 5$	60	$I_0 < 10$	96
$5 \leq I_{30V} < 10$	60	$10 \leq I_0 < 20$	48
$10 \leq I_{30V} < 15$	60	$20 \leq I_0 < 30$	24
$15 \leq I_{30V} < 20$	50	$25 \leq I_0 < 35$	24
$20 \leq I_{30V} < 30$	40	$25 \leq I_0 < 40$	24
$30 \leq I_{30V} < 40$	35	$35 \leq I_0 < 50$	24
$40 \leq I_{30V} < 60$	30	$40 \leq I_0 < 60$	24
$60 \leq I_{30V} < 90$	25	$50 \leq I_0 < 75$	24
$90 \leq I_{30V} < 120$	20	$60 \leq I_0 < 80$	24
$120 \leq I_{30V} < 240$	15	$60 \leq I_0 < 120$	24
$240 \leq I_{30V} < 600$	10	$80 \leq I_0 < 200$	24
$I_{30V} > 600$	10	$I_0 > 200$	6

Appendix 3.4 – Two frost cycles daily varying between –20 and 20 °C during the frost tests.

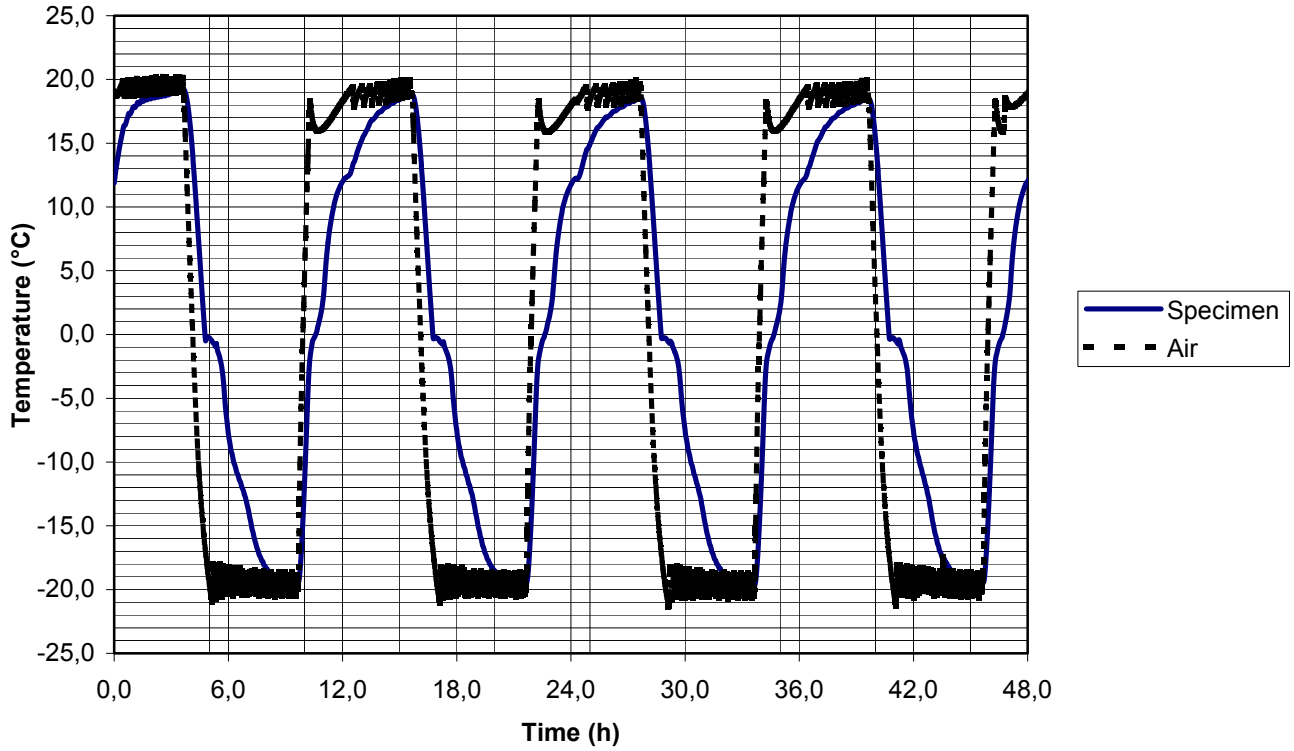

APPENDIX 4

Appendix 4.1 – Strength development of concrete in series 3.

Appendix 4.2 – Shrinkage of concrete in series 3 up to 1 day's age

Appendix 4.3 – Chloride migration coefficient, D, for concretes in series 3 ($x10^{12}$ m^2/s)

Appendix 4.4 – Salt frost scaling for concrete in series 3 (g/sample)

Appendix 4.1 – Strength development of concrete in series 3.

Age (days)	1			7	28			90
Mix proposition	1	2	Average		1	2	Average	Average
KN	19.5	22.0	20.8	50.0	63.5	63.0	63.3	76.0
KOB	26.0	26.0	26.0	63.0	83.0	84.0	83.5	92.0
KN8	14.0	14.0	14.0	38.0	49.5	50.0	49.8	58.0
KO	23.5	24.0	23.8	56.0	74.0	75.0	74.5	81.0
KOT	23.5	24.0	23.8	56.0	74.0	75.0	74.5	81.0
SO	16.0	16.0	16.0	45.0	60.0	61.0	60.5	70.0
RO	24.5	24.5	24.5	54.0	67.5	67.5	67.5	79.0
ROII	16.5	16.5	16.5	48.0	62.5	62.5	62.5	75.0

Notations: B = increased amount of filler; K = Köping 500 limestone filler; N = new way of mixing (filler last); O = ordinary way of mixing (filler first); R = reference; S = Ignaberga 200 limestone filler; T = 5.5 m hydrostatic pouring pressure instead of 0.23 m; II = second; 8 = 8 % air content.

Appendix 4.2 – Shrinkage of concrete in series 3 up to 1 day's age

Mix composition	Measured 25 mm from the surface (mm)	Measured 75 mm from the surface (mm)	Estimated in the surface (‰)
KN	0.043	0.021	0.18
KOB	0.056	0.045	0.13
KN8	0.028	-0.052	0.23
KO	0.055	0.043	0.20
KOT	0.055	0.043	0.20
SO	0.050	0.039	0.20
RO	0.03	0.020	0.15

Notations: B = increased amount of filler; K = Köping 500 limestone filler; N = new way of mixing (filler last); O = ordinary way of mixing (filler first); R = reference; S = Ignaberga 200 limestone filler; T = 5.5 m hydrostatic pouring pressure instead of 0.23 m; II = second; 8 = 8 % air content.

Appendix 4.3 – Chloride migration coefficient, D, for concretes in series 3 (x10 ^{12} m2/s)

Mix proportion	Sample 1						Sample 2						Sample 3						Average
Value	U	T	L	x_d	t	D	U	T	L	x_d	t	D	U	T	L	x_d	t	D	$D_{average}$
KN 28	25	22.15	50	25.6	24	14.41	25	22.2	50.0	29	24	16.46	25	22.15	50	28.25	24	16.00	15.62
KN 90	30	22.2	50	20.1	24	9.27	30	22.2	50.0	24.1	24	11.24	30	22.2	50	22	24	10.20	10.24
KOB 28	25	21.5	50	24.14	24	13.50	25	21.5	50.0	24.86	24	13.94	25	21.5	50	23.57	24	13.16	13.72
KOB 90	30	21.7	50	20	24	9.20	30	21.8	50.0	18.7	24	8.6	30	21.7	50	19.3	24	8.86	8.88
KN8 28	25	22.3	50	25.1	24	14.11	25	22.3	50.0	26.9	24	15.20	25	22.3	50	28.9	24	16.40	15.24
KN8 90	30	22.7	49	27.9	24	12.90	25	22.7	49.0	20.3	24	11.05	25	22.7	49	22.3	24	12.22	11.98
KO 28	20	23	51	31.9	24	23.39	20	23.0	51.0	32.3	24	23.70							23.55
KO 90	25	21.75	50	19.9	24	10.98	25	21.8	50.0	20.3	24	11.22							11.10
KOT 28	25	23.3	50	22	24	12.29	25	23.3	50.0	23.7	24	13.32	25	23.3	50	22.3	24	12.47	12.70
KOT 90	30	23.2	50	20.9	24	9.69	30	23.2	50.0	18.4	24	8.46	25	23.2	50	17	24	9.30	9.07
SO 28	25	21.8	50	27.2	25	14.74	25	21.8	50.0	26.3	25	14.22	25	21.8	50	29.1	25	15.84	14.48
SO 90	25	21	52.5	18.9	24	10.84	25	21.0	52.5	21	24	12.15	25	21	52.5	18.3	24	10.47	11.49
RO 28	30	21.5	50	20	24	9.20	30	21.5	50.0	18.9	24	8.66							8.93
RO 90	30	20.8	50	18.5	24	8.44	30	20.8	50.0	14	24	6.25	30	20.8	50	14.8	24	6.64	7.11
RO 28 – 90h lagr.	30	21.5	50	22	24	10.18	30	21.5	50.0	18.3	24	8.36	30	21.5	50	20	24	9.20	9.25
ROII 28	25	21.2	51	18.1	24	10.08	25	21.2	51.0	16.2	24	8.93	25	21.2	51	17.9	24	9.96	9.66
ROII 90	30	21.5	52	12.1	24	5.54	30	21.5	52.0	14.7	24	6.84	30	21.5	52	12.7	24	5.84	6.07

Notations: see above; 90 = 90 days' starting age.

Appendix 4.4 – Salt frost scaling for concrete in series 3 (g/sample)

Betong	Start				28 cycles				56 cycles				112 cycles			
Sample	1	2	3	Average	1	2	3	Average	1	2	3	Average	1	2	3	Average
KN 28	626.0	637.3	619.7	627.7	613.3	625.3	609.3	466.3	606.9	616.9	600.0	786.5	600.7	610.2	591.7	1068
KN 90	661.4	647.9	656.0	655.1	653.8	638.0	647.4	346.8	647.0	632.0	641.5	595.2	640.9	624.0	635.8	858
KOB 28	659.1	659.9	653.6	657.5	652.2	654.4	643.4	300.3	646.2	647.9	623.9	725.4	634.8	639.2	623.6	996
KOB 90	635.9	635.9	657.7	643.2	632.6	631.3	654.4	148.8	626.0	622.0	645.1	483.6	621.1	614.8	640.9	700
KN8 28	619.3	637.7	620.1	625.7	613.8	633.1	614.8	204.6	609.9	627.9	609.1	401.2	602.6	622.0	601.4	679
KN8 90	619.3	631.9	634.2	628.5	620.1	624.1	622.8	244.5	612.1	625.3	628.2	263.1	606.9	622.0	621.4	466
KO 28	628.7	631.9	634.2	631.6	620.1	624.1	622.8	369.4	614.5	616.8	610.9	698.8	603.6	606.6	595.7	1181
KO 90	638.4	639.7	640.3	639.5	631.2	630.6	632.2	324.2	627.1	624.5	626.2	539.4	619.4	615.9	614.7	909
KOT 28	655.1	644.3	643.3	647.6	646.9	635.0	634.8	345.4	641.0	627.2	631.3	574.0	631.3	615.3	618.7	1028
KOT 90	657.9	657.1	658.9	658.0	649.4	650.0	650.0	325.5	643.8	642.7	642.0	603.2	632.3	634.6	639.7	894
SO 28	631.3	622.6	613.7	622.5	620.7	612.8	604.7	390.6	617.6	609.5	600.0	538.1	612.9	604.8	595.4	724
SO 90	629.2	635.8	619.1	628.0	624.9	632.5	615.1	154.1	622.9	631.5	613.1	220.5	618.2	626.5	604.4	465
RO 28	644.6	649.6	650.9	648.4	638.5	643.7	644.8	240.5	627.6	634.2	634.7	645.7	618.0	626.8	625.6	992
RO 90	650.5	647.0	652.5	650.0	642.1	638.8	642.3	356.1	630.6	630.7	634.8	716.1	622.1	617.5	624.1	1147
ROII 28	639.0	661.9	677.9	659.6	636.3	658.9	674.4	122.2	633.7	657.2	671.1	223.2	629.2	652.4	668.1	387
ROII 90	599.8	591.8	625.3	605.6	598.4	590.1	622.5	78.4	596.1	587.7	618.6	192.6	592.6	583.7	614.3	349

Notations: B = increased amount of filler; K = Köping 500 limestone filler; N = new way of mixing (filler last); O = ordinary way of mixing (filler first); R = reference; S = Ignaberga 200 limestone filler; T = 5.5 m hydrostatic pouring pressure instead of 0.23 m; II = second; 8 = 8 % air content.

APPENDIX 5

Appendix 5.1 – Internal frost resistance of mix proportions D, F, G, RO II and T in series 2

Mix	Test	Sort	Start value				100 cycles				300 cycles			
Sample			1	2	3	Av..	1	2	3	Est.	1	2	3	Est..
D 28	Frequency	(Hz)	6400.0	6430.0	6610.0	6480.0	6470.0	6470.0	6640.0	0.7	6370.0	6200.0	6470.0	-2.1
	Length	(mm)	151.9	152.0	147.9	150.6	151.7	152.2	147.7	-0.4	151.8	152.1	147.8	-0.2
	Mass	(g)	679.3	678.8	656.2	671.4	679.8	679.6	657.2	0.0	672.8	673.5	648.7	-0.2
F 28	Frequency	(Hz)	6550.0	6720.0	6570.0	6613.3	6610.0	6780.0	6620.0	0.9	6600.0	6750.0	6550.0	0.3
	Length	(mm)	152.8	150.8	153.8	152.5	152.6	150.4	153.4	-2.2	152.5	150.5	153.5	-2.0
	Mass	(g)	702.8	695.1	703.6	700.5	704.3	696.6	705.2	0.1	703.5	696.0	704.3	0.0
G 28	Frequency	(Hz)	6840.0	6700.0	6640.0	6726.7	6850.0	6810.0	6660.0	0.7	6800.0	6700.0	6570.0	-0.5
	Length	(mm)	148.9	151.0	152.0	150.6	148.9	151.0	152.0	0.0	149.2	151.0	152.2	1.1
	Mass	(g)	689.8	698.8	702.9	697.2	690.8	699.5	703.9	0.0	689.6	697.6	700.8	0.0
ROII 28	Frequency	(Hz)	6420.0	6480.0	6880.0	6593.3	6300.0	6660.0	6920.0	0.5	6270.0	6500.0	6620.0	-2.0
	Length	(mm)	150.9	151.3	146.4	149.5	150.9	151.2	146.7	0.4	150.8	151.3	146.3	-0.4
	Mass	(g)	711.7	708.3	687.8	702.6	706.6	706.4	684.1	-0.1	692.0	697.6	667.9	-0.6
T 28	Frequency	(Hz)	6780.0	6830.0	6800.0	6803.3	6800.0	6870.0	6830.0	0.4	6820.0	6910.0	6890.0	1.0
	Length	(mm)	150.1	150.8	151.4	150.8	150.2	150.8	151.4	0.2	150.2	150.8	151.3	0.0
	Mass	(g)	696.5	693.8	696.5	695.6	696.6	694.3	696.6	0.0	695.8	694.2	696.3	0.0

Notations: D = Danish fly ash mix composition; F = optimum fly ash mix composition; G = glass filler mix composition; RO II = reference mix composition; T = German slag mix composition. Est. = estimation of change of fundamental frequency (%), length (‰) and mass loss (kg/m³).

Appendix 5.2 – Internal frost resistance of mix proportions KN, KOB, KN8 and KO in series 3

Mix	Test	Sort	Start value				100 cycles				300 cycles			
Sample			1	2	3	Av..	1	2	3	Est.	1	2	3	Est..
KN 28.	Frequency	(Hz)	6720.0	6770.0	6620.0	6703.3	6680.0	6740.0	6570.0	-0.6	6540.0	6560.0	6280.0	-3.6
	Length	(mm)	149.1	150.5	150.4	150.0	149.0	150.5	150.5	0.0	149.0	150.8	150.6	0.9
	Mass	(g)	686.0	695.2	696.2	692.5	686.9	694.7	696.1	0.0	675.6	685.8	689.1	-0.3
KN 90	Frequency	(Hz)	6750.0	6720.0	6880.0	6783.3	6750.0	6800.0	6970.0	0.8	6580.0	6680.0	6860.0	-1.1
	Length	(mm)	149.9	149.9	150.8	150.2	150.3	150.4	150.5	1.3	150.0	150.3	150.6	0.7
	Mass	(g)	698.5	700.4	704.4	701.1	699.0	701.2	706.1	0.0	689.0	695.5	702.9	-0.2
KOB 28	Frequency	(Hz)	6810.0	6630.0	6760.0	6733.3	6870.0	6690.0	6750.0	0.5	6720.0	6560.0	6700.0	-1.1
	Length	(mm)	151.3	152.3	150.7	151.4	151.1	152.2	150.7	-0.7	151.2	152.3	150.6	-0.4
	Mass	(g)	717.1	720.1	713.4	716.9	718.3	722.5	715.9	0.1	714.4	720.0	712.4	0.0
KOB 90	Frequency	(Hz)	6920.0	6930.0	6900.0	6916.7	6880.0	6900.0	6870.0	-0.5	6710.0	6680.0	6790.0	-2.7
	Length	(mm)	151.2	151.5	150.9	151.2	151.1	151.6	150.9	0.0	151.2	151.4	151.0	0.0
	Mass	(g)	717.9	714.6	714.8	715.8	720.4	717.8	716.9	0.1	711.7	703.9	714.4	-0.2
KN8 28	Frequency	(Hz)	6420.0	6450.0	6360.0	6410.0	6190.0	6400.0	6170.0	-2.4	5820.0	6120.0	5950.0	-7.0
	Length	(mm)	150.7	150.9	151.4	151.0	150.7	151.2	151.5	0.9	150.9	151.3	151.6	1.8
	Mass	(g)	679.8	686.5	682.3	682.9	680.7	688.1	683.0	0.0	660.7	674.2	665.5	-0.6
KN8 90	Frequency	(Hz)	6300.0	6350.0	6570.0	6406.7	6190.0	6290.0	6380.0	-1.9	5870.0	5910.0	6210.0	-6.4
	Length	(mm)	149.5	150.5	151.2	150.4	149.8	150.5	150.7	-0.4	150.1	150.6	151.1	1.3
	Mass	(g)	678.2	681.2	681.6	680.3	676.6	680.0	681.2	0.0	660.6	660.4	661.7	-0.7
KO 28	Frequency	(Hz)	6600.0	6260.0	6560.0	6473.3	6660.0	6190.0	6540.0	-0.2	6540.0	6650.0	6500.0	1.4
	Length	(mm)	150.9	150.6	150.6	150.7	151.0	150.7	150.5	0.2	151.1	151.6	150.8	3.1
	Mass	(g)	691.3	688.6	690.5	690.1	691.3	687.2	688.4	0.0	684.9	644.1	682.5	-0.7
KO 90	Frequency	(Hz)	6740.0	6740.0	6730.0	6736.7	6680.0	6740.0	6600.0	-0.9	6570.0	6660.0	6520.0	-2.3
	Length	(mm)	151.2	151.1	150.7	151.0	151.1	150.9	150.7	-0.7	151.0	150.9	150.7	-0.9
	Mass	(g)	696.0	697.4	698.1	697.2	697.2	697.6	696.8	0.0	690.3	688.4	690.2	-0.3

Notations: B = increased amount of filler; K = Köping 500 limestone filler; N = new way of mixing (filler last); O = ordinary way of mixing (filler first); R = reference; S = Ignaberga 200 limestone filler; T = 5.5 m hydrostatic pouring pressure instead of 0.23 m; II = second; 8 = 8 % air content. Est. = estimation of change of fundamental frequency (%), length (‰) and mass loss (kg/m³).

Appendix 5.3 – Internal frost resistance of mix proportions KOT, SO, RO and ROII in series 3

Mix	Test	Sort	Start value				100 cycles				300 cycles			
Sample			1	2	3	Av..	1	2	3	Est.	1	2	3	Est..
KOT 28	Frequency	(Hz)	6660.0	6780.0	6820.0	6753.3	6730.0	6780.0	6910.0	0.8	6700.0	6750.0	6850.0	0.2
	Length	(mm)	151.0	151.4	150.7	151.0	151.3	151.6	150.5	0.7	151.4	151.7	150.7	1.5
	Mass	(g)	714.8	717.4	712.3	714.8	716.2	719.1	714.0	0.1	713.3	718.2	712.3	0.0
KOT 90	Frequency	(Hz)	6920.0	6910.0	6870.0	6900.0	6890.0	6840.0	6840.0	-0.6	6870.0	6830.0	6750.0	-1.2
	Length	(mm)	150.3	150.7	150.8	150.6	150.4	150.7	150.9	0.4	150.2	150.6	150.8	-0.4
	Mass	(g)	712.8	717.5	717.5	715.9	714.1	719.6	719.3	0.1	710.8	712.2	714.3	-0.1
SO 28	Frequency	(Hz)	6320.0	6360.0	6680.0	6453.3	6430.0	6470.0	6770.0	1.6	6440.0	6480.0	6720.0	1.4
	Length	(mm)	150.7	150.6	149.4	150.2	150.8	150.5	149.3	-0.2	150.7	150.4	149.4	-0.4
	Mass	(g)	696.6	692.3	690.7	693.2	698.8	694.7	691.8	0.1	694.3	689.7	683.3	-0.1
SO 90	Frequency	(Hz)	6570.0	6560.0	6530.0	6553.3	6510.0	6580.0	6540.0	-0.2	6400.0	6510.0	6470.0	-1.4
	Length	(mm)	150.5	150.4	150.8	150.6	151.2	150.2	150.7	0.9	151.1	150.4	150.8	1.3
	Mass	(g)	701.1	690.6	697.5	696.4	702.5	693.3	699.8	0.0	693.6	687.8	692.7	-0.2
RO 28	Frequency	(Hz)	6650.0	6700.0	6800.0	6716.7	6600.0	6400.0	6700.0	-2.2	3250.0	1260.0	1380.0	-70.8
	Length	(mm)	152.2	151.8	151.6	151.8	152.4	152.0	151.6	1.1	152.1	152.6	153.1	5.0
	Mass	(g)	717.9	714.8	714.4	715.7	715.5	712.5	712.5	-0.1	686.4	667.6	648.5	-1.8
RO 90	Frequency	(Hz)	6770.0	6650.0	6930.0	6783.3	5760.0	6060.0	4050.0	-22.0	1500.0	1300.0	900.0	-81.8
	Length	(mm)	151.4	151.3	151.2	151.3	151.7	151.5	151.7	2.2	152.3	152.8	153.0	9.3
	Mass	(g)	715.0	713.8	710.5	713.1	712.0	711.3	700.6	-0.2	664.0	664.0	594.0	-2.6
ROII 28	Frequency	(Hz)	6420.0	6480.0	6880.0	6593.3	6300.0	6660.0	6920.0	0.5	6270.0	6500.0	6620.0	-2.0
	Length	(mm)	150.9	151.3	146.4	149.5	150.9	151.2	146.7	0.4	150.8	151.3	146.3	-0.4
	Mass	(g)	711.7	708.3	687.8	702.6	706.6	706.4	684.1	-0.1	692.0	697.6	667.9	-0.6
ROII 90	Frequency	(Hz)	6710.0	6750.0	6710.0	6723.3	6700.0	6800.0	6740.0	0.3	6400.0	6780.0	6640.0	-1.7
	Length	(mm)	150.6	150.3	151.3	150.7	150.7	150.5	151.2	0.4	150.9	150.6	151.3	1.3
	Mass	(g)	710.6	710.9	704.9	708.8	710.5	709.2	705.3	0.0	699.6	703.2	696.6	-0.3

Notations: B = increased amount of filler; K = Köping 500 limestone filler; N = new way of mixing (filler last); O = ordinary way of mixing (filler first); R = reference; S = Ignaberga 200 limestone filler; T = 5.5 m hydrostatic pouring pressure instead of 0.23 m; II = second; 8 = 8 % air content. Est. = estimation of change of fundamental frequency (%), length (‰) and mass loss (kg/m³).

Appendix 5.4 – Resistance to sulphates (5 °C, internal fundamental frequency, Hz)

Mix	Test	Sort	Start value			90 days			450 days		
			H_2O	H_2O-sea	Na_2SO_4	H_2O	H_2O-sea	Na_2SO_4	H_2O	H_2O-sea	Na_2SO_4
KN 28	Frequency	(Hz)	6600.0	6820.0	6830.0	6660.0	6880.0	6950.0	6970.0	7170.0	7220.0
	Length	(mm)	150.3	149.6	148.6	150.3	149.5	148.7	150.4	149.7	148.9
	Mass	(g)	693.3	693.8	684.9	696.1	696.6	687.1	698.0	701.4	689.8
KN 90	Frequency	(Hz)	6900.0	6850.0	6970.0	7060.0	6870.0	7040.0	7220.0	7110.0	7190.0
	Length	(mm)	149.8	150.5	151.0	149.9	150.7	151.4	149.8	150.6	151.6
	Mass	(g)	703.2	702.3	701.4	707.5	707.0	704.9	708.5	708.5	708.5
KOB 28	Frequency	(Hz)	6800.0	6780.0	6960.0	6990.0	7000.0	7180.0	7110.0	7140.0	7280.0
	Length	(mm)	151.1	150.9	151.1	151.3	151.3	151.1	151.3	151.3	151.1
	Mass	(g)	714.4	715.5	722.2	719.7	719.2	726.0	720.5	719.8	727.8
KOB 90	Frequency	(Hz)	6760.0	6990.0	6810.0	6890.0	7150.0	6980.0	6980.0	7210.0	6980.0
	Length	(mm)	151.9	150.4	151.7	152.1	150.1	151.7	152.1	150.3	151.7
	Mass	(g)	714.2	703.7	717.2	724.2	713.1	721.1	726.4	715.1	722.9
KN8 28	Frequency	(Hz)	6250.0	6420.0	6280.0	6280.0	6450.0	6310.0	6570.0	6800.0	6660.0
	Length	(mm)	151.0	151.0	150.9	150.8	150.9	150.8	151.0	151.2	151.1
	Mass	(g)	673.1	681.2	677.0	676.1	683.9	678.7	677.2	684.7	681.5
KN8 90	Frequency	(Hz)	6340.0	6380.0	6430.0	6570.0	6560.0	6630.0	6630.0	6630.0	6670.0
	Length	(mm)	151.3	150.7	151.0	151.4	150.5	151.1	151.5	150.6	151.3
	Mass	(g)	678.4	679.2	683.0	682.7	683.3	686.1	682.8	685.3	688.7
KO 28	Frequency	(Hz)	6600.0	6620.0	6130.0	6770.0	6820.0	6470.0	6920.0	7000.0	6610.0
	Length	(mm)	150.7	150.5	150.3	150.9	150.5	150.7	151.0	150.7	150.6
	Mass	(g)	692.7	692.8	691.7	697.2	697.0	695.4	698.5	700.5	698.9
KO 90	Frequency	(Hz)	6720.0	6860.0	6770.0	6940.0	6950.0	6960.0	7130.0	7030.0	7000.0
	Length	(mm)	149.7	150.5	150.5	149.9	150.5	150.4	149.8	150.7	150.3
	Mass	(g)	702.9	697.6	702.3	707.2	701.9	705.3	707.0	702.2	707.6
KOT 28		(Hz)	6850.0	6800.0	6870.0	7010.0	6970.0	7010.0	7180.0	7150.0	7180.0
		(mm)	151.3	151.5	150.9	151.3	151.6	150.8	151.5	151.8	151.0
		(g)	714.1	721.0	717.0	718.0	724.8	720.2	719.8	726.7	722.3
KOT 90		(Hz)	6920.0	6920.0	7000.0	7000.0	7020.0	7010.0	7110.0	7110.0	7220.0
		(mm)	150.8	150.5	150.5	150.9	150.6	150.6	150.8	150.6	150.6
		(g)	716.3	710.9	718.0	719.9	715.0	721.0	720.3	716.1	722.5
SO 28		(Hz)	6520.0	6420.0	6530.0	6780.0	6750.0	6920.0	6900.0	6870.0	6950.0
		(mm)	150.3	149.4	149.2	150.4	149.4	149.2	150.5	149.4	149.2
		(g)	696.4	689.7	700.2	701.7	694.7	704.8	702.0	699.7	707.3
SO 90		(Hz)	6720.0	6610.0	6520.0	6870.0	6750.0	6700.0	6930.0	6820.0	6780.0
		(mm)	150.4	150.8	150.2	150.3	150.8	150.3	150.5	150.7	150.3
		(g)	700.0	696.5	690.4	704.0	703.3	694.1	705.9	703.0	696.9
RO 28		(Hz)	6640.0	6510.0	6960.0	6770.0	6640.0	7130.0	7000.0	6860.0	7330.0
		(mm)	152.0	152.0	151.0	152.5	152.4	151.2	152.6	152.5	151.3
		(g)	722.0	720.0	714.0	723.3	722.3	715.2	724.8	727.9	717.9
RO 90		(Hz)	6660.0	6630.0	6840.0	6830.0	6770.0	6990.0	6960.0	6930.0	7120.0
		(mm)	151.4	151.6	150.9	151.5	151.7	151.0	151.4	151.9	152.2
		(g)	712.8	704.0	716.6	717.1	707.8	719.2	718.6	710.6	721.2

B = increased amount of filler; K = Köping limestone filler; N = new way of mixing (filler last); O = ordinary way of mixing (filler first); R = reference; S = Ignaberga 200; T = 5.5 m hydrostatic pouring pressure instead of 0.23 m; 8 = 8 % air content.

Appendix 5.5 – Resistance to sulphates – Estimation of change of fundamental frequency (%), length (‰) and mass loss (kg/m³).

Age (days)	90				450		
Fundamental frequency (%)	H2O	H2O-sea	Na2SO4		H2O	H2O-sea	Na2SO4
KN 28	0.91	0.88	1.76	KN 28	5.61	5.13	5.71
KN 90	2.32	0.29	1.00	KN 90	4.64	3.80	3.16
KOB 28	2.79	3.24	3.16	KNB 28	4.56	5.31	4.60
KOB 90	1.92	2.29	2.50	KNB 90	3.25	3.15	2.50
KN8 28	0.48	0.47	0.48	KN8 28	5.12	5.92	6.05
KN8 90	3.63	2.82	3.11	KN8 90	4.57	3.92	3.73
KO 28	2.58	3.02	5.55	KO 28	4.85	5.74	7.83
KO 90	3.27	1.31	2.81	KO 90	6.10	2.48	3.40
KOT 28	2.34	2.50	2.04	KOT 28	4.82	5.15	4.51
KOT 90	1.16	1.45	0.14	KOT 90	2.75	2.75	3.14
SO 28	3.99	5.14	5.97	SO 28	5.83	7.01	6.43
SO 90	2.23	2.12	2.76	SO 90	3.13	3.18	3.99
RO 28	1.96	2.00	2.44	RO 28	5.42	5.38	5.32
RO 90	2.55	2.11	2.19	RO 90	4.50	4.52	4.09
Change of length (‰)	H2O	H2O-sea	Na2SO4		H2O	H2O-sea	Na2SO4
KN 28	0.00	-0.67	0.67	KN 28	0.67	0.67	2.02
KN 90	0.67	1.33	2.65	KN 90	0.00	0.66	3.97
KOB 28	1.32	2.65	0.00	KNB 28	1.32	2.65	0.00
KOB 90	1.32	-1.99	0.00	KNB 90	1.32	-0.66	0.00
KN8 28	-1.32	-0.66	-0.66	KN8 28	0.00	1.32	1.33
KN8 90	0.66	-1.33	0.66	KN8 90	1.32	-0.66	1.99
KO 28	1.33	0.00	2.66	KO 28	1.99	1.33	2.00
KO 90	1.34	0.00	-0.66	KO 90	0.67	1.33	-1.33
KOT 28	0.00	0.66	-0.66	KOT 28	1.32	1.65	0.66
KOT 90	0.66	0.66	0.66	KOT 90	0.00	0.66	0.66
SO 28	0.67	0.00	0.00	SO 28	1.33	0.00	0.00
SO 90	-0.66	0.00	0.67	SO 90	0.66	-0.66	0.67
RO 28	3.29	2.63	1.32	RO 28	3.95	3.29	1.99
RO 90	0.66	0.66	0.66	RO 90	0.00	1.98	8.61
Mass loss	H2O	H2O-sea	Na2SO4		H2O	H2O-sea	Na2SO4
KN 28	0.40	0.40	0.32	KN 28	0.68	1.10	0.72
KN 90	0.61	0.67	0.50	KN 90	0.75	0.88	1.01
KOB 28	0.74	0.52	0.53	KNB 28	0.85	0.60	0.78
KOB 90	1.40	1.34	0.54	KNB 90	1.71	1.62	0.79
KN8 28	0.45	0.40	0.25	KN8 28	0.61	0.51	0.66
KN8 90	0.63	0.60	0.45	KN8 90	0.65	0.90	0.83
KO 28	0.65	0.61	0.53	KO 28	0.84	1.11	1.04
KO 90	0.61	0.62	0.43	KO 90	0.58	0.66	0.75
KOT 28	0.55	0.53	0.45	KOT 28	0.80	0.79	0.74
KOT 90	0.50	0.58	0.42	KOT 90	0.56	0.73	0.63
SO 28	0.76	0.72	0.66	SN 28	0.80	1.45	1.01
SO 90	0.57	0.98	0.54	SN 90	0.84	0.93	0.94
RO 28	0.18	0.32	0.17	RO 28	0.39	1.10	0.55
RO 90	0.60	0.54	0.36	RO 90	0.81	0.94	0.64

B = increased amount of filler; K = Köping limestone filler; N = new way of mixing (filler last); O = ordinary way of mixing (filler first); R = reference; S = Ignaberga 200; T = 5.5 m hydrostatic pouring pressure instead of 0.23 m; 8 = 8 % air content.

Appendix 5.6 – Air void structure of concrete KN

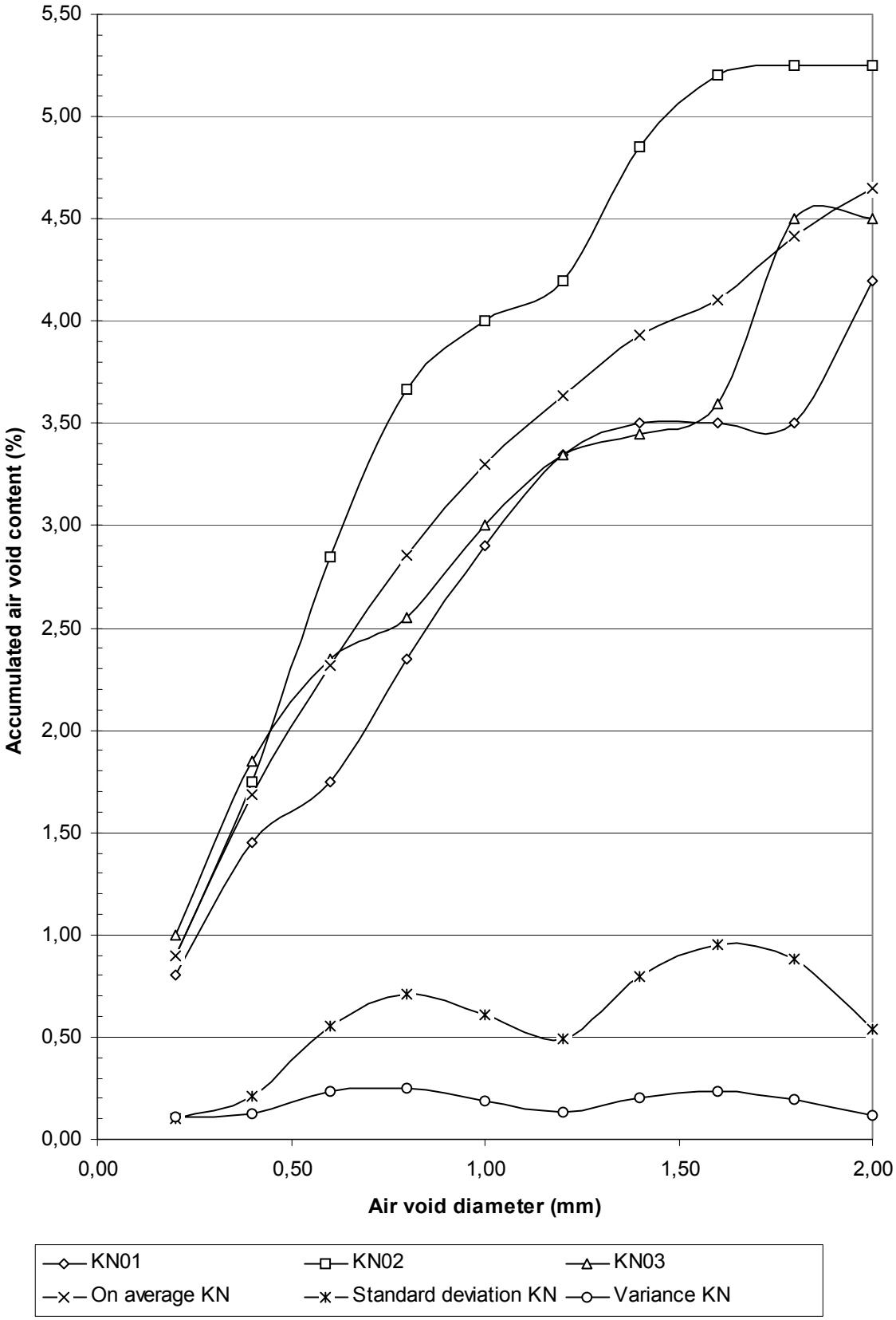

Appendix 5.7 – Air void structure concrete KO

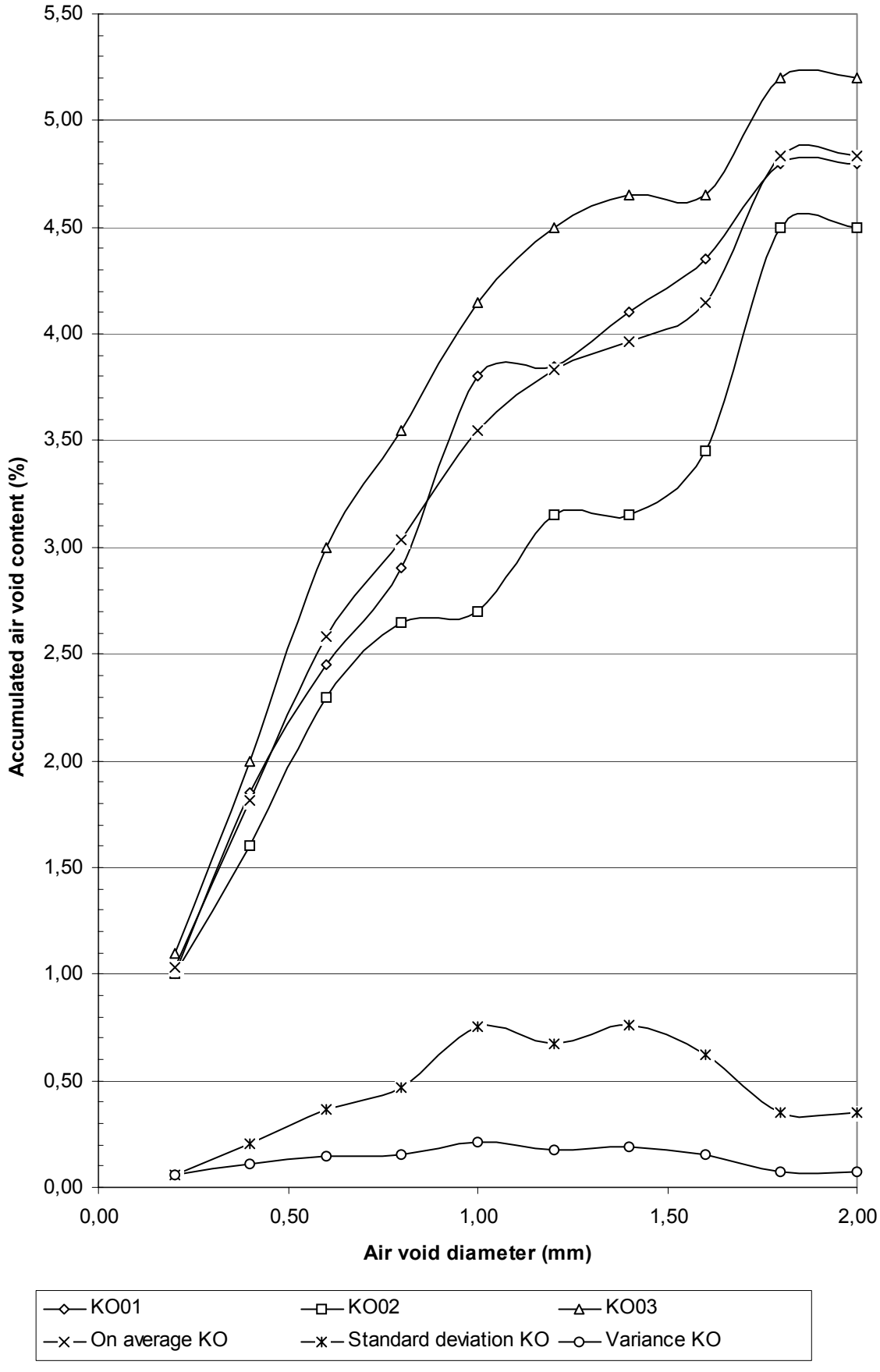

Appendix 5.8 – Air void distribution for concrete KOT

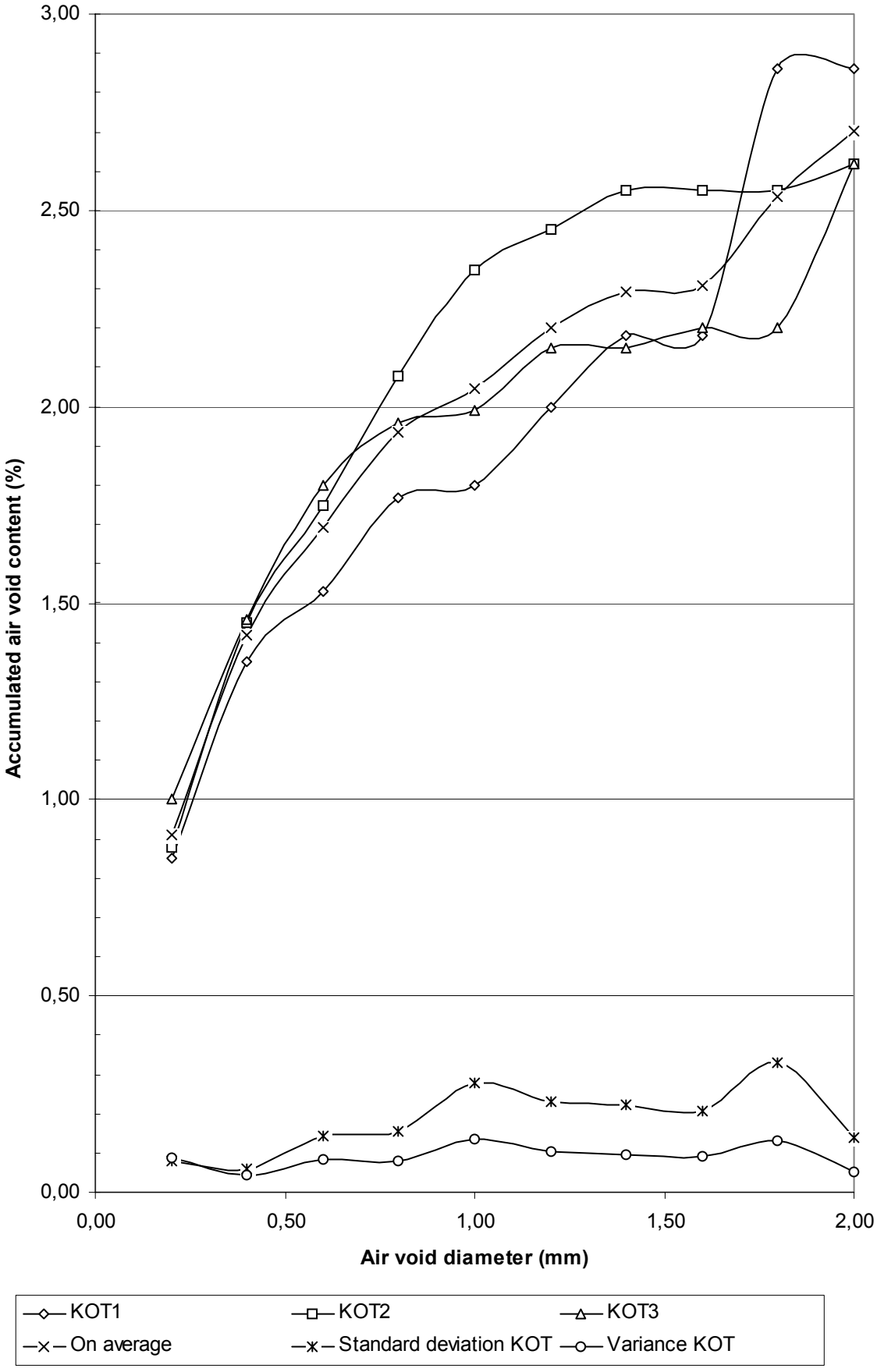

Appendix 5.9 – Air void structure of concrete RO I

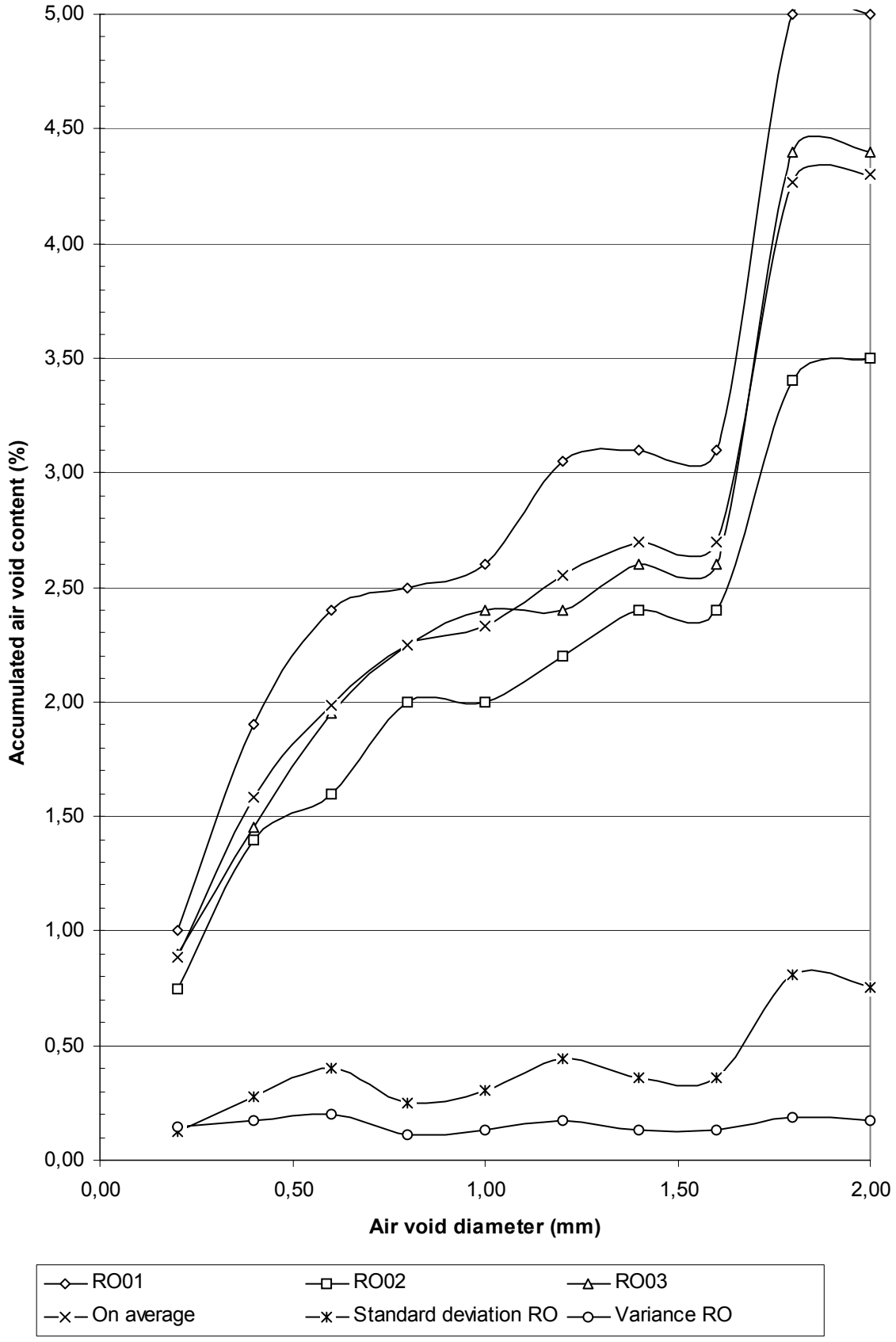

APPENDIX 6

Appendix 6.1 – Coefficient of variation of repeated tests of chloride migration coefficient, D, for concretes in series 3.

Concrete	KOB	KOT	SO	KN8	KN	ROII	RO	KO
Coefficient of variation (%)	3.5	5.5	7.0	8.0	8.5	9.0	10.0	10.5

Notations: B = increased amount of filler; K = Köping 500 limestone filler; N = new way of mixing (filler last); O = ordinary way of mixing (filler first); R = reference; S = Ignaberga 200 limestone filler; T = 5.5 m hydrostatic pouring pressure instead of 0.23 m; II = second reference concrete.

Appendix 6.2 – Significance test for the chloride migration coefficient, D, for concretes in series 3 (x10 $^{-12}$ m^2/s) – Effect of way of compaction (x10^{12} m^2/s).

Age of testing (days)	z	mK	mR	x
28	3.1	16.4	9.4	2.2
90	3.2	10.4	6.6	1.2

Notations: m = average; n = number of specimen; s = standard deviation; $x = \sqrt{(s_{KO}^2/n_{KO} + s_{RO}^2/n_{RO})}$; $z = (m_{KO}-m_{RO})/x$; K = Köping limestone powder; R = reference concrete (without filler).

Appendix 6.3 – Chloride migration coefficient, D, for concretes in series 3 (x10^{12} m^2/s) – Effect of mixing order and type of compaction.

Mix proportions	Ordinary mixing order (filler at first)	New mixing (filler last	Normal compacting concrete
KN 28		15.62	
KN 90		10.24	
KOB 28	13.72		
KOB 90	8.88		
KN8 28		15.24	
KN8 90		12.06	
KO 28	26.44		
KO 90	11.10		
KOT 28	12.70		
KOT 90	9.15		
SO 28	14.93		
SO 90	11.15		
RO 28			8.93
RO 90			7.11
RO 28 – 90h lagr.			9.25
ROII 28			9.66
ROII 90			6.07
Total	13.51	13.29	8.20

Notations: B = increased amount of filler; K = Köping 500 limestone filler; N = new way of mixing (filler last); O = ordinary way of mixing (filler first); R = reference; S = Ignaberga 200 limestone filler; T = 5.5 m hydrostatic pouring pressure instead of 0.23 m; II = second reference concrete; 8 = 8 % air content.

Appendix 6.4 – Chloride migration coefficient, D, for concretes in series 3 (x10 $^{-12}$ m^2/s) – Effect of age at testing and way of compaction.

Mix proportions	28 days	90 days
KN	15.6	10.2
KOB	13.7	8.9
KN8	15.2	12.1
KO	26.4	11.1
KOT	12.7	9.1
SO	14.9	11.2
RO	8.9	7.1
ROII	9.7	6.1
Average SCC	16.4	10.4
Average NC	9.3	6.6

Notations: B = increased amount of filler; K = Köping 500 limestone filler; N = new way of mixing (filler last); O = ordinary way of mixing (filler first); R = reference; S = Ignaberga 200 limestone filler; T = 5.5 m hydrostatic pouring pressure instead of 0.23 m; II = second reference concrete; 8 = 8 % air content.

Appendix 6.5 – Significance test for the hypothesis that SCC with ordinary mixing order had larger salt frost scaling after 112 cycles than NC had (g/m²).

Age at start of testing (days)	z	mKO	mRO	x	sK	sR
28	2.2	1181.1	689.5	224.4	307.2	336.6
90	0.8	908.8	748.0	196.7	136.5	441.3

Notations: m = average; n = number of specimen; s = standard deviation; $x = \sqrt{(s_{KO}^2/n_{KO} + s_{RO}^2/n_{RO})}$; $z = (m_{KO}-m_{RO})/x$; K = Köping limestone powder; O = ordinary mixing order; R = reference concrete (without filler).

Appendix 6.7 – Significance test for the hypothesis that SCC with 6% air content had larger salt frost scaling after 112 cycles than SCC with 8% had (g/m²).

Age at start of testing (days)	z	mKN	mKN8	x	sKN	sKN8
28	8,2	1068,2	678,9	47,5	55,0	61,1
90	6,6	858,3	466,3	59,7	82,2	62,9

Notations: m = average; n = number of specimen; s = standard deviation; $x = \sqrt{(s_{KN}^2/n_{KN} + s_{KN8}^2/n_{KN8})}$; $z = (m_{KN}-m_{KN8})/x$; K = Köping limestone powder; N = new mixing order; 8 = air content (%).

Appendix 6.8 – Significance test for the hypothesis that SCC with more filler had larger frost scaling after 112 cycles than SCC with normal filler content had (g/m²).

Age at start of testing (days)	z	mKO	mKOB	x	sKO	sKOB
28	0.9	1181.1	996.5	207.8	307.2	187.6
90	1.9	908.8	700.2	108.3	136.5	128.8

Notations: m = average; n = number of specimen; s = standard deviation; $x = \sqrt{(s_{KO}^2/n_{KO} + s_{KOB}^2/n_{KOB})}$; $z = (m_{KO}-m_{KO8})/x$; B = increased amount of filler; K = Köping limestone powder; O = ordinary mixing order.

Appendix 6.6 – Significance test for salt frost scaling of NC and SCC at different age of start of testing (kg/m²).

Significance test	28 cycles	56 cycles	112 cycles
mR	0.18	0.43	0.69
s28R	0.08	0.30	0.43
m28K6	0.37	0.70	1.07
s28K6	0.07	0.09	0.08
x_{28}	0.07	0.22	0.31
z_{28}	-2.75	-1.21	-1.24
m28K8	0.20	0.40	0.68
m28S6	0.39	0.54	0.72
m90R	0.22	0.45	0.75
s90R	0.20	0.37	0.56
m90K6	0.29	0.56	0.84
s90K6	0.09	0.06	0.10
x_{90}	0.15	0.26	0.40
z_{90}	-0.47	-0.38	-0.23
m90K8	0.24	0.26	0.47
s90S6	0.15	0.22	0.47

Notations: m = average; n = number of specimen; s = standard deviation; $x = \sqrt{(s_{KO}^2/n_{KO} + s_{RO}^2/n_{RO})}$; $z = (m_{KO}-m_{RO})/x$; B = increased amount of filler; K = Köping 500 limestone filler; N = new way of mixing (filler last); O = ordinary way of mixing (filler first); R = reference; S = Ignaberga 200 limestone filler; T = 5.5 m hydrostatic pouring pressure instead of 0.23 m; 6 = 6% air entrainment; II = second reference concrete.

Appendix 6.9 – Significance test for the hypothesis that large pouring pressure caused larger frost scaling after 112 cycles than normal pouring pressure did (g/m²).

Age at start of testing (days)	z	mKO	mKOT	x	sKO	sKOT
28	0.8	1181.1	1028.3	188.8	307.2	112.0
90	0.1	908.8	894.2	108.0	136.5	128.0

Notations: m = average; n = number of specimen; s = standard deviation; $x = \sqrt{(s_{KO}^2/n_{KO} + s_{KOT}^2/n_{KOT})}$; $z = (m_{KO}-m_{KOT})/x$; K = Köping 500 limestone filler; O = ordinary way of mixing (filler first); T = 5.5 m hydrostatic pouring pressure instead of 0.23 m.

Appendix 6.10 – Significance test for the hypothesis that SCC with Köping filler had larger frost scaling after 112 cycles than SCC with Ingaberga filler had (g/m²).

Age at start of testing (days)	z	mKO	mSO	x	sKO	sSO
28	2,6	1181,1	724,1	177,5	307,2	12,9
90	4,4	908,8	465,0	101,4	136,5	110,4

Notations: m = average; n = number of specimen; s = standard deviation; $x = \sqrt{(s_{KO}^2/n_{KO} + s_{SO}^2/n_{SO})}$; $z = (m_{KO}-m_{SO})/x$; K = Köping 500 limestone filler; O = ordinary way of mixing (filler first); S = Ignaberga 200 limestone filler.

Appendix 6.11 – Change on average of fundamental frequency, length and loss of weight of SCC mix proportions with Köping limestone filler and 6% air content

Test	Sort	Mix	Age at start of testing	100 Cycles	300 cycles
Frequency	%	K6	28	0.44	-5.49
Length	‰	K6	28	0.00	0.93
Mass	kg/m²	K6	28	0.03	-0.25
Frequency	%	K6	90	-0.46	-1.76
Length	‰	K6	90	0.67	0.13
Mass	kg/m²	K6	90	0.07	-0.20
Frequency	%	K6	28+90	-0.01	-3.62
Length	‰	K6	28+90	0.33	0.53
Mass	kg/m²	K6	28+90	0.05	-0.22

Appendix 6.12 – Change on average of fundamental frequency, length and loss of weight of SCC mix proportions with Köping limestone filler and 8% air content

Test	Sort	Mix	Age at start of testing	100 Cycles	300 cycles
Frequency	%	K8	28	-2.44	-6.97
Length	‰	K8	28	0.88	1.77
Mass	kg/m²	K8	28	0.04	-0.58
Frequency	%	K8	90	-1.87	-6.40
Length	‰	K8	90	-0.44	1.33
Mass	kg/m²	K8	90	-0.04	-0.71
Frequency	%	K8	28+90	-2.16	-6.68
Length	‰	K8	28+90	0.22	1.55
Mass	kg/m²	K8	28+90	0.00	-0.65

Appendix 6.13 – Change on average of fundamental frequency, length and loss of weight of NC mix proportions with 6% air content

Test	Sort	Mix	Age at start of testing	100 Cycles	300 cycles
Frequency	%	RO+ ROII	28	-0.86	-36.37
Length	‰	RO+ ROII	28	0.77	2.30
Mass	kg/m²	RO+ ROII	28	-0.10	-1.18
Frequency	%	RO+ ROII	90	-10.83	-41.78
Length	‰	RO+ ROII	90	1.32	5.29
Mass	kg/m²	RO+ ROII	90	-0.10	-1.48
Frequency	%	RO+ ROII	28+90	-5.85	-39.07
Length	‰	RO+ ROII	28+90	1.05	3.80
Mass	kg/m²	RO+ ROII	28+90	-0.10	-1.33

Appendix 6.14 – Significance test for a hypothesis that SCC with 6% air content had smaller change of fundamental frequency after 300 cycles than with 8% air (Hz).

Age at start of testing (days)	z	mKN	mKN8	x	sKN	sKN8
28	2.2	-243.3	-446.7	93.9	85.0	138.7
90	6.3	-76.7	-410.0	53.3	81.4	43.6

Notations: m = average; n = number of specimen; s = standard deviation; $x = \sqrt{(s_{KN}^2/n_{KN} + s_{KN8}^2/n_{KN8})}$; $z = (m_{KN}-m_{KN8})/x$; K = Köping; N = new mixing order; 8 = air content (%).

Appendix 6.15 – Significance test for the hypothesis that SCC with 6% air content had smaller length change after 300 cycles than SCC with 8% air content (mm).

Age at start of testing (days)	z	mKN	mKN8	x	sKN	sKN8
28	-1.0	0.1	0.3	0.1	0.2	0.1
90	-0.4	0.1	0.2	0.3	0.3	0.4

Notations: m = average; n = number of specimen; s = standard deviation; $x = \sqrt{(s_{KN}^2/n_{KN} + s_{KN8}^2/n_{KN8})}$; $z = (m_{KN}-m_{KN8})/x$; K = Köping; N = new mixing order; 8 = air content (%).

Appendix 6.16 – Significance test for the hypothesis that SCC with 6% air content had smaller mass change after 300 cycles than SCC with 8% had (g)

Age at start of testing (days)	z	mKN	mKN8	x	sKN	sKN8
28	3,2	-9,0	-16,1	2,2	1,7	3,5
90	5,6	-5,3	-19,4	2,5	4,0	1,7

Notations: m = average; n = number of specimen; s = standard deviation; $x = \sqrt{(s_{KN}^2/n_{KN} + s_{KN8}^2/n_{KN8})}$; $z = (m_{KN}-m_{KN8})/x$; K = Köping; N = new mixing order; 8 = air content (%).

Appendix 6.17 – Significance test for the hypothesis that SCC had smaller change of fundamental frequency after 300 cycles than NC had, both with 6 % air (Hz).

Age at start of testing (days)	z	mKO	m(RO+RO II)	x	sKO	s(RO+RO II)
28	4.6	90.0	-4883.3	1088.2	259.8	2640.1
90	4.5	-153.3	-5666.7	1221.1	66.6	2989.7

Notations: m = average; n = number of specimen; s = standard deviation; $x = \sqrt{(s_{KO}^2/n_{KO} + s_R^2/n_R)}$; $z = (m_{KO}-m_R)/x$; K = Köping; O = ordinary mixing order; R = reference.

Appendix 6.18 – Significance test for the hypothesis that SCC had a smaller length change after 300 cycles than NC had, both with 8% air content (mm).

Age at start of testing (days)	z	mKO	m(RO+RO II)	x	sKO	s(RO+RO II)
28	-0.6	0.5	0.7	0.4	0.5	0.7
90	-5.7	-0.1	1.6	0.3	0.1	0.7

Notations: m = average; n = number of specimen; s = standard deviation; $x = \sqrt{(s_{KO}^2/n_{KO} + s_R^2/n_R)}$; $z = (m_{KO}-m_R)/x$; K = Köping; O = ordinary mixing order; R = reference.

Appendix 6.19 – Significance test for the hypothesis that SCC had smaller mass change after 300 cycles than NC had. both concretes with 6% air content (g)

Age at start of testing (days)	z	mKO	m(RO+RO II)	x	sKO	s(RO+RO II)
28	3.0	-19.6	-65.0	15.0	21.6	20.6
90	4.3	-7.5	-81.4	17.3	1.7	42.3

Notations: m = average; n = number of specimen; s = standard deviation; $x = \sqrt{(s_{KO}^2/n_{KO} + s_R^2/n_R)}$; $z = (m_{KO}-m_R)/x$; K = Köping; O = ordinary mixing order; R = reference.